Charles University in Prague
Faculty of Science

Field of study: Chemistry
Specialization: Physical Chemistry

Mgr. Lenka Škrabalová

Nucleation of sulphuric acid and water – experimental and atmospheric observations

Nukleace kyseliný sírové a vody - experimentální a atmosférická pozorování

Doctoral thesis

Supervisor: Ing. Vladimír Ždímal, Dr.
Prague, 2015

Acknowledgement

I would like to thank to my supervisor, Dr. Vladimír Ždímal, for his guidance and support during my studies and to all of my colleagues for creating a pleasant working environment. My very special thanks belong to Dr. David Brus, who enabled me to work in a laboratory at Finnish meteorological institute and introduced me into nucleation experiments. I am also very grateful to Ing. Josef Kugler for his immense help and technical support during the laboratory experiments.

Prohlášení:

Prohlašuji, že jsem závěrečnou práci vypracovala samostatně a že jsem uvedla všechny použité informační zdroje a literaturu. Tato práce ani její podstatná část nebyla předložena k získání jiného nebo stejného akademického titulu.

V Praze, dne 27. 11. 2015

Podpis

Název práce: *Nukleace kyseliny sírové a vody – experimentální a atmosférická pozorování*

Autor: *Mgr. Lenka Škrabalová*

Katedra: *Katedra fyzikální a makromolekulární chemie*

Vedoucí dizertační práce: *Ing. Vladimír Ždímal, Dr.*

ABSTRAKT: Tato práce se zabývá studiem nukleace kyseliny sírové a vody, která představuje klíčový děj spojený se vznikem sekundárního atmosférického aerosolu procesem kondenzace plynných prekurzorů. Zkoumali jsme především rychlost nukleace, vznik nových aerosolových částic a dynamiku růstu těchto částic. Tyto procesy byly studovány v laboratorních i atmosférických podmínkách.

Laboratorní experimenty byly zaměřeny na určení rychlosti nukleace kyseliny sírové a vody a rychlosti růstu nově vzniklých částic; byl také studován vliv experimentálních podmínek na růst částic. Koncentrace H_2SO_4 měla ze všech experimentálních podmínek největší vliv na výsledné rychlosti růstu částic, což je v souladu s atmosférickými pozorováními tohoto jevu. Dále byl navržen model, který předpovídá růst částic vzniklých nukleací H_2SO_4 - H_2O a při modelování růstu částic model uvažuje kromě přítomnosti H_2SO_4 a H_2O také kondenzaci třetí složky – NH_3 v různých koncentracích. Při porovnání atmosférických a experimentálních rychlostí růstu částic bylo zjištěno, že H_2SO_4 je hlavní kondenzující složka zodpovědná za růst částic pouze lokálně především v silně znečištěných oblastech a v globálním měřítku dominují během počátečního růstu částic sekundárního aerosolu jiné složky, především NH_3 a aminy.

Atmosférická pozorování H_2SO_4 - H_2O nukleace a vzniku nových částic v atmosféře byla založena na analýze dvouleté časové řady měření velikostních distribucí a koncentrací atmosférického aerosolu. Analýza dat byla zaměřena především na dynamiku růstu nově vzniklých částic a byl zkoumán nedávno popsaný jev – vypařování částic následující po předchozím vzniku nových částic sekundárního aerosolu. Byla popsána sezónní variabilita tohoto jevu a byl také studován vliv meteorologických parametrů a vliv koncentrací polutantů na vypařování částic. Bylo zjištěno, že na vypařování částic se nejvíc podílí prudký pokles intenzity globální radiace a také vertikální promíchávání atmosféry výrazně přispívá k intenzitě tohoto jevu.

Klíčová slova: nukleace kyseliny sírové a vody, vznik nových aerosolových částic, růst částic, vypařování částic

Title: *Nucleation of sulphuric acid and water experimental and atmospheric observations*

Author: *Mgr. Lenka Škrabalová*

Department: *Department of Physical and Macromolecular Chemistry*

Supervisor: *Ing. Vladimír Ždímal, Dr.*

ABSTRACT: This work is dedicated to the study of nucleation of sulphuric acid and water, which presents the key process associated with secondary aerosol formation via gas to particle conversion. We investigated the nucleation rates, new aerosol particles formation and growth dynamics of newly nucleated particles. These processes were explored in both laboratory and field experiments.

In the laboratory measurements, we explored the H_2SO_4 - H_2O nucleation rates and growth rates of newly formed particles under well-defined conditions and we also investigated the effect of experimental conditions on particle growth dynamics. Furthermore, we proposed a model, which predicts the particle growth and accounts for condensation of H_2SO_4, H_2O and NH_3. The comparison of experimental growth rates with atmospheric ones was made and resulting implications of the chemical nature of compounds involved in the early growth of nucleated particles is also presented.

To investigate the atmospheric H_2SO_4 - H_2O nucleation and new particle formation, we analysed a two-year long dataset of particle number size distributions, obtained from a urban background station in Prague Suchdol. A special attention was given to a recently reported special feature of particle growth dynamics - a particle shrinkage following previous new particle formation. We determined the basic characteristics of observed new particle formation and particle shrinkage events and their seasonal variability was investigated as well. We also focused on the analysis of the meteorological and atmospheric conditions favouring the particle shrinkage.

Key words: sulphuric acid water nucleation, new particle formation, particle growth, particle shrinkage

Preface

The formation of new aerosol particles in the atmosphere via gas to particle conversion presents a key phenomenon associated with the atmospheric aerosol system. Model calculations suggest that up to half of secondary aerosol particles may originate from this process. Atmospheric nucleation i.e. the formation of nanometer sized stable clusters from gaseous precursors is the first step in secondary aerosol formation. The atmospheric new particle formation is a very active area of aerosol research owing to the role of aerosol particles in the Earth‘s climate and because of aerosol‘ influence on the atmospheric chemistry and human health. Our current limited knowledge about new particle formation translates into uncertainties in the magnitude of such effects. Despite extensive research, fundamental questions about formation of new aerosol particles remain open, especially about the mechanism responsible for atmospheric nucleation and overall extent of this phenomenon. Once formed, the aerosol particles have to reach sizes over 50 nm in order to influence climate and cloud formation processes. The particle growth following new particle formation event is thus the dominant factor, which determines the magnitude of aerosol impact on climate and human health. More work is therefore needed to clarify the factors, which govern the growth of newly formed particles.

This thesis is dedicated to the study of H_2SO_4 - H_2O nucleation and new particle formation with special interest in growth dynamics of formed particles. This work reports on two sets of observations an experimental study of H_2SO_4 - H_2O particles growth, which was performed in the laboratory of Climate change department at the Finnish Meteorological Institute in Helsinki, and field work on atmospheric new particle formation and particle shrinkage, conducted at the urban background station at Prague Suchdol. The primary objectives of the presented work include to:

- determine the growth rates of particles formed via H_2SO_4 - H_2O nucleation under various conditions in a laboratory study
- compare the experimental growth rates with a model prediction
- compare the experimental growth rates with growth rates of newly formed atmospheric aerosol particles
- analyze a long-term time series of atmospheric observations of new particle formation and particle shrinkage events from Prague Suchdol station

- identify the atmospheric conditions influencing the growth dynamics of newly formed particles

The thesis is divided into five chapters. Chapter (1) introduces recent findings related to atmospheric new particle formation and particle growth. Chapter (2) describes methods used for both laboratory and field investigation of atmospheric nucleation and also gives an overview of laboratory nucleation experiments. Chapter (3) includes description of experimental setup and results from a laboratory study of H_2SO_4 – H_2O nucleation and particle growth, while Chapter (4) is dedicated to the field observation of atmospheric new particle formation and brings together the growth dynamics of formed particles and the atmospheric conditions. Finally, Chapter (5) concludes the results.

Contents

1. Introduction

We will briefly introduce atmospheric aerosols, their sources and properties here. Recent findings related to the process of secondary aerosol formation, atmospheric nucleation and subsequent growth of newly formed particles will be discussed in detail in this chapter. An emphesis will be given to the nucleation of sulphuric acid and water, because these compounds are key components of atmospheric nucleation and particle growth. The presented work is devoted to both experimental investigation and atmospheric observation of this phenomenons.

1.1 Atmospheric aerosol

Aerosol is defined as a suspension of liquid and solid particles in a gas (Hinds, 1999). Atmospheric aerosol particles exert an important influence on Earth's climate through their effect on the global radiation budget, on chemical composition of atmosphere, on cloud formation, cloud lifetime and the whole hydrological cycle (Charlson et al., 1992). Aerosol also affects human health owing to exposure in both ambient and occupational environments. Aerosol particles span the size range from 1 nm to 100 μm. The particle size is the most important parameter determining the behaviour of aerosol.

Aerosol particles can be divided into several modes according to particle size. Particles smaller than 1 μm form fine mode, whereas particles spanning the sizes from 1 to 10 μm belong to coarse mode. Particles from these two modes are generated from various processes and thus differ significantly in residence time in atmosphere and in chemical composition. There is also quite low mass exchange between these modes (Hinds, 1999). Coarse mode particles are either anthropogenic mechanically produced particles (from mining, construction works, agriculture etc) or sea spray salt particles and windblown dust. Their lifetime in the atmosphere is typically from several hours to several days due to its settling down or impacting various surfaces. The fine mode can be further divided into 3 distinctly different modes nucleation, Aitken and accumulation mode. The nucleation mode contains particles in sizes from 1 to 25 nm, which are formed by gas to particle conversion or during high temperature (combustion) processes. They have short lifetime in the atmosphere, since they coagulate quickly with each other or with particles in Aitken and accumulation mode. The Aitken mode consists of particles in sizes from 25 to 100 nm, which are generated during combustion processes, from traffic exhausts or have grown from nucleation mode via condensation or coagulation. These particles can serve as cloud condensation nuclei and have a relatively short atmospheric lifetime owing to rapid coagulation and growth

into larger sizes. The accumulation mode (particle sizes from 100 to 1000 nm) includes aerosol particles grown by coagulation or by condensation from smaller particles or aerosol formed by combustion processes and smog particles. Because the removal processes from this mode are weak, the particles accumulate in this mode and have significantly longer lifetime in the atmosphere compared to particles from nucleation and Aitken modes (Hinds, 1999).

Secondary aerosol formation

Primary aerosol is introduced into atmosphere directly (via volcanic eruption, as sea spray etc.), whereas secondary aerosol particles are formed in the atmosphere via chemical reactions of gas phase species. The first step of the secondary aerosol formation is nucleation, which is generally defined as a formation of molecular clusters (embryos) of a new phase during any phase transition. Atmospheric nucleation (a gas to particle conversion) is therefore in principle analogous to any phase transformation i.e. freezing of liquids or crystallization of supersaturated solutions. The molecular clusters during nucleation are formed via random collisions and rearrangements of atoms and molecules of the existing phase. Each step of cluster formation, growth and decay can be described as a reversible stepwise process characterized by kinetic rate theories. According to the Classical Nucleation Theory (Becker and Döring, 1935) the free energy of cluster formation, Δ G, reaches maximum when the cluster has critical size i* and beyond this point the growth of the clusters and thus the phase transition are spontaneous (Fig.1).

There are three main theoretical approaches to characterize the formation of these molecular clusters. The Classical Nucleation Theory (CNT), formulated in 1935 (Becker and Döring, 1935) on the basis of kinetic theory of nucleation (Volmer and Weber, 1926), uses thermodynamic and kinetic variables in order to obtain the nucleation rate. The CNT approximates the clusters as spherical droplets with a sharp interface having macroscopic thermodynamic properties, such as the surface tension or bulk liquid density. Up to date, the CNT forms basic theoretical framework of nucleation. Recently, several binary and ternary nucleation parametrizations based on CNT have been introduced and are widely used in atmospheric modelling (Wilemski, 1984; Kulmala et al., 1998; Wehkämaki et al., 2002; Yu, 2008). The kinetic models present another approach to study nucleation theoretically. These models deduce the cluster distribution and hence the nucleation rate by determining the rate constants for formation and decay of clusters, avoiding to evaluate the cluster formation energies from macroscopic properties. Some of these theories are based on solving the Smoluchowski or Fokker - Planck equations describing the motion of a single molecule in a potential well around

the cluster (Nowakowski and Ruckenstein, 1991a; Nowakowski and Ruckenstein, 1991b), while other treat nucleation as a multistep binary collision process between nucleating molecules and clusters (Kathman, 2006; Kathman et al., 2009). Finally, the molecular level approach to nucleation is represented by Monte Carlo or molecular dynamics simulations (ten Wolde et al., 1999; Frenkel and Smith, 2002). These methods aim to determine the cluster structure and the free energy of cluster formation. However, use of these models is limited owing to their extensive demand of computational and time capacity. Apart from above mentioned theoretical approaches, the Nucleation theorem (Kashchiev, 1982), provides the insight into the molecular composition of the critical nucleus. This theorem states that the slope of the logarithm of the nucleation rate versus the logarithm of the concentration of the nucleating vapor is closely related to the number of molecules in the critical nucleus.

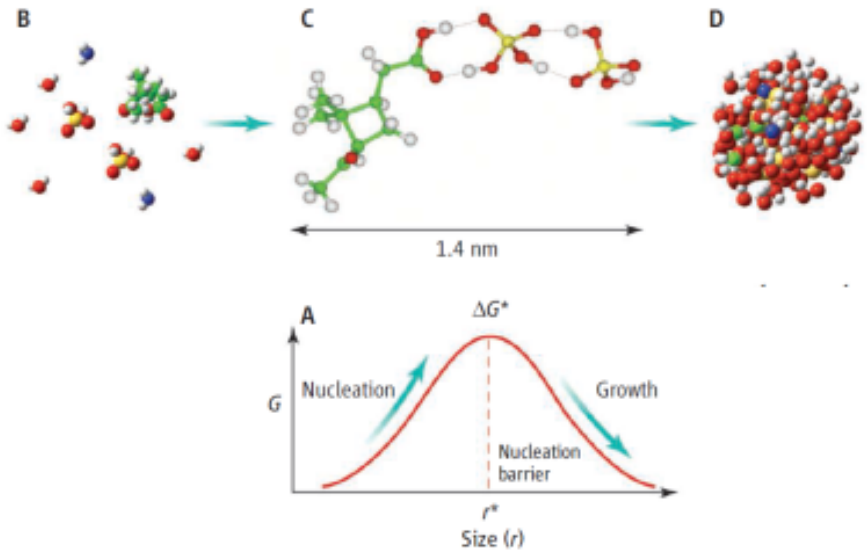

Fig. 1: Schematic description of the formation of critical cluster (stage C) from free molecules and corresponding free energy variation. Figure taken from Zhang, 2010.

1.2 Atmospheric nucleation

Atmospheric nucleation (i. e. formation of new aerosol particles) is a key process associated with atmospheric aerosol system (Kulmala et al., 2013). Aerosol particles influence the global radiative balance and Earth´s climate directly via scattering and absorbing solar radiation and indirectly by acting as cloud condensation nuclei (Charlson et al., 1992) and also affect visibility. New particle formation through the photochemical reactions of gaseous species

significantly influences the number concentrations and size distributions of atmospheric aerosol. Also aerosol models suggest that atmospheric nucleation is very likely a major source of aerosol particles in the global atmosphere (Spracklen et al, 2006) and is a significant source of cloud condensation nuclei (Spracklen et al., 2008, Merikanto et al., 2009). Atmospheric nucleation events are a global phenomenon and have been observed to take place in many different atmospheric environments (Kulmala, 2003). There are large variations in intensities and spatial scales of these events – it can be a huge regional event extending over a thousand kilometres or it can occur in intensive localised burst i.e. on a coastline (O'Dowd et al., 2002).

Atmospheric new particle formation is a complicated set of processes, which includes the production of nanometer-sized clusters from gaseous precursors, the growth of these clusters to larger sizes and the removal of growing clusters via coagulation with the pre-existing aerosol particles (Kulmala et al, 2012). Several mechanisms of new particle formation have been proposed, including the binary homogeneous nucleation of water and sulphuric acid (Vehkamäki et al., 2002), ternary homogeneous nucleation of water, sulphuric acid and ammonia or amines (Ball et al., 1999; Korhonen et al., 1999; Benson et al., 2009; Berndt et al., 2010; Kirkby et al., 2011), ion-induced nucleation (Lee et al., 2003; Lovejoy et al., 2004; Yu et al., 2010; Kerminen et al., 2010; Hirsikko et al., 2011) and homogeneous nucleation involving iodine species (Kulmala, 2003). However, it still remains an open question which nucleation mechanism is dominant in the atmosphere (Kulmala et al., 2004), because the preferred new particle formation mechanism is likely to vary with the geographical location and atmospheric conditions. In Fig. 2 is presented the schematic description of atmospheric new particle formation mechanism (Kulmala, 2003). The atmospheric nucleation involves the formation of stable clusters of size ~1.5 nm from gaseous precursors and the growth of these clusters to large sizes. Despite intensive investigation, the overall magnitude of this aerosol source is still poorly known compared to any other major source producing aerosol particles. Our current inability to quantify new particle formation correctly results in huge uncertainties into the assessment of the direct and indirect effects of aerosols on climate change in the climatic models (Spracklen et al., 2006, Merikanto et al., 2009).

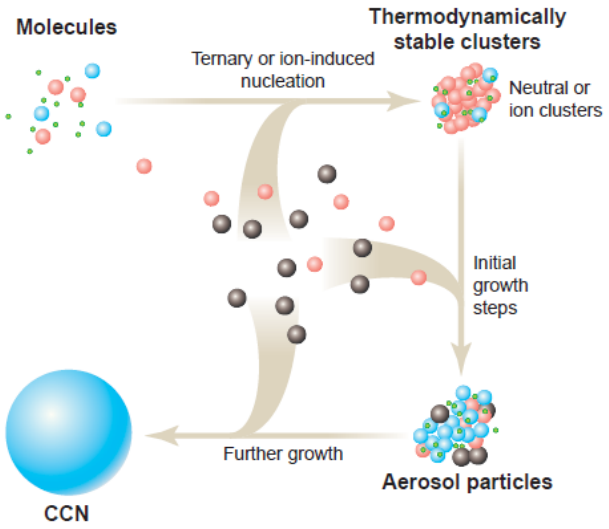

Fig. 2: The new particle formation is initiated by a formation of stable clusters via ternary or ion-induced nucleation. The subsequent growth of formed particles involves condensation of various vapours and the particles are expected to grow faster with increasing size due to enhanced condensational flux caused by decreasing Kelvin effect. Finally, cloud condensation nuclei (CCN) are formed when particles reach sizes of 50 nm and larger. Figure taken from Kulmala (2003).

Atmospheric nucleation mechanism

New particle formation (NPF) events are usually characterized by two quantities: particle formation rate (cm^{-3} s^{-1}) which presents the rate at which new particles are being produced and particle growth rate (nm h^{-1}) which describes, how rapidly newly formed particles grow to larger sizes. The measured NPF rate is usually not the actual atmospheric nucleation rate, but rather the rate at which nucleated particles appear in the smallest detectable sizes, which are currently ~3 nm in commonly used instruments (Kulmala et al., 2012). The particle detection devices, which are used to measure particle number concentration, are characterized by a certain cut-off size. The cut-off size is defined as the lowest particle diameter at which the instrument detects at least 50 % of the particles. The cut-off diameter and the steepness of the cut-off curve are determined by the diffusional losses of particles in the device and by the activation probability of the particles (Kulmala et al., 2012). However, recent technical development enabled for the first time to measure the concentrations and size distributions of molecular clusters and nanoparticles in the sub-2nm size range, where the key steps of atmospheric nucleation occur (Kulmala et al., 2013).

Almost constant presence of neutral clusters in sizes ≤ 2 nm was observed, which implies continuous formation of neutral clusters and their subsequent growth to larger sizes. Three size segregated regimes in the sub-2nm range, identified in these experiments, build up a consistent framework for neutral nucleation path, which strongly dominates over the ion induced nucleation in the atmosphere. The clusters exhibit very different behaviour in these 3 size regimes. Whereas cluster concentration and its diurnal pattern in the first size regime (from 0.9 to 1.3 nm) were very similar between event days (the day when NPF is observed) and non event days (the day with no NPF event), the opposite is truth for clusters in the other size regimes (from 1.3 to 1.7 nm and from 1.7 to 2.1 nm). Concentrations of these clusters exhibit a clear daytime maximum on the NPF event days, which was absent on non event days. When investigating the growth rates, the growth of clusters in the first two size regimes can be fully explained by H_2SO_4 condensation provided that clusters in the second size regime (sizes from 1.3 to 1.7 nm) are stabilized by ammonia, amines or organic vapours (Kulmala et al., 2013). On the other hand, the clusters from the third size group grow two to four times faster than can be explained by H_2SO_4 condensation indicating involvement of other species in the growth process. Organic vapours were found to be the most likely candidates. The overview of these conclusions is schematically depicted in Fig. 3. To summarize these findings, which present current state-of-the-art knowledge, the atmospheric new particle formation is assumed to consist of two separated steps. In the first step (in sizes from 1.3 to 1.7 nm) the atmospheric nucleation (i.e. the formation of stabilized clusters) occurs. The second step, initiated from sizes 1.7 to 2.1 nm, is characterized by enhanced cluster growth due to assumed condensation of organic vapours. Although this study revealed many important conclusions, there are still many open questions, that limit our current understanding of the atmospheric nucleation. For example the quantitative measurements of the ternary vapours involved in nucleation or the role of ions in nucleation mechanism are still lacking, as well as molecular composition of the critical clusters has not been directly measured yet and remains unknown. Deeper investigation on this subject is therefore needed to fully understand this process and to add nucleation parametrization into the climatic models.

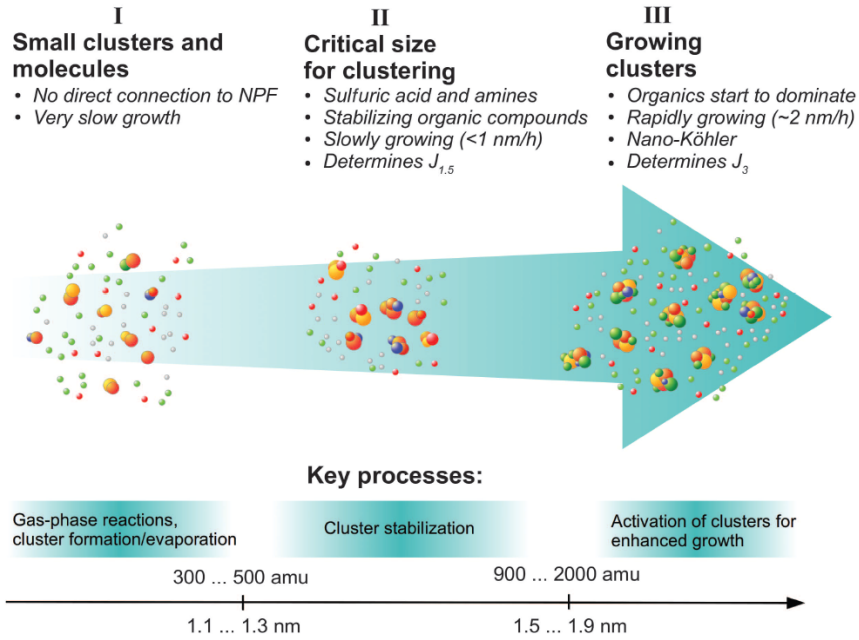

Fig. 3: The neutral molecular clusters in the sub-2nm size bin observed in the atmosphere were found to form three size segregated ranges. The key processes of atmospheric nucleation are related to the second size regime (from 1.3 to 1.7 nm) and the formation rate of stable clusters of size 1.5 nm presents the true nucleation rate $J_{1.5}$ connected to the NPF event. The figure was taken from Kulmala et al. (2013).

Field studies of atmospheric nucleation

Field studies have shown that atmospheric nucleation occurs ubiquitously in different atmospheric environments, ranging from the boundary layer just above the Earth's surface to the upper troposphere and lower stratosphere. A large number of field campaigns has been performed at various altitudes, different geographical locations, in clean environments like Antarctica as well as in heavily polluted areas (Kulmala et al., 2004). There are quite large differences in reported formation rates among studies performed at various locations. Typical formation rates of 3 nm particles, measured during regional NPF events in the boundary layer, span the range from 0.01 to 10 cm^{-3} s^{-1}, even though much higher values are often reported from urban areas: 100 cm^{-3} s^{-1} and in local bursts in coastal zones or industrial plumes the formation rates can reach up to 10^4-10^5 cm^{-3} s^{-1}. Investigation of atmospheric nucleation requires measurements of both chemical and physical properties of nucleation mode particles (≤ 25 nm) as well as the ambient aerosol number size distributions. Simultaneous measurements of nucleating vapours or their proxies and chemical analysis of formed particles provide further informations

about the nucleation mechanism. Field measurements suggest that nucleation rate depends only weakly on the H_2SO_4 concentration, implying that according to Nucleation theorem (Kashchiev, 1982) there are 1 or 2 H_2SO_4 molecules in the critical cluster (McMurry et al., 2005). Quantum chemistry simulations suggest, that a hydrated H_2SO_4 dimer has a diameter ~0.7 nm, which is too small to overcome the nucleation barrier (Zhang, 2010). All these findings imply, that critical cluster containing H_2SO_4 and H_2O is stabilized by presence of a third species (Kerminen et al., 2010). Favourable candidates are NH_3, amines or organic acids; however these compounds have different ability to stabilize H_2SO_4 clusters (Fig. 4). Amines and ammonia were observed to be the most effective compounds to provide stabilization of H_2SO_4 clusters.

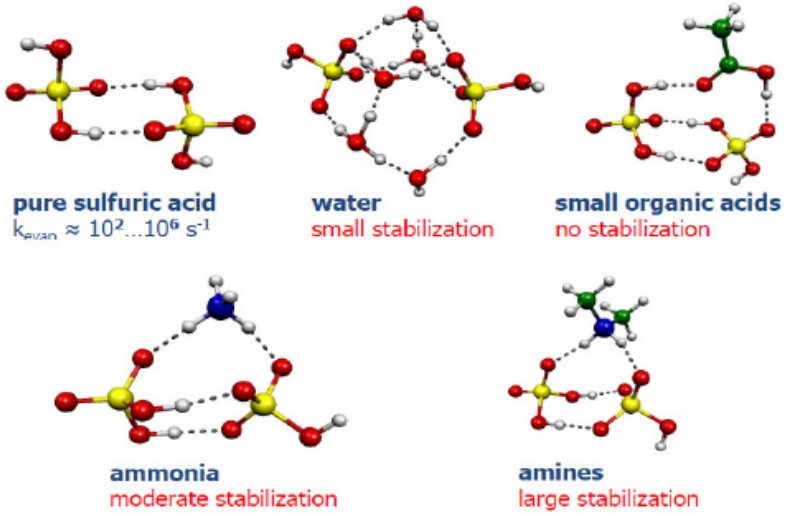

Fig. 4: Relative stability of H_2SO_4 clusters with different stabilizing species (H_2O, organic acids, NH_3 and dimethyl amine) based on the evaporation rates k_{evap} determined from quantum chemistry simulations. The atoms are presented with different colors: yellow – sulfur, red – oxygen, grey – hydrogen, blue – nitrogen and green – carbon and the dashed lines depict hydrogen bonds. Figure taken from Kerminen et al. (2010).

The number size distribution of aerosol particles is governed by the formation processes and subsequent physical and chemical transformations in the atmosphere. The particle number concentration as a function of time is the primary data set needed for determination of particle formation rate. The number concentrations of atmospheric particles are usually measured by condensation technique using Condensation Particle Counters (CPCs) and number size distributions are commonly measured by a Differential Mobility

Particle Sizer (DMPS) or a Scanning Mobility Particle Sizer (SMPS). Detaited description of these instrumenst will be given in Chapter (2). Identifying the atmospheric new particle formation from the ambient measurements is based on inspecting the measured size distribution data (Kulmala et al, 2012). Owing to aerosol dynamic processes in the atmosphere, the ambient aerosol size distribution is usually composed of one or more log-normally distributed modes. A new particle formation event leads to the formation of a distinctly new mode – the nucleation mode. An example of particle size distributions observed on days with and without new particle formation is presented in Fig. 5. Observed evolution of the nucleation mode in time can be used to determine the dynamic parameters of the new particle formation (Dal Maso et al., 2005).

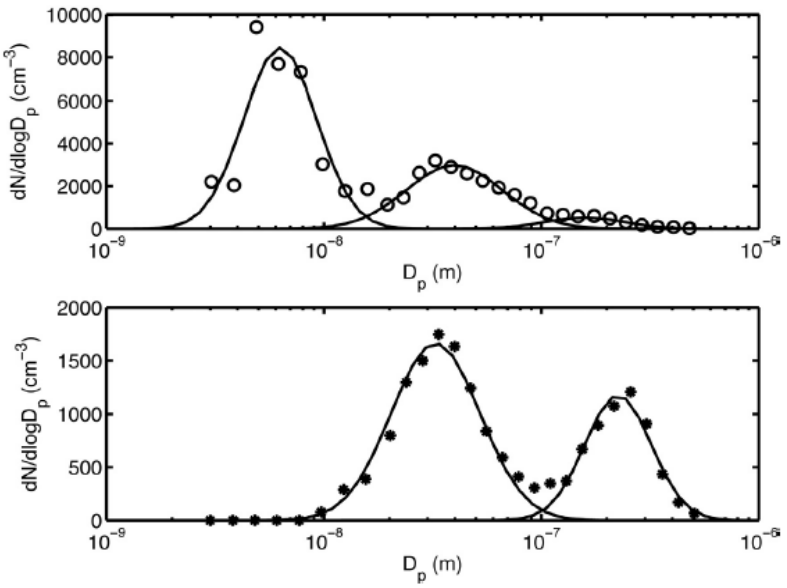

Fig. 5: The depicted number size distributions were observed in a boreal forest at Hyytiälä station, Finland. The lower panel shows typical size distributions observed on a day without new particle formation consisting of a bimodal size distribution. The upper panel depicts the size distribution observed on a day with a new particle formation. 3 modes are present here – the nucleation mode (size from 1 to 25 nm), Aitken mode (25 – 100 nm) and accumulation mode (≥ 100 nm). Figure taken from Dal Maso et al. (2005).

Atmospheric new particle formation event characterization

Recently, a detailed procedure describing basic methodology to characterize the NPF event in order to obtain particle formation rates (especially during regional NPF) has been proposed (Kulmala et al., 2012). Firstly, measured particle size distributions from SMPS or DMPS have to be inverted (this procedure will be described in more detail later) and verified. The data inversion of particle size distribution gives particle number concentration density function $dN/d(\log d_p)$, which is by convention plotted as flat surface plots, where x axis is time, y axis presents the particle diameter on a logarithmically spaced scale and z axis shows the particle number concentration density, commonly presented by different colors (Fig. 6). The NPF event classification is based on visual or automatic inspection of these surface plots showing time evolution of the number size distribution. The investigated days are classified as an event day, a non event day or an undefined day. Because the clarity of NPF typical features can significantly vary between different events, 3 features have to be observed to classify a regional particle formation event: 1) a distinctly new particle mode must appear in size distribution in the nucleation size range (≤ 25 nm) 2) the new mode is prevailing for at least several hours 3) growth of the newly formed particles is observed for several hours (Dal Maso et al., 2005).

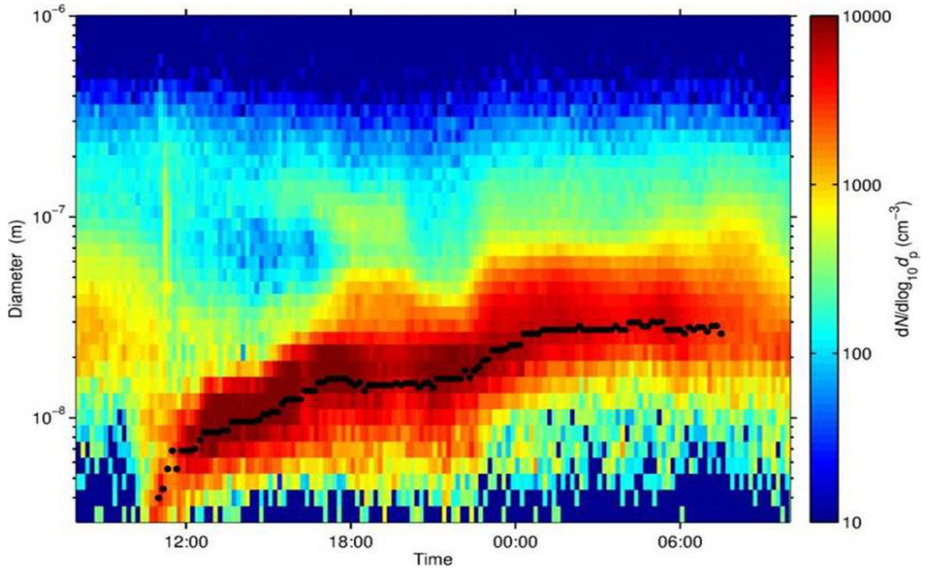

Fig. 6: An example of the plot of NPF event. The aerosol particle concentration is depicted as a function of particle diameter and time. The nucleation mode geometric mean diameters obtained by log-normal fitting are shown as black points. Figure taken from Ehn et al. (2014).

After NPF event classification, the observed particle growth rate GR is determined as the rate of change of the diameter d_p representing the whole growing particle population, which is determined using either maximum concentration method or log-normal distribution function method:

$$GR = \frac{d_{p2} - d_{p1}}{t_2 - t_1}, \quad (1)$$

where d_{p1} and d_{p2} are the representative particle diameters at times t_1 and t_2, respectively (Kulmala et al., 2012).

With the maximum concentration method, the timing of maximum concentration in each size fraction is followed and the representative diameter is determined as the center of the measured size bin (Lehtinen and Kulmala, 2002). In the second method, the log-normal distribution is fitted to the measured size distribution and the geometric mean of the fitted distribution is used in the calculations (Dal Maso et al., 2005). The GR is then calculated from the slope of a linear fit to the data points determined in the previous step. The slope can be determined for the whole time period of the particle formation to obtain the overall GR or can be determined for selected size ranges or time periods to obtain size- or time- dependent GRs. An example of GR determination from measured size distributions using both above described methods is depicted in Fig. 7A and 7B. The correction of the observed GR for self-coagulation and coagulation scavenging is necessary, since the overall GR is given by the real growth of newly formed particles, by the self-coagulation of the growing particle population as well as by the selective coagulation scavenging by the larger pre-existing particles (Leppa et al, 2011). Next, the size distribution-dependent particle loss parameters have to be determined CoagS, which presents the coagulation sink at size d_p and CS, which is the condensational sink and presents the condensing vapour sink caused by the particle population. The final step is the determination of a formation rate of particles with certain diameter. The time evolution of particle number concentration in size range (d_p, $d_p + \Delta d_p$) can be described as the difference between production (i. e. formation rate at particle size d_p, i.e. J_3 for 3 nm particles) and losses, which include coagulation losses by pre-existing larger particles and condensational growth out of the considered size range using equations given in Kulmala et al. (2012).

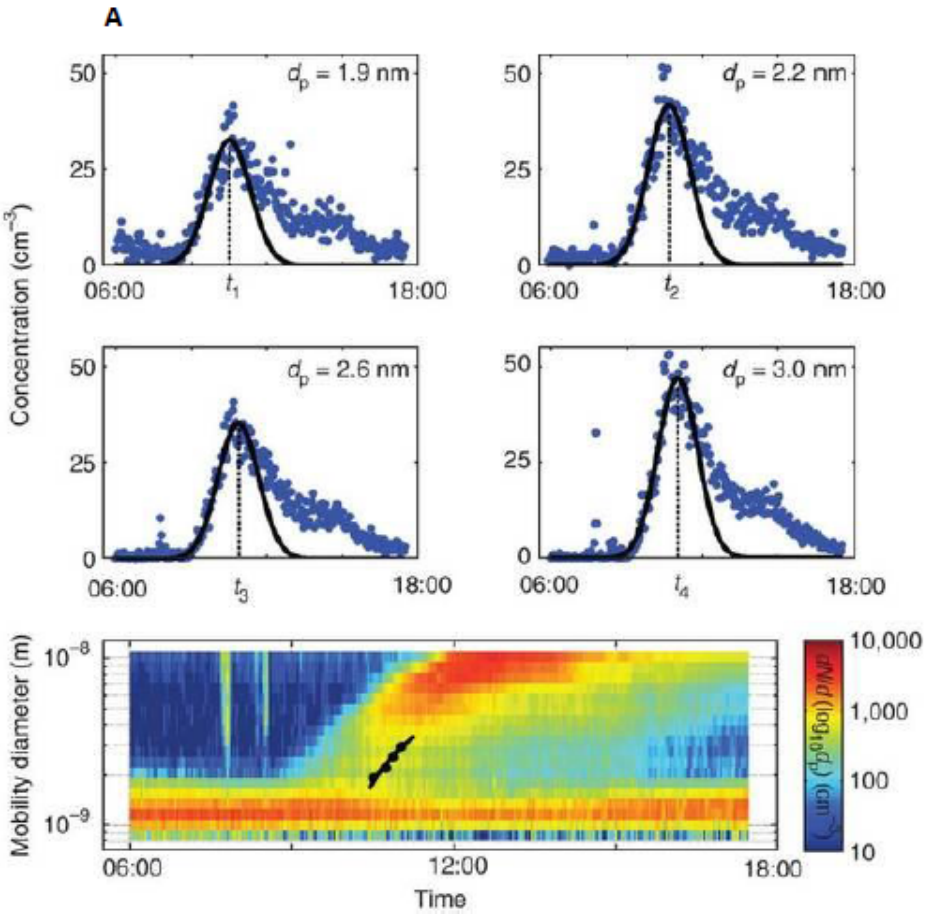

Fig. 7A: An example of particle growth determination from particle size distribution plots using above described maximum concentration function method. Figure taken from Kulmala et al. (2012).

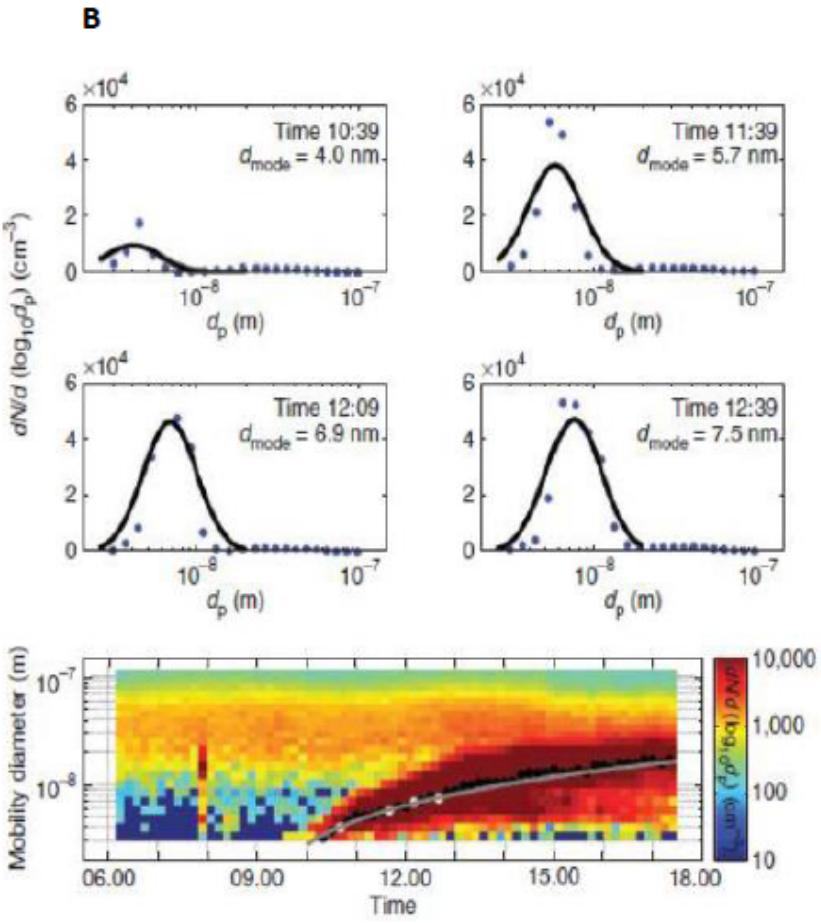

Fig. 7B: An example of particle growth determination from particle size distribution plots using above described log-normal distribution function method. The growth rate is determined by a linear least-square fitting to the data points obtained from treatment of the size distributions. Figure taken from Kulmala et al. (2012).

It is neccesary to distinguish between the terms nucleation rate and particle formation rate. The particle formation rate (cm^{-3} s^{-1}) is commonly refered as J_2 or J_3 (depending on the size of the smallest detectable particles) and presents the rate at which particles of a certain size are being formed in the atmosphere. The nucleation rate presents the rate at which critical clusters (i. e. clusters which have the same probability to grow or to decay) of size ~1.5 nm are being formed. Coagulation by pre-existing particles scavenge a certain fraction of formed critical clusters as they grow to larger sizes; therefore the true nucleation rate is always larger then observed particle formation rates (Kulmala et al., 2012). When taking into account condensational growth and coagulation scavenging, the relation between atmospheric nucleation rate J^*

and measured formation rate J_{dp} of smallest detectable particles of d_p can be found (Kerminen and Kulmala, 2002).

1.3 Growth of atmospheric nanoparticles

Atmospheric nucleation is followed by the growth of newly formed particles. The fate of nucleated particles is governed by the competition between scavenging by pre-existing aerosol and growth to larger sizes. The initial growth is the crucial process determining the fraction of nucleated particles growing to cloud condensation nuclei sizes (~50 nm and larger) and hence subsequently participating in cloud formation processes (Dusek et al. 2006; Andreae and Rosenfeld 2008; Kulmala and Kerminen, 2008). The vast majority of particle growth rates observed during atmospheric measurements lies in the range of 1–10 nm h^{-1} and it takes about 12 - 72 hours before the nucleated particles grow to cloud condensation nuclei sizes (Kulmala et al., 2004). Occasionally, growth rates up to 100 nm h^{-1} are reported from coastal zones or industrial plumes. Many recent studies have suggested that sulphuric acid plays a key role in the atmospheric nucleation and also participates in subsequent growth of newly formed particles (Sipillä et al, 2010; Brus et al. 2011; Kirkby et al., 2011). However, growth rates based entirely on the condensation of sulphuric acid vapour greatly underestimate the growth rates observed in atmospheric measurements (Sihto et al, 2006, Nieminen et al., 2010), mainly because low-volatile organic species are responsible for up to 90% of the observed growth (Makëla et al., 2001, Smith et al., 2008).

The processes governing the growth of particles in a nucleation mode size range are condensation, self-coagulation and coagulation scavenging (Leppä et al., 2011). After formation, the particles grow by multiple condensations of different organic and inorganic species (Kulmala, 2003). The condensation rate of different chemical compounds is influenced by the Kelvin effect, which increases the equilibrium vapour pressure with decreasing particle size and increasing molar volume of the condensing species. According to the Nano-Köhler theory (Kulmala et al., 2004), the non-volatile or low-volatile compounds are responsible for the initial growth of freshly formed particles and the condensation of more volatile components increases with increasing particle size (Zhang et al., 2004). The coagulation between particles in the same size mode (i.e. self-coagulation) increases the mean particle diameter and decreases the number concentration in this mode. Unless the particle number concentration of freshly formed particles is 1×10^6 cm^{-3} or higher, self-coagulation is only a minor contributor to the initial growth of nucleation mode particles (Kulmala and Kerminen, 2008). The coagulation scavenging of nucleation

mode particles with pre-existing larger particles results in a decrease of the total particle number concentration and an increase of the diameter describing the whole aerosol population. The growth of nucleation mode particles due to coagulation scavenging is thus only apparent, because none of the particles in this mode grow larger (Leppä et al., 2011).

2 Methodology

A brief description of various experimental devices and common instrumentation for investigation of nucleation will be given in this chapter. An overview of recent findings from nucleation laboratory experiments will be also outlined.

2.1 Experimental devices for nucleation laboratory experiments

Several experimental devices have been developed in the past decades to study the nucleation process. These devices enable to measure nucleation rates spanning more than 20 orders of magnitude from 10^{-4} to 10^{17} cm^{-3} s^{-1}. The main difference between the various methods is the mechanism used to achieve the supersaturated state. In a single component system, the preffered approach to reach supersaturation is by cooling the vapour either by temperature gradient or by adiabatic expansion. In multi component systems, the supersaturated state is typically obtained by turbulent mixing of vapours or in situ production of one the nucleating vapour by photochemical reactions.

Adiabatic expansion devices

These experimental devices are based on vapour cooling by a rapid adiabatic expansion, which causes supersaturation and initiates nucleation. One of these devices is a shock tube (Peters, 1982; Luijten et al., 1997), in which a diaphragm separates high pressure vapour/carrier gas mixture from section maintained at low pressure (Fig. 8). Rupturing the diaphragm leads to the adiabatic expansion with subsequent supersaturation and nucleation. Another expansion based method is a fast expansion chamber, where a piston is moved to initiate adiabatic expansion of vapour/carrier gas mixture. This method has been used to measure nucleation rates of a single component systems i.e. water, alcohols, toluene or binary mixtures, such as water and ethanol system (Wagner et al., 1981; Strey et al., 1986; Viisanen et al., 1994).

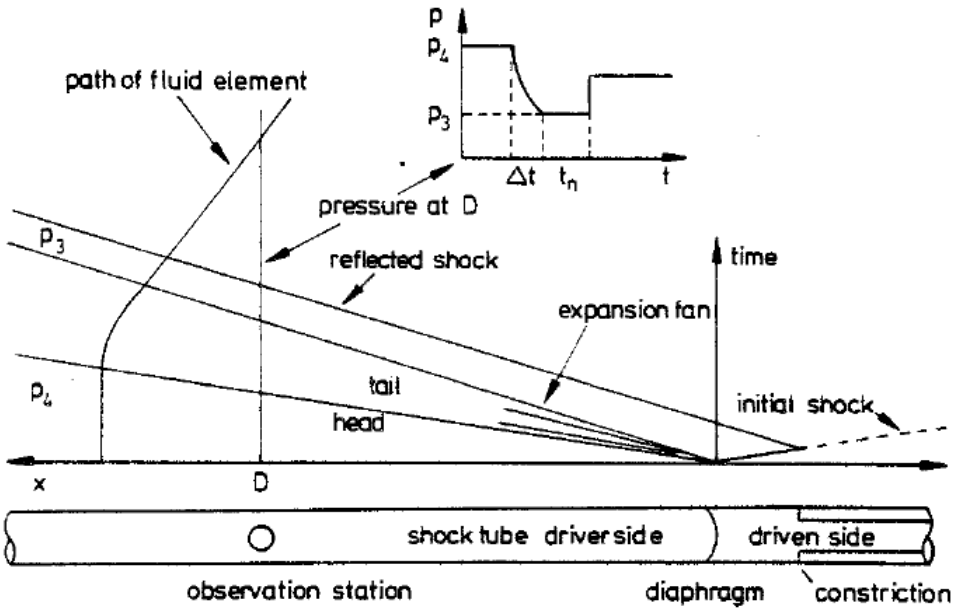

Fig. 8: Schematic description and operational principle of a shock tube. Figure taken from Peters (1983).

Diffusion chambers

These devices work continuously and can be used to measure nucleation rates of both single and multi component systems (Fig. 9). Diffusion chambers consist of two plates; the bottom one is heated and covered with a liquid pool and the upper one is cooled. The supersaturation is achieved by establishing the temperature gradient between the two plates. The liquid evaporates from the bottom plate, diffuses towards the upper plate and its partial pressure decreases with the distance. The temperature difference between the plates can be adjusted in order to obtain desired levels of supersaturation. When supersaturated, the vapour starts to nucleate and the formed particles grow to larger sizes. When the particles reach a certain size, they start to settle down and are then detected and counted using a laser beam. This method has been used to measure critical supersaturations and nucleation rates of both individual and mixed vapors (Katz and Ostermier, 1967; Heist and He, 1994; Brus et al., 2005; Brus et al., 2008).

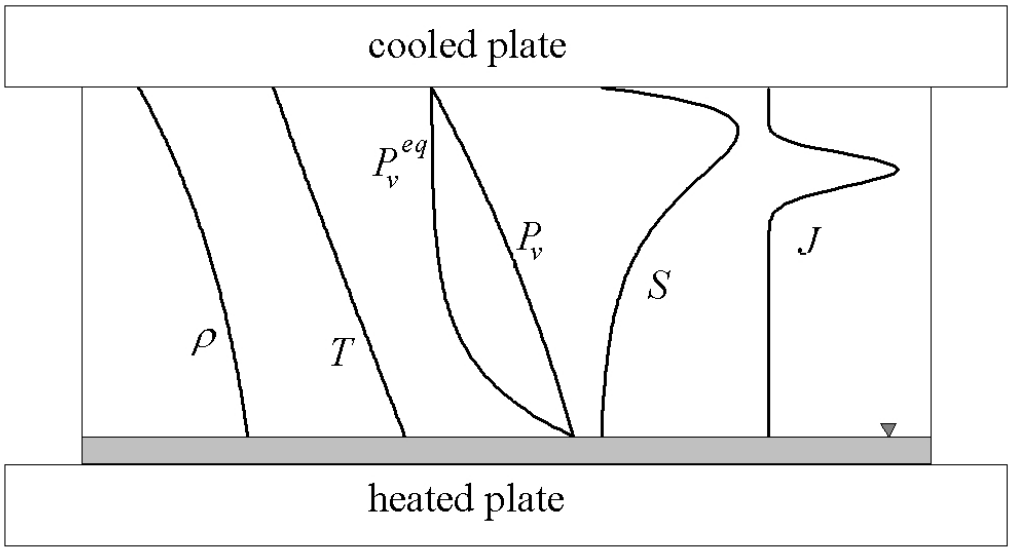

Fig. 9: Operation principle of a diffusion chamber, where ρ is density profile; T is temperature profile; P_v^{eq} is saturation pressure curve; P_v is pressure profile; S is saturation curve and J is nucleation rate curve. Figure taken from Ždímal (1998).

Flow tubes

The flow tubes are also based on the diffusion principle. In these devices, two or more carrier gas flows are saturated with the nucleating vapour in saturators and then are turbulently mixed in the next section (Fig. 10). After mixing, the total flow is then introduced into the flow tube, where the particles nucleate and grow. Alternatively, the nucleating compound can be chemically or photochemically produced in situ. Major drawback of these devices is the diffusion of nucleating species towards the flow tube walls, which can deplete the initial concentration significantly. For example the molecules of H_2SO_4 are lost on almost every collision with the surface and corrections are therefore necessary to obtain the residual concentration. Neverthless, flow tubes are widely used to investigate the atmospherically important binary and ternary nucleation systems (Ball et al., 1999; Benson et al., 2008; Benson et al, 2009; Berndt et al., 2010; Benson et al., 2011, Brus et al., 2011).

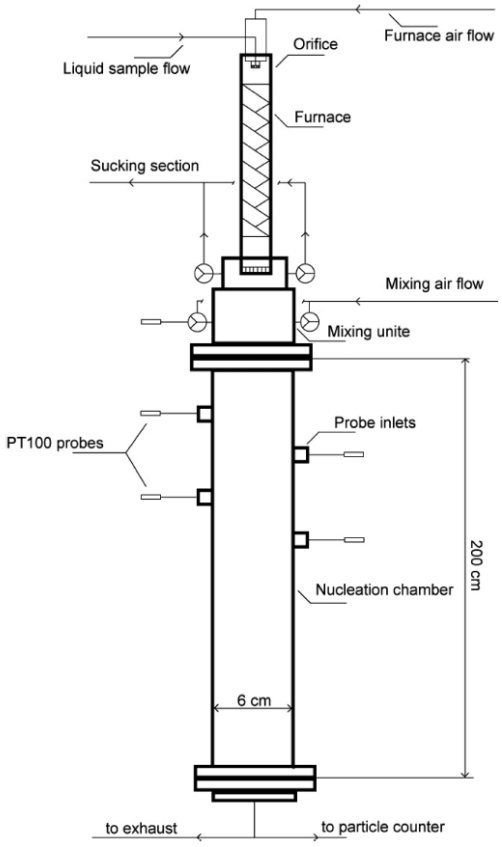

Fig. 10: Schematic description of a flow tube. A furnace was used in this experimental setup to produce gas phase H_2SO_4 via evaporation of a liquid H_2SO_4 solution of a known amount and concentration. Figure taken from Hermann et al. (2010).

A laminar co-flow tube (LCFT) presents a special type of the flow tubes. This device has been recently developed in the Laboratory of Phase Transition Kinetics in the Institute of Thermomechanics, v. v. i. in collaboration with the Laboratory of Aerosol Chemistry and Physics in the Institute of Chemical Processes Fundamentals, v. v. i. of the Academy of the Sciences of the Czech Republic. This flow tube has been primarely designed to study the H_2SO_4 - H_2O nucleation. The whole experimental setup consists of mixture preparation device and the flow tube. The reacting mixture is prepared in a set of 3 saturators allowing arbitrary involvement of a third compound in H_2SO_4 - H_2O nucleation. The carrier gas flows saturated with desired vapour are introduced into the flow tube, which has a unique design. The laminar co-flow tube consists of two coaxial tubes of radii d (inner tube) and D (outer tube), see Fig. 11.

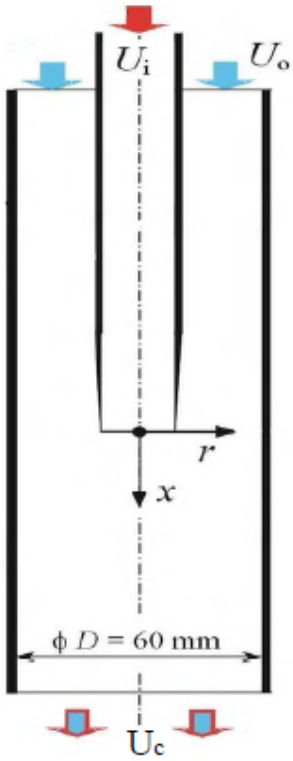

Fig. 11: The schematic description of laminar co-flow tube design. U_i presents the laminar profile velocity in the inner tube, U_o presents the laminar profile velocity in the outer tube and U_c presents the laminar profile velocity in the co-flow region. The corresponding coordinates are also depicted. Figure taken from Krejčí (2010).

One stream of the carrier gas saturated with H_2SO_4 flows in the inner tube, while the second stream of the carrier gas saturated with H_2O flows in the annulus between inner and outer tube in paralel direction. Downstream from the inner tube end, both streams flow together in a duct of radius D. The length of inner tube L_i and outer tube L_o are sufficiently long to ensure that the fully developed laminar profiles are established in each of the tubes. The magnitudes and ratio of the flow rates are mantained to keep the flow laminar behind the opening of the inner tube. In the co-flow region, the reacting vapour from the inner tube flow diffuses into the gas stream coming from the inner tube and vice versa. In the region where the concentration of both vapors is sufficiently high, nucleation is initiated. The nucleation rate is determined using the computational fluid dynamics (CFD) model, which accounts for the flow and concentration fields in the LCFT of the known mixture composition, the LCFT operating conditions and the detected number concentration of the nucleated particles. The main advantage of this design is the limitation of H_2SO_4 wall losses in case of short residence times in the flow tube, which ensures sufficient $[H_2SO_4]$ for nucleation and subsequent particle growth.

The whole experimental setup has been recently tested in the Laboratory of Aerosol Chemistry and Physics of the Institute of Chemical Processes Fundamentals and a series of nucleation experiments has been succesfully performed. A major improvement of the original setup presents the use of novel device to detect nucleated particles - Particle Size Magnifier (PSM 09, Airmodus), which enables detection of particles as small as ~1 nm in mobility diameter (Vanhanen et al., 2011). This device thus detects all nucleated particles and the resulting particle number concentration is not influenced by the particle growth. A paper summarizing experimental setup and firts results in now in preparation. Owing to the fact that the results from this device have not been published yet, the experimental results from the LCFT have therefore not been included in this thesis.

2.2 Instrumentation for field and laboratory experiments

Condensational Particle Counter

Investigation of nucleation in some laboratory and most of field observations is based on measurements of particle number concentration and size distribution. The condensation technique is widely used method to determine the aerosol particle concentration (Kulmala et al., 2012). The working principle of Condensational Particle Counter (CPC) is to expose the aerosol sample to a supersaturated vapour (Fig. 12). The vapour condensates on the particles, which subsequently grow to sizes large enough to be observed optically. These particle detection devices, which are used to measure particle number concentration, are characterized by a certain cut-off size. The cut-off size is the diameter of particles which the device detects with 50 % efficiency. The cut-off size and the steepness of the cut-off curve are crucial factors characterizing the instrument. The commonly used CPCs have the lower detection limit typically between 3 and 10 nm, however recently developed instrumentation enables detection of particles as small as 1 nm. The modern CPCs are suitable for field measurements due to their fast response time and continuous flow rate.

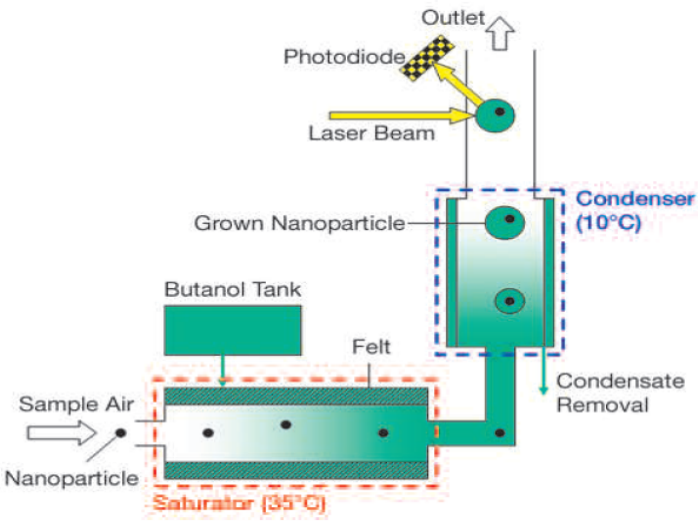

Fig. 12: Schematic description of operational principle of Condensational Particle Counter. Figure taken from: http://www.grimmaerosol.com/phocadownload/Datasheets/GrimmAerosolTechnikNanoMobileCPC.pdf

Differential Mobility Particle Sizer

Differential Mobility Particle Sizer (DMPS), a commonly used device to measure particle size distributions, consists of a Differential Mobility Analyzer (DMA), which transmits only particles with a certain electrical mobility and CPC, which counts these particles (Fig. 13). DMA separates electrically charged particles according to their electrical mobility, which governs the move of charged particle across the electrical field. Before entering the DMA, the particles pass through a neutralizer, which brings them into a well-defined charge distribution (a Boltmann distribution of positive and negative charged particles). The DMA is a cylindrical capacitor, which consist of 2 electrodes. The incoming sample flow with polydisperse aerosol is directed between the electrodes. At a certain voltage, only particles with corresponding electrical mobility reach the gap at the outlet of the DMA, pass it and are subsequently counted. The obtained data have to be inverted. The data inversion process transforms electrical mobility into particle diameter and accounts for numerous factors i.e. flow rate, scan time, transfer function of the DMA etc. As a result of data inversion, the particle size distribution is obtained. By changing the DMA voltage, the desired particle diameter can be changed and the particle size distribution of aerosol sample can be obtained in a wide size range.

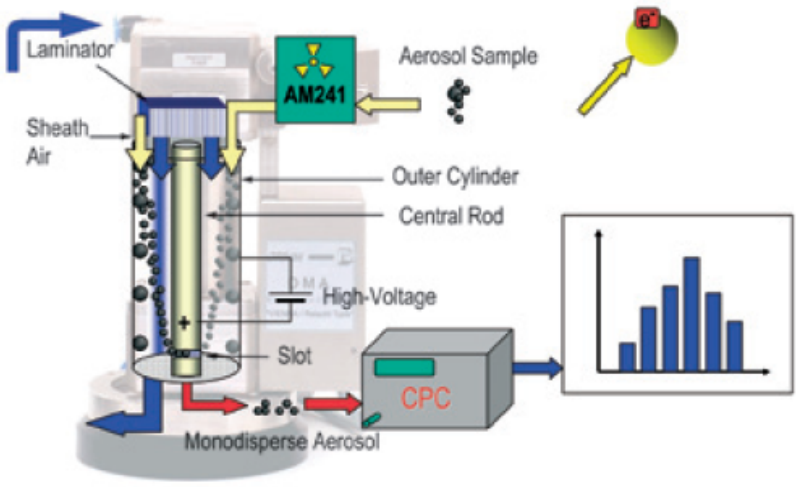

Fig. 13: The schematic description of operational principle of Differential Mobility Particle sizer consisting of Differential Mobility Analyzer (DMA) and a CPC. Figure taken from http://www.grimmaerosol.com/phocadownload/Datasheets/E_Catalogue_Nano_2014.pdf

2.3 Laboratory studies of atmospherically relevant nucleation systems

Technical challenges

The binary nucleation of H_2SO_4 and H_2O presents one of the most relevant atmospheric nucleation systems (Benson et al., 2008). It is widely accepted that the atmospheric NPF is dominated by ternary nucleation involving third species; amines, NH_3 or organic species are likely compounds involved in these processes. Understanding the impact of a third species on the overall process requires detailed knowledge of the system being affected i. e. binary nucleation of H_2SO_4 and H_2O. Although the nucleation of H_2SO_4 and H_2O has been experimentally investigated for a long time, the number of studies on this system is limited. Moreover, there are quite large discrepancies of measured nucleation rate J (cm^{-3} s^{-1}) and the dependency of J on [H_2SO_4] reported from different studies. There are several experimental aspects which directly contribute to the uncertainties in measured J and [H_2SO_4] needed for nucleation and cause that experimental results are often not reproducible between different studies.

Two main methods to produce the gas phase H_2SO_4 in these experiments are used: in situ production of H_2SO_4 is achieved via reaction of OH^- radicals with SO_2 inside the reactor providing continuous production of

H_2SO_4 or an acid saturator is used to produce H_2SO_4 vapour by passing a stream of a carrier gas over the liquid sample. Different paths to produce H_2SO_4 vapour deteriorate the comparability of different studies (Young et al., 2008). To illustrate how a slight modification of H_2SO_4 production method influences the H_2SO_4 concentration profile in a flow tube, two experiments using photochemical reaction of OH^- with SO_2 are presented (Fig. 14A and 14B). In case of the first experiment (Berndt et al., 2010), the flow tube was illuminated by a UV lamp to generate OH^- radicals by photolysis of water vapour to react with SO_2 and H_2SO_4 was therefore continuously produced in situ. The resulting H_2SO_4 concentration profile was quite uniform (Fig. 14A). In the second experiment (Young et al., 2008), the nucleating gases were produced in a photolysis cell and mixed before entering the flow tube and the H_2SO_4 profile inside the tube is very different from the first experiment. [H_2SO_4] exhibits significant steady decay owing to wall loses of H_2SO_4 (Fig. 14B).

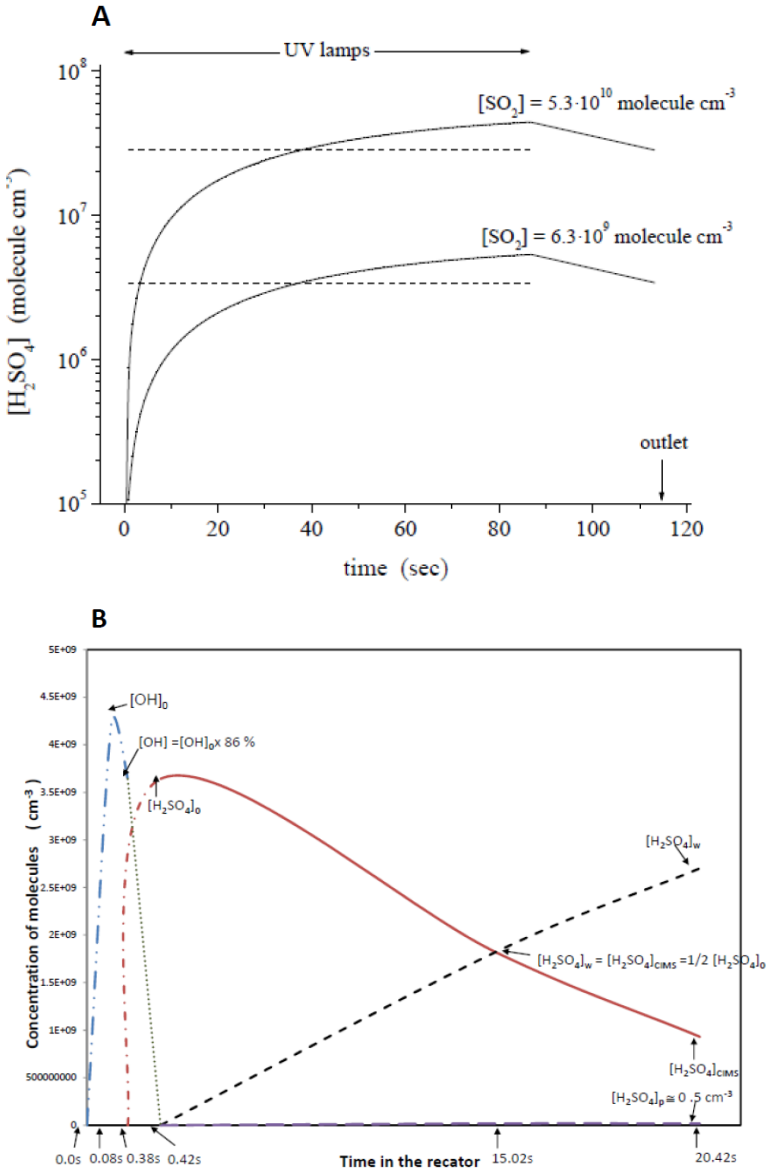

Fig 14A: The concentration profile of H_2SO_4 in a flow tube, where H_2SO_4 was produced photochemically in situ. The dashed lines present the average H_2SO_4 concentrations at different initial concentrations of SO_2. Figure taken from Berndt et al. (2010). 14B: Concentration profile of H_2SO_4 in a flow tube, where the reacting gases containing H_2SO_4 were mixed before entering the flow tube. The solid red line presents the $[H_2SO_4]$ in the flow tube, whereas the dashed line presents the wall losses of H_2SO_4. Figure taken from Young et al. (2008).

Another challenge in nucleation experiments presents the quantification of H_2SO_4 wall losses and correct determination of $[H_2SO_4]$ in the flow tube. Since the H_2SO_4 molecules attach to the inner surfaces of experimental devices during experiments, the corrections of the initial $[H_2SO_4]$ are necessary in order to determine the residual $[H_2SO_4]$. The initial $[H_2SO_4]$ can be measured with mass spectrometry using a Chemical Ionization Mass Spectrometer (CIMS) (Young et al., 2008) or calculated from the estimated $[OH^-]$ and $[SO_2]$ in the reactor (Benson et al., 2011). The H_2SO_4 wall losses are commonly calculated from a first order rate equation (Hanson and Eisele, 2000) assuming that wall loss is a diffusion-limited process or are determined from the difference in $[H_2SO_4]$ measured at the beginning and the end of the nucleation reactor using CIMS. Since nucleation is a non-linear proces and J is extremely sensitive to precursors concentrations (H_2SO_4 and H_2O), the correct determination of precursors concentration is of a great importance.

Another important aspects of nucleation experiments are detection limit of particle detector and residence time (Berndt et al., 2011; Sipilä et al., 2010). Because the growth of particles following their formation governs the measured particle concentration, sufficient residence time is required to ensure that the nucleated particles grow to detecteble sizes. Using inappropriate particle detector, which is unable to detect small particles, may result in underestimation of measured N and subsequent incorrect determination of J. Another major limitation of H_2SO_4 - H_2O nucleation studies is unavoidable presence of impurities like NH_3, amines or organic compounds in the system since these chemical species are ubiquitous in the ambient environment. Many studies report that these compounds enhance nucleation very effectively even in trace concentrations (Ball et al., 1999; Berndt et al., 2014). Although high purity H_2SO_4 and H_2O and different scrubbers are routinely used during experiments in order to avoid unwanted impurities, the presence of these compounds at low concentrations cannot be totally excluded in the case of laboratory measurements. All these above mentioned experimental parameters directly influence the measured nucleation rate J and corresponding $[H_2SO_4]$ and contribute to the discrepancies of measured J reported from different studies.

Overview of laboratory studies of H_2SO_4 - H_2O nucleation

Early studies of binary H_2SO_4 and H_2O nucleation, conducted from 1970s to early 1990s, were performed using expansion chamber (Reiss et al., 1976), thermal diffusion chamber (Mirabel et al., 1978) and turbulent mixing chamber (Wyslouzil et al., 1991; Viisanen et al., 1997). The gas phase H_2SO_4 in these experiments was produced by evaporation of a liquid solution and $[H_2SO_4]$ in

the nucleation chamber was not measured directly, but calculated based on thermodynamic data and various assumptions. The threshold nucleation rate J of 1 cm^{-3} s^{-1} obtained from these experiments performed in temperature (T) range from 283 to 303 K corresponds to $[H_2SO_4]$ in nucleation chamber from 10^{10} to 10^{11} molecule cm^{-3}. First study, where $[H_2SO_4]$ in the nucleation reactor was measured directly using CIMS was performed in 1999 (Ball et al., 1999) and the residual $[H_2SO_4]$ was corrected for wall losses. The particle number concentration was measured using Ultrafine Condensational Particle Counter (UCPC) with lower detection limit of ~3 nm. The threshold nucleation rate J of 1 cm^{-3} s^{-1} measured at T 295 K corresponds to $[H_2SO_4]$ 6×10^{10} molecule cm^{-3}. Several later studies, which also produced H_2SO_4 vapour from a liquid sample, report nucleation rate J of 1 cm^{-3} s^{-1} to occur under similar $[H_2SO_4] \sim 10^9$ to 10^{10} molecule cm^{-3} (Zhang et al, 2004; Brus et al., 2011). The nucleation rates J, obtained from these experiments, exhibit similar slope of dependence of J on the $[H_2SO_4]$, as shown in Fig. 15.

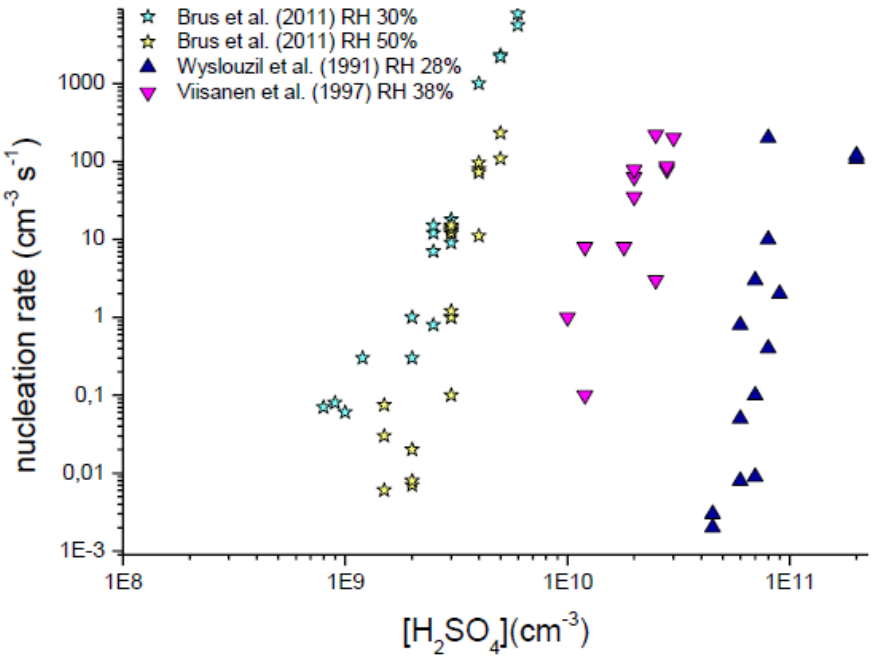

Fig. 15: The nucleation rates, obtained from studies using liquid sample to produce gas phase H_2SO_4 in experimental devices, exhibit similar slope of dependence of J on $[H_2SO_4]$. Data taken from Wyslouzil et al. (1991), Viisanen et al. (1997) and Brus et al. (2011).

Substantially different results are obtained from studies, where H_2SO_4 is produced in situ via reaction of OH^- radicals with SO_2 inside the flow tube

(Young et al., 2008; Benson et al., 2008). The threshold nucleation rate J of 1 cm^{-3} s^{-1} reported in these studies was observed at $[H_2SO_4] \sim 10^7$ molecule cm^{-3}, which is close to typical atmospheric $[H_2SO_4]$ measured during new particle formation. Similar results are also reported from later studies using photochemically produced H_2SO_4 (Sipilä et al., 2010; Berndt et al., 2011; Berndt et al., 2014). The disagreement between studies conducted with H_2SO_4 produced from liquid sample and with H_2SO_4 produced in situ was attributed to different H_2SO_4 concentration profiles in nucleation reactor. In case of photochemical in situ production, the H_2SO_4 profile is almost uniform and the growth of nucleated particles to detectable sizes is sufficient. In contrary, in the case of a liquid sample, the H_2SO_4 concentration decreases rapidly with time owing to significant wall losses and the particle growth is therefore limited.

A recent study (Sipilä et al., 2010) using high efficiency particle detection device enabling detection of particles as small as ~1.5 nm reports for the first time the binary H_2SO_4 - H_2O nucleation to occur at atmospherically relevant $[H_2SO_4] \sim 10^6$ molecule cm^{-3}. Sipilä et al. (2010) also observed the experimental slope of $d(\ln J)/d(\ln[H_2SO_4])$, which according to nucleation theorem corresponds to number of H_2SO_4 molecules in a critical cluster, to range from 1 to 2, which is in agreement with most atmospheric observations (Sihto et al., 2006; Riipinen et al., 2007). A nucleation rate of unity was measured at $[H_2SO_4] \sim 1.1 \times 10^6$ molecule cm^{-3} which is also in accordance with most atmospheric measurements. In their study H_2SO_4 was produced both in situ and from a liquid sample and the observed nucleation rates were found to be independent of the source of gaseous H_2SO_4. This observation was attributed to use of high efficiency particle counters with lower detection limit ~1.5 nm. Fig 16. shows the comparison of experimental results from studies performed under different methods to produce gas phase H_2SO_4 (liquid sample vs. in situ production). As mentioned previously, the differences among experiments may be attributed to different technical and experimental aspects, which directly contribute to the discrepancies of measured *J*.

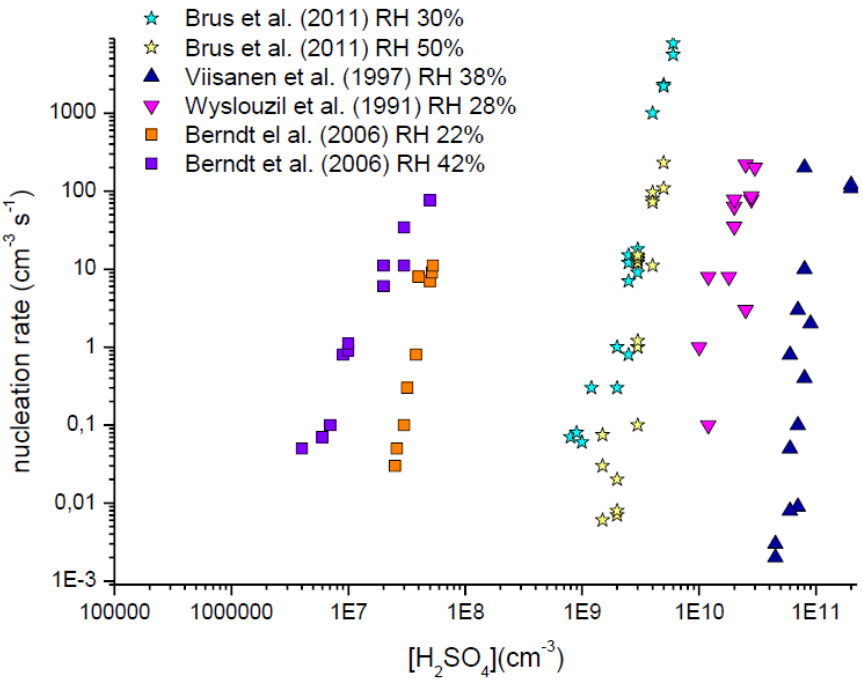

Fig. 16: The nucleation rates obtained from studies using different approaches to produce gas phase H_2SO_4 in experimental devices are compared here. All studies show similar slope of dependence of J on $[H_2SO_4]$, however J obtained from experiments using in situ (photochemically) produced H_2SO_4 (Berndt et al., 2006) is close to $[H_2SO_4]$ observed in atmospherical measurements. Data taken from Wyslouzil et al. (1991), Viisanen et al. (1997), Berndt et al. (2006) and Brus et al. (2011).

Laboratory studies of H_2SO_4 - H_2O nucleation involving ternary species

The experimental studies of binary H_2SO_4 and H_2O nucleation serve as a basis for investigation of third species enhancement of this process. Recent study revealed that binary H_2SO_4 and H_2O nucleation will proceed at extremely low rates in atmospheric boundary layer, which implies that additional species are therefore involved in atmospheric new particle formation (Kirkby et al., 2011). Atmospheric nucleation is known to be promoted by the presence of third species such as NH_3, amines or oxidized organic compounds (Kulmala et al., 2004). Ammonia is ubiquitous in the atmosphere and has typical mixing ratio between 0.1 and 10 ppb. Interaction with H_2SO_4 creates ammonium sulfate and bisulfate salts and therefore greatly lowers the partial pressure of H_2SO_4. NH_3 was found to significantly enhance H_2SO_4 and H_2O nucleation up to a factor 1000 during laboratory experiments (Ball et al., 1999; Benson et al., 2011; Berndt et al., 2014). However, the experimental slopes of $d(\ln J)/d(\ln[H_2SO_4])$ as well as $[H_2SO_4]$ required for nucleation were significantly higher than those

observed in atmosphere, suggesting that other species might be involved in atmospheric nucleation.

Amines, organic derivatives of NH_3, are likely candidates. They are strong bases and form more stable salts and complexes with H_2SO_4 (Kurten et al., 2008). Amines are consistently identified to be more effective in H_2SO_4 and H_2O nucleation enhancement compared to NH_3 at similar concentration levels (Berndt et al., 2010; Berndt et al., 2014). However amines are in atmosphere present at much lower concentrations compared to NH_3 and therefore, on a global scale, their impact on atmospheric nucleation might be limited. Several studies also investigated the effect of organic acids, because the organic compounds were identified to be present in the freshly nucleated atmospheric particles. A large fraction of low volatility organic species found in particulate phase is formed via photo-oxidation of volatile compounds. Several organics acids (benzoic, p-toluic, m-toluic) were found to increase both nucleation rate and growth of newly formed particles in experimental study (Zhang et al., 2004) and also atmospheric observations imply that organic compounds play an important role in early growth of aerosol particles (Kulmala et al., 2013). However, it is not obvious at the moment how the organic oxidation products take part in the atmospheric nucleation since the current concept of this process is based on interaction of a strong acid (H_2SO_4) with a strong base (NH_3 or amines) (Berndt et al., 2014). To sum up, it still remains unclear which nucleation mechanism is dominant in the atmosphere (Kulmala et al., 2004), mainly because the preferred new particle formation mechanism depends on the atmospheric conditions and geographical location.

3 Laboratory study of H_2SO_4 - H_2O nucleation and particle growth

In this chapter are presented findings of laboratory experiments of nucleation of H_2SO_4 and H_2O and growth behaviour of formed particles. First the comprehensive description of the experimental setup, operational principle of flow tube used and typical conditions of the experiments are outlined. Detailed description of a model, which predicts the growth of nucleated particles formed in the experiments then follows. Finally, an overview of experimental results and particle growth is given in the following section.

3.1 Measurements and experimental setup

The experiments of the homogeneous nucleation of H_2SO_4 and H_2O presented here were carried out in a laminar flow tube at the Finnish Meteorological Institute, Helsinki, Finland. The detailed description of the flow tube design and performance is given in Brus et al. (2010) and Neitola et al (2013). The experimental setup used in our measurements consists of four main parts: a saturator, a mixing unit, laminar flow tube and a particle detection system Differential Mobility Particle Sizer (DMPS) and Ultrafine Condensational Particle Sizer (UCPC) and is presented in Fig. 17. The laminar flow tube is vertically mounted cylindrical tube made from stainless steel of total length of 200 cm with an inner diameter of 6 cm. The whole tube was insulated and kept at a constant temperature with a liquid circulating bath (Lauda RK-20). The tube consists of two interchangeable 1 meter long parts; one of them is equipped with 4 ports in the distance of 20 cm from each other. The gas phase H_2SO_4 was produced by passing a stream of a carrier gas through a saturator filled with 97% H_2SO_4. The saturator is a horizontal iron cylinder with Teflon insert of inner diameter 5 cm and was thermally controlled with a liquid circulating bath (LAUDA RC 6). The temperature inside the saturator was measured with a PT100 resistence thermometer (± 0.05 K). A stream of the carrier gas saturated with H_2SO_4 was introduced into the mixing unit made of Teflon and turbulently mixed with a second stream of humidified carrier gas. The gas mixture was then introduced into the flow tube. The mixing unit was kept at room temperature and was not insulated. The mixing unit dimensions are: outer diameter = 10 cm, inner diameter = 7 cm and height = 6 cm. The second stream of the carrier gas – the mixing air - was humidified with one pair of Nafion humidifiers (Perma Pure MH-110-12) connected in parallel, where the total flow of the mixing air was split into half for longer residence time and better humidification in both humidifiers. Ultrapure water (Millipore,

TOC less than 10 ppb, resistivity 18.2 MΩ cm^{-1} at 25°C) was circulating in both humidifiers, which were temperature controlled with a liquid circulating bath (Lauda RC-6 CS). Both lines of the carrier gas (saturator air and mixing air) were controlled by a mass flow controller (MKS type 250) to within ±3 %. The relative humidity in the flow tube was measured at the centre and the far end with two humidity and temperature probes (Vaisala HMP37E) and a humidity data processor (Vaisala HMI38) to within ± 3 %.

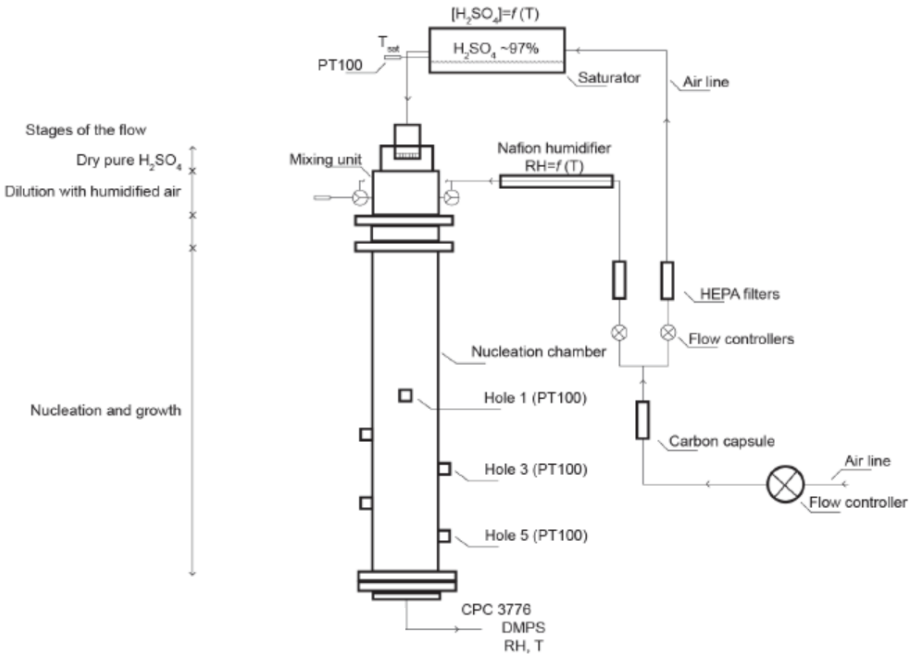

Fig. 17: The schematic description of experimental setup used in laboratory measurements of H_2SO_4 - H_2O nucleation.

Experimental conditions

The nucleation rates and subsequent growth of newly formed nanoparticles under different conditions were investigated. The measurements were performed at relative humidities of ~1% and ~30%, presented here as dry and wet conditions, respectively. The flow tube was kept at constant temperature during the measurements and the nucleation temperatures investigated were 283, 293 and 303 K. Dry and particle-free air served as the carrier gas in this study. Both lines of the carrier gas (saturator and mixing flows) were controlled by a mass flow rate controller and the total gas flow inside the tube was maintained to provide four residence times in the tube: 30, 45, 60 and 90 s. H_2SO_4 vapour was produced from a liquid reservoir by passing a stream of carrier gas through a saturator filled with H_2SO_4 and the initial H_2SO_4 concentration in the flow tube ranged from 2×10^8 to 1.4×10^{10} molecule cm^{-3}.

Although no measurement of the NH_3 concentration was done during the experiments, NH_3 was assumed to be present in the system (Brus et al., 2011; Neitola et al., 2013). Since NH_3 and other chemical compounds are ubiquitous in the ambient environment, the presence of these species at very low concentrations cannot be excluded in the case of laboratory measurements (Benson et al., 2011; Kirkby et al., 2011). The nucleated nanoparticles in our experiments containing sulphuric acid and water were thus partially neutralized to $(NH_4)_2SO_4$ and $(NH_4)HSO_4$ during the measurements. The extent of the partial neutralization is dependent on the particle size and relative humidity and is highest for the smallest particles and highest relative humidities (Biskos et al., 2009). In a study with identical experimental setup and comparable experimental conditions (Neitola et al., 2013), the concentration of NH_3 was measured with the online ion chromatograph Monitor for AeRosols and Gases in ambient Air (MARGA; Metrohm Applikon) (ten Brink et al., 2007). The average NH_3 concentrations were 60 pptv under dry conditions (relative humidity ~1%) and 126 pptv under wet conditions (relative humidity ~30%). These concentrations did not change significantly in the course of measurements under different conditions and thus the NH_3 was assumed to originate from the carrier gas and from the ultrapure water used to humidify the mixing flow.

Determination of H_2SO_4 concentration

The temperature of the H_2SO_4 saturator was increased stepwise in 7 increments of 5 K during each measurement resulting in a gradually growing concentration of H_2SO_4 in the flow tube. In order to determine the concentration of gas-phase H_2SO_4 in the tube, the saturation vapour pressure of H_2SO_4 in the saturator was calculated first using the following equation (Kulmala and Laaksonen, 1990):

$$\ln p_{SA} = \ln p_{SA,0} + \frac{\Delta Hv(T_0)}{R}\left[-\frac{1}{T}+\frac{1}{T_0}+\frac{0{,}38}{T_c - T_0}\times\left(1+\ln\frac{T_0}{T}-\frac{T_0}{T}\right)\right], \qquad (2)$$

where p_{SA} is the saturation vapour pressure (atm) of H_2SO_4 at a temperature T (K), $p_{SA,0}$ is the saturation vapour pressure of H_2SO_4 at the temperature T_0 = 360 K (Ayers et al., 1980), ΔH_v is the enthalpy of vaporization of H_2SO_4, T is the temperature of the saturator and T_c is the critical temperature (T_c = 905 K). Equation (2) is commonly used in studies on binary or ternary nucleation theories and in their parametrizations (Vehkamäki et al., 2002; Merikanto et al., 2007). Also, its accuracy has been investigated by Neitola et al. (2013) who reported a comparison of H_2SO_4 concentrations calculated from H_2SO_4 saturation vapour pressure using Eq. (2) and experimental concentrations

measured with online ion chromatograph Monitor for AeRosols and Gases in ambient Air (MARGA; Metrohm Applikon), displaying good agreement (Fig. 18).

The amount of substance of sulphuric acid (moles) in the pre-defined volume of 1 cm^3 in the acid saturator was determined using the ideal gas equation of state:

$$n = \frac{pV}{RT} \quad (3)$$

where p is the saturation vapour pressure of H_2SO_4 (Pa), V is pre-defined volume of 1 cm^3, R is the ideal gas constant (J mol^{-1} K^{-1}) and T is the temperature of the acid saturator (K). The calculated number of moles of H_2SO_4 was multiplied by Avogadro constant A_v (6.02×10^{23}) to obtain the sulphuric acid vapour concentration in the saturator $[H_2SO_4]_{SAT}$ (molecule cm^{-3}):

$$[H_2SO_4]_{SAT} = nA_v \quad (4)$$

The H_2SO_4 vapour concentration in the flow tube $[H_2SO_4]_0$ was then calculated by applying the mixing law, i.e. dividing the sulphuric acid vapour flux leaving the saturator by the total flow (saturator flow Q_{SAT} and the mixing flow Q_{MIX}) in the laminar flow tube:

$$[H_2SO_4]_0 = \frac{[H_2SO_4]_{SAT} Q_{SAT}}{Q_{SAT} + Q_{mix}} \quad (5)$$

The initial concentrations $[H_2SO_4]_0$, at which newly formed particles were detected during the experiments, covered the range from 2×10^8 to 1.4×10^{10} molecule cm^{-3}. The wall losses of H_2SO_4 in the flow tube were assumed to be a diffusion controlled first-order rate process, which can be described by a simple equation given by Hanson and Eisele (2000):

$$[H_2SO_4]_t = [H_2SO_4]_0 e^{-kt} \quad (6)$$

where $[H_2SO_4]_0$ is the initial concentration of H_2SO_4, $[H_2SO_4]_t$ is the concentration after time t and k is the rate constant given by the equation:

$$k = 3.65 \frac{D}{r^2} \quad (7)$$

where r is the radius of the flow tube and D is the diffusion coefficient of H_2SO_4.

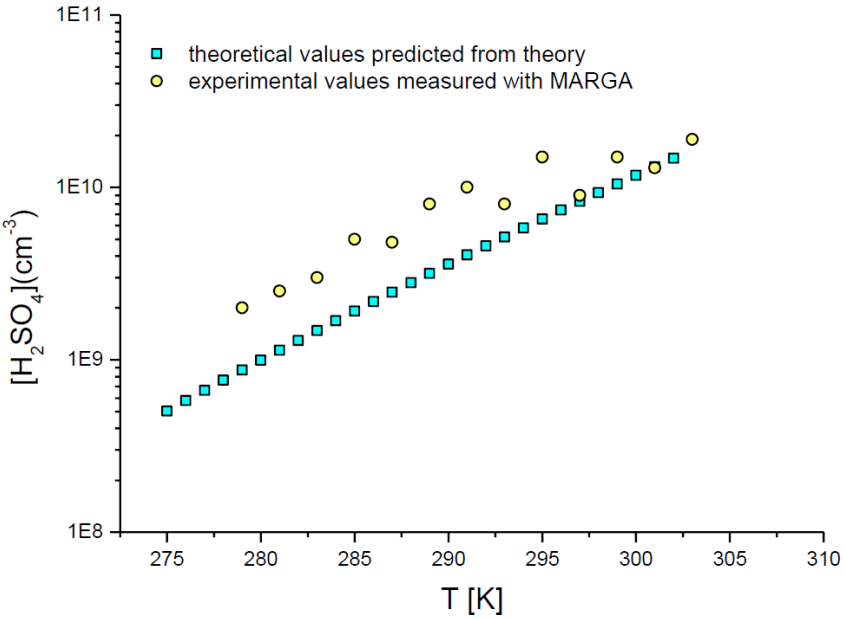

Fig. 18: A comparison of H_2SO_4 concentration calculated from H_2SO_4 saturation vapour pressure determined from Eq. (2) and experimental concentration measured with online ion chromatograph Monitor for AeRosols and Gases in ambient Air (MARGA; Metrohm Applikon), performed by Neitola et al. (2013). A good agreement can be seen, especially under high [H_2SO_4].

Data treatment

During experiments the number concentrations of the produced particles were measured using an Ultrafine Condensation Particle Counter (UCPC, Model 3776, TSI Inc., USA) and particle size distributions were measured using a Differential Mobility Particle Sizer (DMPS). The raw DMPS data were inverted to yield the number size distributions of the formed particles. The charging efficiencies were calculated using the parametrization given in Wiedensohler and Fissan (1991). The same modification to UCPC TSI 3776 has been done as described in Brus et al., (2010) to obtain a d_{50}cut-off of 2.25 nm. The saturator temperature was increased from 39°C up to 40°C, the condenser temperature was decreased from 10°C down to 8°C. At these new temperatures no homogenous nucleation was observed inside the counter. During each measurement, which was performed under a constant nucleation temperature, residence time and relative humidity, the temperature of the H_2SO_4 saturator was increased in seven consecutive steps of 5 K every two hours, resulting in a significant increase of the H_2SO_4 concentration in the gas phase and a subsequent distinct rise of the particle number concentration. The stability of particle number concentration was not achieved immediately, but it

took about 30 minutes to obtain a steady particle production. The first 30 minutes of every period of constant saturator temperature were therefore excluded from the analysis. The values of particle concentrations obtained from the DMPS were then averaged over the whole period analysed to receive one data point characterizing each saturator temperature and the data from the UCPC were averaged over two equal periods of 45 minutes to receive two data points. Apart from nucleation rate, the growth rates of newly formed particles were investigated. The obtained number size distributions from DMPS were therefore fitted with the log-normal distribution and the geometric mean diameter of the nucleation mode was determined. In Fig. 19 is depicted such a fitted particle number distribution. The particle growth rates were then obtained from the change of the modal geometric mean diameter as a function of time, analogous to the mode fitting method described in introduction (Fig. 7B).

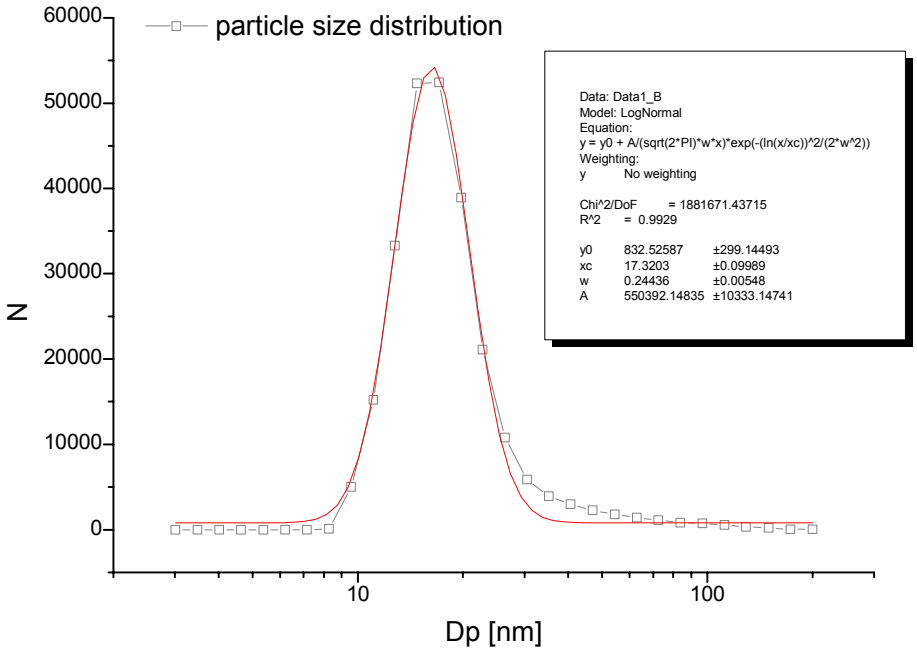

Fig. 19: The particle size distribution obtained by inversion of raw DMPS data is depicted as a black line. The log-normal distribution, presented by red line, was subsequently fitted to the size distribution and its peak presents the geometric mean diameter, which characterizes the whole aerosol population and which was used to calculate the growth rate of the particles.

Particle growth model description

The particle growth inside the laminar flow tube was simulated with a model that accounts for the condensation of H_2SO_4 as well as uptake of H_2O and NH_3 by the particles. The former process was modelled dynamically by calculating the mass transfer rate of H_2SO_4 onto the particles, I_{SA} (molecule s^{-1}), using the Fuchs-Sutugin equation (Fuchs and Sutugin, 1970):

$$I_{SA} = 2\pi d_p D_{SA} FS(\alpha,Kn)(C_{SA} - C_{SA,sat}) \quad (8)$$

$$FS(\alpha,Kn) = \frac{1+Kn}{1+0.337Kn+\left(\frac{1.33}{\alpha}\right)(1+Kn)Kn} \quad (9)$$

$$Kn = \frac{6D_{SA}}{c_{SA}d_p} \quad (10)$$

Here d_p is the particle diameter (m), D_{SA} is the diffusion coefficient ($m^2\ s^{-1}$), α is the mass accommodation coefficient of H_2SO_4, C_{SA} is the gas phase number concentration of H_2SO_4 (molecule cm^{-3}) and $C_{SA,sat}$ is the number concentration of H_2SO_4 at the saturation vapour pressure (molecule cm^{-3}). Moreover, $FS(\alpha, Kn)$ is the so-called Fuchs-Sutugin correction factor which accounts for non-continuum effects in the mass transfer and c_{SA} (m s^{-1}) is the mean molecular speed of H_2SO_4 molecules in the gas phase. Here the value of C_{SA} was taken from the measurements, and $C_{SA,sat}$ was set as equal to zero corresponding to the assumption that H_2SO_4 behaves as a non-volatile vapour. This assumption is reasonable for systems that contain NH_3 (Kulmala et al., 2000). Finally, the value of α was set as equal to unity based on the measurements conducted by Hanson (2005).

The uptake of the considered semi-volatile compounds, NH_3 and H_2O, was modelled as follows. First, since there were no direct measurements of the ammonia concentration levels in the system, we applied three different degrees of particle neutralization: 1) no NH_3 was assumed to be taken up by the aerosols, 2) NH_3 was assumed to condense along with H_2SO_4 so that a 1:1 molar ratio was maintained between NH_3 and H_2SO_4, corresponding thus to a $(NH_4)HSO_4$ solution, and 3) two NH_3 molecules were assumed to condense with each H_2SO_4 molecule which corresponds to an $(NH_4)_2SO_4$ solution. The particles were assumed to be aqueous regardless of the relative humidity and the particle H_2O content was calculated as a function of the H_2O activity (a_w) using the appropriate molality data taken from the literature (Staples, 1981, for H_2SO_4, and Tang and Munkelwitz, 1994, for $(NH_4)HSO_4$ and $(NH_4)_2SO_4$).

Here the H_2O activity a_w was calculated using the relation a_w= RH/Ke where RH is the relative humidity in the instrument and Ke is the Kelvin term (Seinfeld and Pandis, 1998). Finally, the particle surface tension and density were calculated using the model presented by Hyvärinen et al. (2005).

The initial particle diameter d_{init} was taken from the measurements at the lowest temperature of the saturator and the initial chemical composition was set so that the particles were in equilibrium with respect to H_2O and NH_3. The increase of the particle diameter as a function of the increasing H_2SO_4 concentration (owing to growing temperature of the saturator) was then simulated. The particle size was increased after each time step by first converting the total particle mass (obtained as described above) to a corresponding volume and further to a diameter d_p by assuming that the particles are spherical. At the end of the simulation, the growth rate of particles during the experiment, GR, was calculated as follows:

$$\mathrm{GR} = \frac{d_p - d_{init}}{t_{\exp}}, \qquad (11)$$

where d_p is the particle diameter at the end of the experiment, and $t_{\exp}$ is the residence time in the laminar flow tube. The applied time step was 0.1 seconds in all of the performed calculations.

3.2 Experimental results

An overview of experimental observations of the growth behaviour of sulphuric acid nanoparticles produced by nucleation of H_2SO_4 and H_2O is given in the following section. The main focus of this study was to assess the effect of various experimental conditions on the growth of freshly nucleated particles. Part of the presented results has been published in Skrabalova et al. (2014). To our best knowledge, this is the first comprehensive laboratory study investigating the growth of H_2SO_4 nanoparticles under different conditions.

Reproducibility of the measurements

The optimized experimental procedure proceeded in the following way. First all the experimental conditions (relative humidity, temperature of the H_2SO_4 saturator and flow tube, flow rates) were adjusted. Then the experiment was run for 5 hours at the lowest temperature of the H_2SO_4 saturator in order to obtain a steady state. After this period the saturator temperature was increased of 5 K every 2 hours, while all other experimental conditions were kept constant. The series of the experiments started at the lowest nucleation temperature (283 K) and at the low RH (1%). The total flow rates were gradually decreased to provide 4 residence times in the flow tube (30, 45, 60 and 90 s) and the RH was then increased to 30% and measurements with 4 residence times were performed again. The series of the experiments then proceeded to higher nucleation temperatures. In total 25 measurements, each lasting for 17 hours, were performed. The carrier gas was left flowing overnight under the initial conditions through the humidifiers and saturator in order to maintain the steady state in the flow tube. Overall, the carrier gas saturated with nucleating vapours was flowing through the whole experimental setup for more then a month without an interruption.

In order to investigate the reproducibility of the measurements, one experiment was performed under the same experimental conditions twice. The obtained results are illustrated in Figs. 20A and 20B, which show the results of experiments at a temperature of 283 K, a residence time of 60 s and under dry conditions (RH ~1%) taken one day apart. The total particle concentrations as a function of the H_2SO_4 concentration measured by DMPS for both experiments are presented in Fig. 20A. Except the first points, which show larger scatter and with a ratio of these concentrations of 1:1.17, the ratios of the remaining concentrations range from 1:1.01 to 1:1.07. The observed variation of the median particle diameters as a function of the initial H_2SO_4 concentrations with standard deviations as error bars is shown in Fig. 20B. At the same temperature, relative humidity, residence time and comparable H_2SO_4 concentrations, the maximum difference of single median particle diameters

determined from both experiments was 0.6 nm with most diameters varying by 0.3 or 0.4 nm. These results show that the measurements of the particle diameters and particle number concentrations were very reproducible.

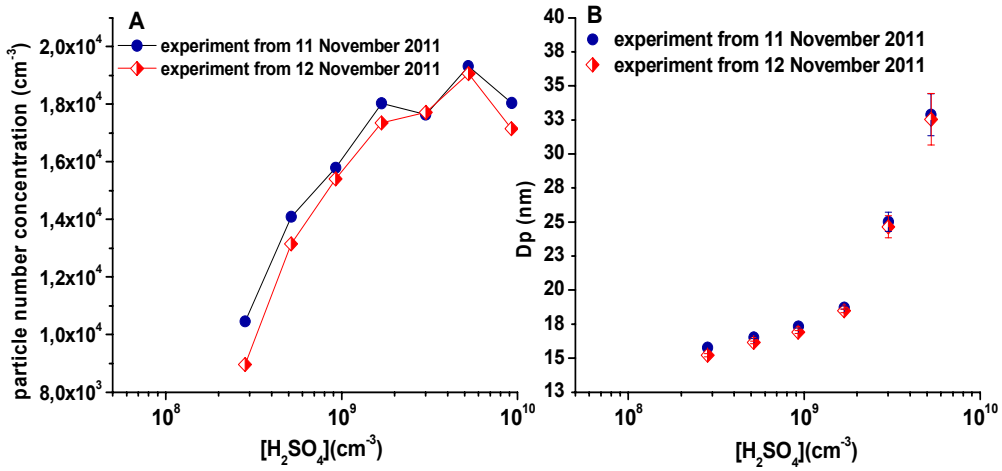

Fig. 20A: The variation of the total particle concentrations determined from DMPS from measurements performed at T=283 K, with a RH of ~1% and a residence time of 60 s taken one day apart. Fig. 20B: The median particle diameters determined from measurements performed at T=283 K, with a RH of ~1% and a residence time of 60 s taken one day apart. The standard deviations of the median particle diameters are depicted as error bars.

Variation of particle number concentrations and particle size distributions

During each experiment, the temperature of the saturator was increased in 7 consecutive steps, resulting in a distinct increase of the H_2SO_4 concentration in the gas phase and a subsequent significant rise of the particle number concentration. The stability of particle production was not achieved immediately after changing the experimental conditions, but it took a certain time to reach a steady state. Here the steady state of particle production is reffered as total number concentration with a maximum ±10% change over at least one hour. It was found out during the measurements that obtaining a steady particle production took approximately 30 minutes, which were therefore excluded. The total number concentrations determined from both instruments were found to be strongly dependent on the residence time of the gaseous mixture in the flow tube. The obtained curves of the particle number concentration as a function of the initial H_2SO_4 concentration measured by both DMPS and UCPC at T=293 K, RH ~30% and at residence times of 45,

60 and 90 s are presented in Fig. 21. The results clearly show that the observed total number concentration is influenced by the growth process and the longer the residence time, the larger the fraction of nucleated particles grows beyond the detection limits of the UCPC and DMPS. For example, during the experiment performed at T=293 K and RH ~30%, at a H_2SO_4 concentration of 6.5×10^8 molecule cm^{-3}, the particle number concentration increases about one order of magnitude from $3.2\times10^3 \pm 0.15\times10^3$ cm^{-3} at a residence time of 45 s to $3\times10^4 \pm 1.1\times10^3$ cm^{-3} at a residence time of 90 s. The values of the total number concentrations during all of the measurements ranged from $1.1\times10^3 \pm 0.17\times10^3$ cm^{-3} to $4.7\times10^4 \pm 1.2\times10^3$ cm^{-3} and were generally higher during experiments performed at RH of ~30% and nucleation temperature of 303 K. The values of the median particle diameter determined from the particle size distributions obtained from the inversion of the raw DMPS data ranged from 14.4 ± 0.1 nm to 39.8 ± 1.6 nm and particles grew larger at a RH of ~30% and at high H_2SO_4 concentrations.

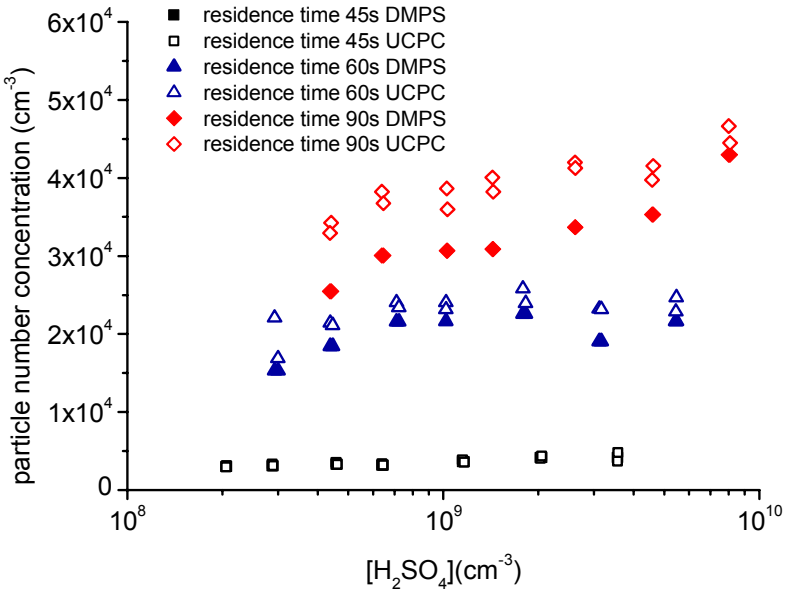

Fig. 21: The observed particle number concentrations at different residence times at T=293 K and with a RH of ~30%. The solid symbols present the number concentrations determined by a DMPS and the open symbols are number concentrations determined by a UCPC.

The total particle concentrations obtained from the DMPS measurements were slightly lower than the values detected with the stand-alone UCPC, due to the lower cut-off diameter (d_{50} = 2.25 nm) of the stand-alone UCPC and the upper limit (200 nm) of the DMPS, which may have caused undercounting of formed particles at higher H_2SO_4 concentrations and longer residence times. However,

by a comparison of the measured particle concentrations from both instruments, we received an almost linear relationship between the data in most cases (Fig. 22). Also when sampling ambient aerosol from laboratory, almost identical particle number concentrations were obtained from both devices. We therefore conclude that the difference in concentrations depicted in Fig. 21 is caused by various detection limits of both instruments.

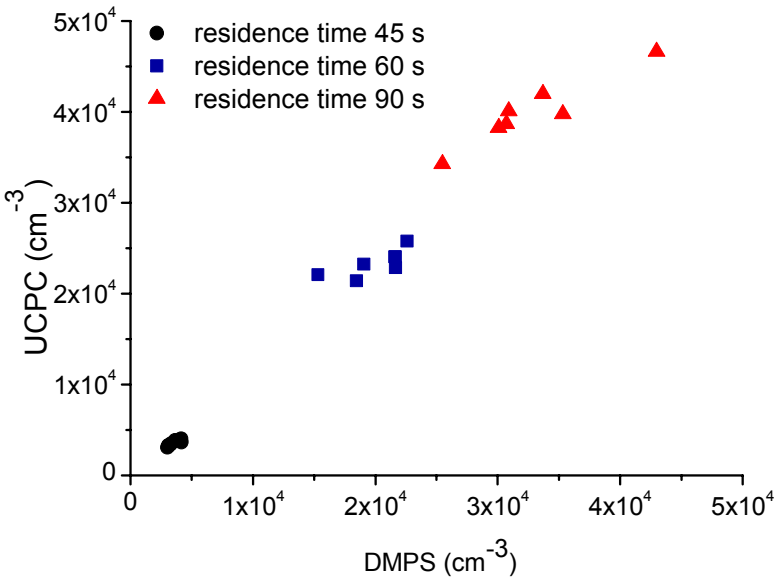

Fig. 22: An almost linear relationship was reached by a comparison of the particle number concentrations determined from a DMPS and a UCPC at different residence times at T=293 K and with the RH set at 30%.

Absolutely no particles were detected during experiments performed at a residence time of 30 s indicating that the nucleated particles were not able to grow to detectable sizes during the first 30 seconds of the experiments. The significance of residence time in nucleation measurements has been discussed in previous studies (Sipilä et al., 2010; Berndt et al., 2010). Several competing processes occur simultaneously in flow tube, such as nucleation, condensational growth, coagulation or wall losses of H_2SO_4. On one hand, short residence time may results in underestimation of particle concentration due to insufficient growth of particles to sizes large enough to ensure their detection. In contrary, at long residence time the condensational growth may dominate over the nucleation due to larger particle surface area and also the H_2SO_4 wall losses are more important with longer residence time (Young et al., 2008). Under these conditions, observed particle concentration may be even anti correlated with [H_2SO_4] (Benson et al., 2008). The residence time greatly influences these

competing processes and nucleation experiments should be therefore conducted under conditions when nucleation dominates over coagulation or condensational growth i. e. prefferably under low [H_2SO_4] and short residence time.

Nucleation rates

The nucleation rates J were determined by dividing the total particle number concentration by the lenght of time over which the nucleation occured, i.e. by the residence time of the gaseous mixture in flow tube given by the total flow. For J values presented here, the number concentration was determined using the UCPC standalone mode, whereas the DMPS was used to provide aerosol sizes. Because critical clusters have size ~1.5 nm (Kulmala et al, 2013), which is under the cut-off size of the UCPC used (~2.25 nm), the J reported here is not the actual nucleation rate, but rather the formation rate of particles with diameters close to ~2.25 nm, so called apparent formation rate. However, in case of experiments when growth of particles via coagulation can be neglected as in our measurements, the J values estimated from this calculation are close to actual nucleation rate (Kulmala et al., 2004). Moreover, extrapolating the measured number concentrations to a specific diameter (i.e. 1.5 nm) would allow to obtain J close to the formation rate of critical cluster (Kulmala et al, 2006). This normalization was however not used here to keep our results directly comparable to other nucleation studies, which commonly report apparent formation rates.

Since the main focus of this study was to investigate the growth of newly formed particles under different conditions, the nucleation rates were measured only in a limited range. Overall, the J values varied from 40 to 560 cm^{-3} s^{-1} and were slightly higher under RH of 30%, but showed only a weak temperature dependency. However, the deduced J values were found to increase with increasing residence time in the flow tube, since the counting efficiency of UCPC governed the observed particle number concentration. J measured at residence times of 60 and 90 s were about a factor of 3 higher compared to J measured at residence time of 45 s. The derived J showed no clear time dependency in experiments conducted under residence times of 60 and 90 s, indicating that in this case the particle growth was not the limiting factor and the majority of nucleated particles was detected. The initial H_2SO_4 concentration in this study ranged from 2×10^8 to 1.4×10^{10} molecule cm^{-3}. The observed J of H_2SO_4 – H_2O nucleation corresponding to this H_2SO_4 concentration range reported from previous studies using liquid sample are 0.1 - 220 cm^{-3} s^{-1} (Young et al., 2008), 0.001 – 10 000 cm^{-3} s^{-1} (Brus et al., 2011)

and 0.01 – 1000 (Ball et al, 1999). Although our experiments were performed under slightly different conditions (RH, T, residence time), our data points fall between those reported from the earlier studies (Fig. 23).

To provide a complete overview, it is a common practise to compare the J values obtained from laboratory experiments with those from field studies. The J of 1 cm^{-3} s^{-1} was observed in atmosphere under H_2SO_4 concentration as low as 2×10^5 molecule cm^{-3} (Sihto et al, 2006) and no laboratory experiment has reproduced this observation yet. However, different methodology is used to perform laboratory studies and field obseravations. Whereas the atmospheric data are often obtained under changing RHs and temperatures and various concentrations of possible third species involved in nucleation mechanism, the laboratory J are deduced from data obtained under constant temperature and RH and presumably in absence of ternary species. These aspects deteriorate the comparability of laboratory and atmospheric observations.

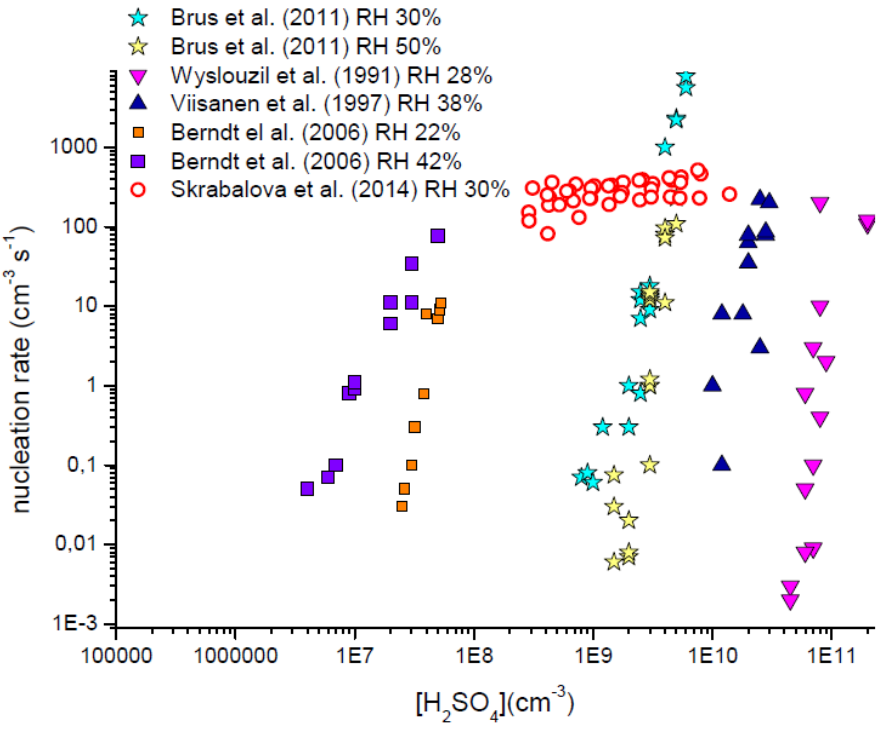

Fig. 23: The comparison of nucleation rates determined in this work with other studies of H_2SO_4 - H_2O nucleation. Data for comparison were taken from Wyslouzil et al. (1991), Viisanen et al. (1997), Berndt et al. (2006) and Brus et al. (2011)

Observed particle growth rates

The experimental growth rates were calculated using Eq. (11), which describes the temporal variation of mean particle diameters, obtained from fitting of the particle size distributions with log-normal distribution (Fig. 19). The observed experimental growth rates range from 20 nm h^{-1} to 890 nm h^{-1} under dry conditions (RH ~1%) and from 7 nm h^{-1} to 980 nm h^{-1} under wet conditions (RH ~30%). The effect of T, RH and [H_2SO_4] on growth rates will be discussed more in detail in the section dealing with the dependence of growth rates on experimental conditions. Qualitatively, the variation of the particle mean diameters has the same pattern under both wet and dry conditions (Fig. 24). The particles are assumed to grow via condensation, because self-coagulation of particles was negligible under observed number concentrations. Apart from the main condensing compounds i.e. H_2SO_4 and H_2O, other species might have influenced the subsequent growth of the freshly formed particles. As mentioned above, trace concentration of NH_3 was detected in this experimental setup in a previous study (Neitola et al., 2013). Assuming that the newly formed particles were fully neutralized by NH_3, the observed growth rates would only increase by a factor of 1.1 compared to pure H_2SO_4 - H_2O particles (Benson et al., 2011). Moreover, the role of NH_3 in the growth process is addressed in the model, which accounts for three degrees of neutralization (pure H_2SO_4 - H_2O, $(NH_4)HSO_4$ and $(NH_4)_2SO_4$ particles). Other impurities, including amines and other organics, were measured by MARGA in the same experimental setup regurlarly (Neitola et al., 2013), and their concentrations were always below the detection limit (~100 pptv for amines). Despite of this, the presence of impurities in the flow tube and their impact on growth dynamics can not be ruled out. Amines, more specifically alkylamines, can displace NH_3 from $(NH_4)_2SO_4$ and form alkylaminium sulfates (Zhang et al., 2012). Alkylaminium sulfates have similar properties as $(NH_4)_2SO_4$ and are even more stable in the particle phase; also aerosol dynamics are very similar to that of $(NH_4)_2SO_4$ and $(NH_4)HSO_4$ (Qiu and Zhang, 2012). If present, these compounds should not therefore influence significantly the growth dynamics of pure H_2SO_4 - H_2O particles.

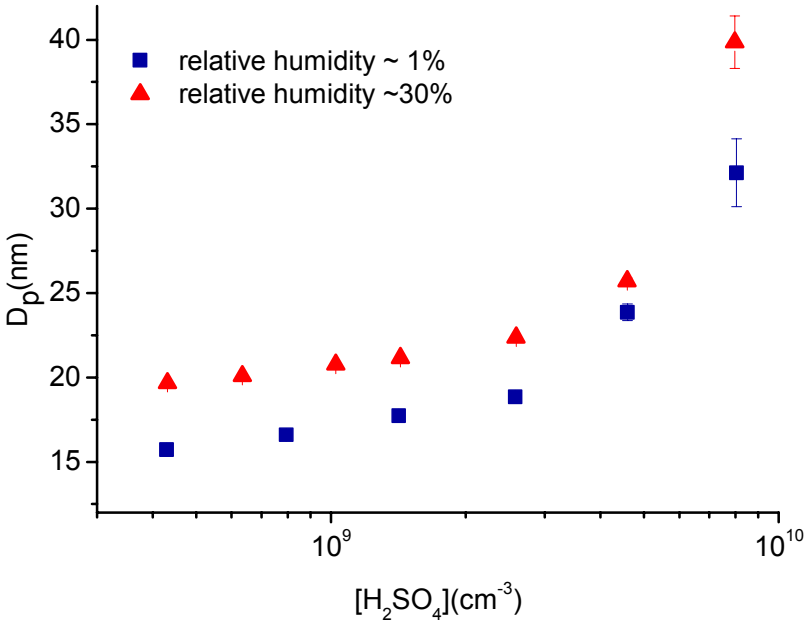

Fig. 24: The variation in the median particle diameters determined from measurements performed at T=303 K, with a residence time of 60 s and at different RHs. The standard deviations of the median particle diameters are depicted as error bars.

Figure 25 depicts the experimental growth rates under wet conditions, at a residence time of 90 s and at three nucleation temperatures and the atmospheric growth rates, obtained in Heidelberg and Hyytiälä during the QUEST project (Fiedler et al., 2005), data obtained in Atlanta during the ANARChE study (Stolzenburg et al., 2005), data from Beijing during the CAREBeijing-2008 campaign (Yue et al., 2010), data from Mace Head during the PARFORCE campaign (O'Dowd et al., 2002) and data from Kent, Ohio (Erupe et al. 2010) are depicted for comparison. A trend line which presents the theoretical predictions of the growth of ammonium sulphate particles under wet conditions (RH=30%) calculated using model introduced in previous section is also depicted. The best agreement with our data was found for sulphuric acid-driven growth rates from a field study by Stolzenburg et al. (2005), who investigated the growth of particles containing ammonium sulphate, which is consistent with the assumed chemical compositions of particles in our study. Most observed atmospheric growth rates correspond to substantially lower H_2SO_4 concentrations and our results thus show that in most cases sulphuric acid alone cannot explain the growth rates observed in

the atmosphere. H_2SO_4 is the main condensing vapour responsible for particle growth only in large urban areas, where it can contribute up to 60 % to the growth (Stolzenburg et al., 2005, Yue et al., 2010). In order to explain the atmospheric growth rates, the condensation of additional chemical species is assumed, mainly organic compounds (Erupe et al., 2010, Fiedler et al., 2010) and iodine species (O'Down et al., 2002, Kulmala et al., 2013).

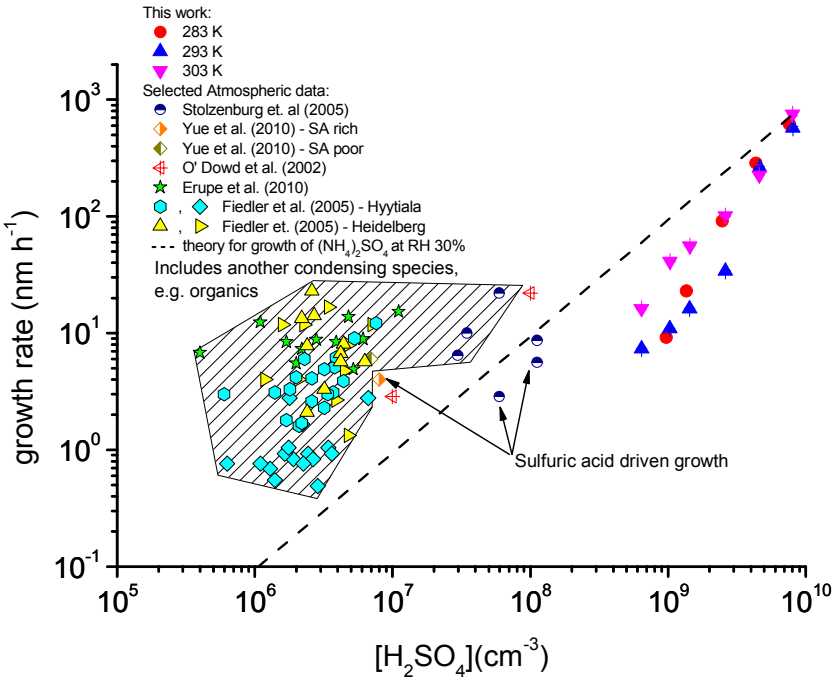

Fig. 25: The experimental growth rates obtained under wet conditions (RH=30%), with a residence time of 90 s and three nucleation temperatures of 283, 293 and 303 K. The atmospheric growth rates, obtained in Heidelberg and Hyytiälä during the QUEST project (Fiedler et al., 2005), data obtained in Atlanta during the ANARChE study (Stolzenburg et al., 2005), data from Beijing during the CAREBeijing-2008 campaign (Yue et al., 2010), data from Mace Head during the PARFORCE campaign (O'Dowd et al., 2002) and data from Kent, Ohio (Erupe et al. 2010), are depicted for comparison. The line presents the theoretical predictions of the growth of ammonium sulphate particles at a RH of 30%.

There are only few previously reported values of particle growth and its dependence on $[H_2SO_4]$ obtained from nucleation laboratory experiments. Young et al. (2008) have studied the binary nucleation of H_2SO_4 – H_2O at T=288 K, RH from 11% to 23% and at $[H_2SO_4]$ from 10^8 to 10^{10} molecule cm^{-3}. The observed particle growth rates in their experiment ranged from 95 nm h^{-1} to 500 nm h^{-1}. Benson et al. (2008) measured the binary nucleation of

H_2SO_4 - H_2O at T=288 K, at RH from 10% to 55% and at $[H_2SO_4]$ from 10^8 to 10^9 molecule cm^{-3}. The particle growth rates estimated from their measurements were roughly from 160 to 490 nm h^{-1}. Keeping in mind different experimental conditions and absence of precise dependence of observed growth rates on $[H_2SO_4]$ in studies of Benson et al. (2008) and Young et al. (2008), we can conclude that the reported values of particle growth rates from these studies are in reasonable agreement with values determined from our experiments (Fig. 26).

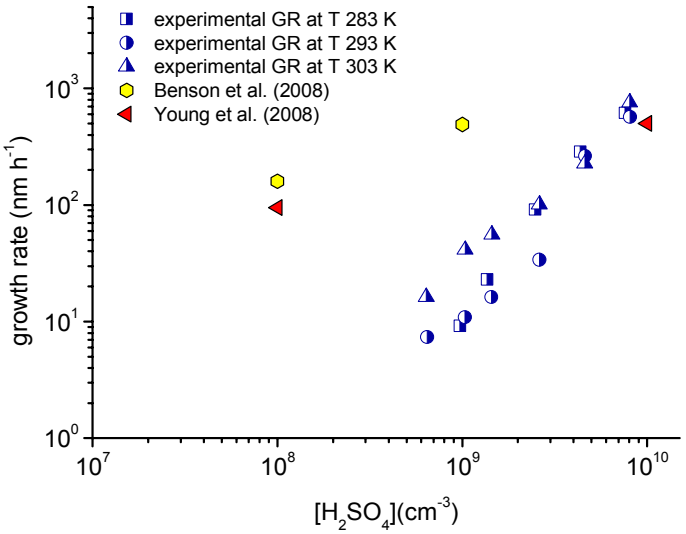

Fig. 26: The experimental growth rates determined from measurements conducted at a RH of 30%, a residence time of 90 s and three nucleation temperatures are compared with the particle growth rates measured in the nucleation experiments made by Benson et al. (2008) at T=288 K and Young et al. (2008) at T=288 K.

Hygroscopic growth

Hygroscopicity of newly formed atmospheric particles is a key parameter, which affects condensational growth by water vapor, particles‘ scattering efficiency, their potential for the formation of cloud condensation nuclei and also influences the uptake of additional condensing species. Atmospheric measurements of hygroscopicity can provide an insight into the chemical composition of formed particles and the composition of condensing vapors. The hygroscopicity of nucleated particles was observed to decrease with increasing particle diameter in size range from 10 to 50 nm. Also the hygroscopicity of 10 nm particles was reported to differ significantly during various NPF events, implying different chemical composition of these particles. This observations indicate that the preferred nucleation mechanism is governed by the atmospheric conditions and concentrations of various nucleation precursors,

which might vary significantly between various NPFs (Wu et al., 2013). Apparently, the chemical nature of the condensating vapours shift during growth process from more to less hygroscopic compounds. Hygrospcopic growth behaviour can be described with the so-called hygroscopic growth factor GF:

$$GF = \frac{D_p(wet)}{D_p(dry)} \tag{12}$$

The species responsible for condensational growth of critical clusters must have a very low volatility in order to overcome the Kelvin effect. The hygroscopic growth of atmospheric nanoparticles was observed to be very sensitive to their extent of neutralization by NH_3 compared to possible nanosize effects on density and surface tension due to Kelvin effect. In a laboratory study, at a fixed relative humidity the hygroscopic growth of $(NH_4)_2SO_4$ particles was found to decrease with decreasing particle size owing to a greater degree of neutralization, since $(NH_4)_2SO_4$ is less hygroscopic than H_2SO_4 (Biskos et al., 2010). This observation of hygroscopicity is not consistent with atmospheric observations, since hygrospocic behaviour of atmospheric particles was observed to have a different trend (Wu et al., 2013). This implies presence of additional species in growing atmospheric particles apart from NH_3, H_2SO_4 and H_2O influencing the particles hygroscopicity. When considering the effect of water vapour on the particle growth, the hydration of H_2SO_4 should be taken into account. The number of water molecules attached to a H_2SO_4 molecule increases significantly with the growing relative humidity and the higher the relative humidity, the higher the growth rate due to the condensation of H_2O on the particles (Nieminen at al., 2010).

The H_2SO_4 - H_2O nucleation in our system was affected by the presence of impurities originating from ultrapure water and carrier gas. The freshly formed H_2SO_4 particles are partially neutralized to $(NH_4)HSO_4$, and $(NH_4)_2SO_4$. When calculating the hygroscopic growth factors using Eq. (12), the dry diameter Dp(dry) corresponds to the median particle diameters obtained from measurements performed at a RH of ~1% and the wet diameters Dp(wet) to the median particle diameters obtained from measurements at a RH of ~30%. Hygroscopic growth factors determined from measurements performed at T=293 K ranged from 1.05 to 1.35 and at T=303 K the values covered the range from 1.1 to 1.42. Our findings were then compared with the results from Biskos et al. (2010), who measured the hygroscopic growth of acidic sulphate nanoparticles over a wide range of relative humidities using the tandem DMA technique. At a relative humidity of ~30%, Biskos et al. (2010) report for dry

diameters from 7.5 nm to 36.1 nm, which are comparable with our study, growth factors from 1.18 to 1.3. The best agreement with our study was found for T=303 K, since most GF values determined at this temperature were close to 1.25 (Fig. 27). At T=293 K, most GFs were around 1.1 and reached values above 1.2 only at a residence time of 90 s and for H_2SO_4 concentrations of 5×10^9 molecule cm^{-3} and higher (Fig. 27). The hygroscopic growth factors were not determined for T=283 K, since the differences in the determined median particle diameters from measurements under wet and dry conditions at all residence times were so small that in most cases they fall within the uncertainity range of the measurements. A dependence of GFs calculated using Eq. (12) on H_2SO_4 concentration was observed. At lower H_2SO_4 concentrations, the GFs slightly decrease and at a H_2SO_4 concentration of ~3×10^9 molecule cm^{-3} GFs start to increase. However, the GFs calculated from our model (described in section 3.1) were not in good agreement with the experimental values, since the model predicted different trend. For this reason, it could not be explained if the trends in the experimental GFs behaviour are real or spurious.

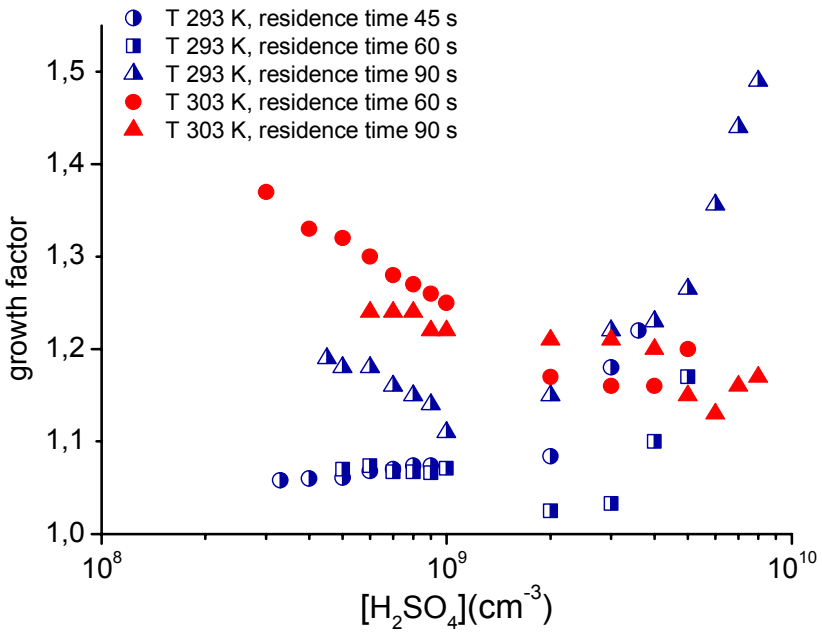

Figure 27: The growth factors as a function of the H_2SO_4 concentration at T=293 and T=303 K at different residence times.

Dependence of growth rates on experimental conditions

The experimental growth rates, determined from Eq (11), range from 20 nm h^{-1} to 890 nm h^{-1} under dry conditions and from 7 nm h^{-1} to 980 nm h^{-1} under wet conditions. When analyzing the dependence on the experimental conditions, the measured growth rates were found to increase with growing H_2SO_4 concentration. The same dependency was observed in atmospheric measurements. In a field study of Stolzenburg et al. (2005) the growth rates of nucleated particles span the range from 0.1 to 120 nm h^{-1} at $[H_2SO_4]$ from 1×10^6 to 1×10^8 molecule cm^{-3} and the growth rates were found to vary aproximately in proportion to observed $[H_2SO_4]$. The influence of the RH is not consistent at lower H_2SO_4 concentrations the growth rates were higher under dry conditions, at H_2SO_4 concentrations of $\sim1\times10^9$ molecule cm^{-3} and above the growth rates were higher under wet conditions. This can be seen in Fig. 24, where at lower $[H_2SO_4]$ the slope of modal diameters under dry conditions is steeper compared to wet conditions. We do not have a plausible explanation of this behaviour. When considering the chemical composition of nucleated particles, the particles formed under dry condition will be more acidic and therefore more hygroscopic compared to particles formed under wet conditions, however this fact does not explain the observed change in growth rates behaviour. In the atmospheric observations, the growth rates of nucleated particles were found to have a negligible correlation with relative humidity (Yli-Juuti et al., 2011). Also growing nucleation temperature was found to have a slight enhancing effect on particle growth rates. This observation is in agreement with atmospheric measurements, since the growth rates of nucleated particles were observed to be positively correlated with ambient temperature (Yli-Juuti et al., 2011). In contrary, the measured growth rates show a negligible dependence on the residence time. As discussed before, the residence time is a crucial parameter for nucleation studies. In our experiments, no particles were detected under residence time of 30 s and the J deduced from meaurements performed at residence time 45 s was found to differ from J deduced from meaurements performed at residence time 60 and 90 s. These findings might partly explain the discrepances of observed J reported from various studies. In case that the particle growth is the limiting factor of observed particle concentration used to derive J, even experiments performed under identical conditions will not provide comparable J when the residence time will not be sufficient.

Model evaluation and wall losses of H_2SO_4

The initial concentrations of H_2SO_4, at which newly formed particles were detected during the experiments, covered the range from 1.8×10^8 to 1.4×10^{10} molecule cm^{-3}. The H_2SO_4 molecules can attach to the inner surfaces of the flow tube during experiments. In order to determine the residual concentration of H_2SO_4 the corrections of the initial concentrations are necessary. The wall loss factor characterizing the diffusion losses of sulphuric acid on the walls of the tube is defined as follows:

$$\mathrm{WLF} = \frac{\left[H_2SO_4\right]_0}{\left[H_2SO_4\right]_t} \tag{13}$$

where $[H_2SO_4]_0$ is the initial concentration of sulphuric acid in the flow tube determined from Eq. (5) and $[H_2SO_4]_t$ is the concentration of sulphuric acid after time t, which can be calculated using Eq. (6). The reliability of these calculations was investigated by Young et al. (2008), who examined WLFs theoretically using this equation and experimentally by measuring the initial and residual $[H_2SO_4]$ using Chemical Ionization Mass Spectrometers (CIMS), which are capable of measuring gas phase H_2SO_4. Very good agreement was observed in their experiments, indicating that WLFs calculated by assuming that H_2SO_4 wall loss is a diffusion limited proces are reasonable (Young et al., 2008).

Since H_2SO_4 wall loss is a first order rate process, WLFs can be determined by using different residence times. The results reported from nucleation laboratory studies are commonly related to either initial or residual $[H_2SO_4]$. In this study, the time t was set as equal to half of the residence time of the gaseous mixture in the flow tube, and thus the concentration $[H_2SO_4]_t$ corresponds approximately to the H_2SO_4 concentration in the middle of the flow tube. The wall losses were determined using Eq. (6) and the value of RH dependent H_2SO_4 diffusion coefficient was determined from equation given in Hanson and Eisele (2000). The calculated wall loss factors span the range from 1.9 to 4.8 under wet conditions and from 2.2 to 6.2 under dry conditions for at from 22 to 45 s, corresponding to half of the initial residence times. However, when using the calculated H_2SO_4 concentrations corrected by WLFs as an input parameter in our model, the experimental values did not agree with the model predictions. This can be seen from Fig. 28, which illustrates the variation of both the measured and calculated median particle diameters at an RH of ~30 %, with T=283K and a residence time of 60 s. The model fails to capture the observed growth rates in all cases since it predicts significantly lower particle growth than observed in experiments, and the deviations are

more profound at RH of ~1% and at higher [H_2SO_4]. This observation indicates that the real mass transfer rate of H_2SO_4 onto the particles, I_{SA} (molecule s^{-1}) is significantly larger than I_{SA} calculated from our model. We conclude that the C_{SA}, which presents the gas phase number concentration of H_2SO_4 (molecule cm^{-3}) in Eq. (8), is significantly greater that H_2SO_4 concentration corrected by WLFs, which was applied in the model. Overall, these results suggest that the H_2SO_4 concentration corresponding to the middle of the flow tube as calculated using WLFs is too low and does not describe the growth behaviour of the particles correctly.

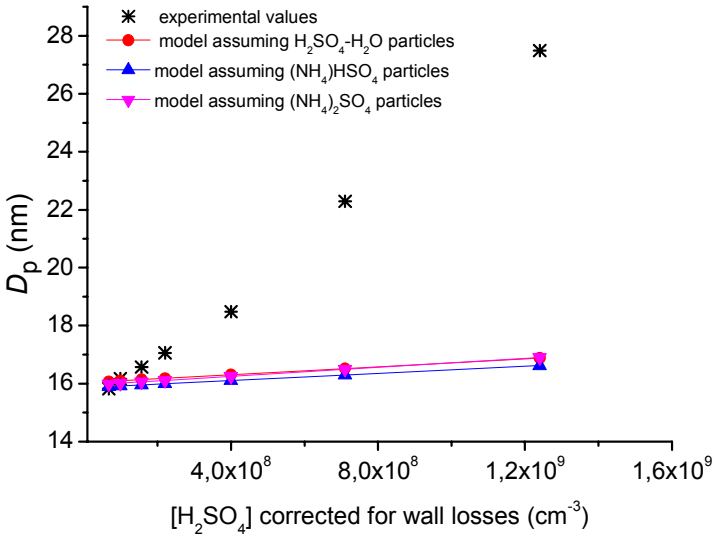

Fig. 28: The comparison of the experimental median particle diameters from a measurement conducted at T=283 K, with a RH of ~30% and a residence time of 60 s and values predicted theoretically from a model using the H_2SO_4 concentration corrected for wall losses, determined according to Hanson and Eisele (2000).

In order to investigate the discrepancy between modelled and measured particle modal diameters, additional calculations were performed with the same model. Instead of using wall loss coefficients determined according to Hanson and Eisele (2000) using Eq. (7), the modelling was performed with wall loss coefficients (0.0047 cm^{-1} for wet conditions and 0.0061 cm^{-1} for dry conditions) accounting for H_2SO_4 diffusion coefficient in air determined by Brus et al. (2011b). In their work the measurements of diffusion coefficient of sulphuric acid in humidified air estimated from the sulphuric acid wall loss coefficients were performed in the same experimental setup, which was used in the this study (Skrabalova et al., 2014). The measurements in the study of Brus et al. (2011b) were carried out under laminar flow conditions in a range of relative

humidities from ~2 to 70 %, at temperatures of 278, 288 and 298 K and at initial H_2SO_4 concentration from 1×10^6 to 1×10^8 molecule cm^{-3}. The concentration of H_2SO_4 was measured continuously with chemical ionization mass spectrometer (CIMS) at 6 different positions along the flow tube. The wall losses of H_2SO_4 were determined from the slopes of the fits to measured H_2SO_4 concentrations as a function of axial position in the flow tube. The observed wall loss rate coefficients were found to decrease slightly with increasing relative humidity and are independent of different initial H_2SO_4 concentrations and different total flow rates (Brus et al., 2011b).

A comparison of the experimental and numerical results is illustrated in Fig. 29, which shows the experiment conducted at T=283 K, an RH of 30% and a residence time of 60 s (compare with Fig. 28). Using the wall loss coefficients accounting for H_2SO_4 diffusion coefficient in air determined by Brus et al. (2011b) provides much better agreement with experimental data compared to calculations based on wall loss coefficients according to Hanson and Eisele (2000). These results are very likely influenced by different carrier gases. Hanson and Eisele (2000) used nitrogen in their work, whereas in our study and study of Brus et al., (2011b) particle free and purified air was used as the carrier gas (the diffusion of H_2SO_4 in air is slower compared to diffusion of H_2SO_4 in nitrogen).

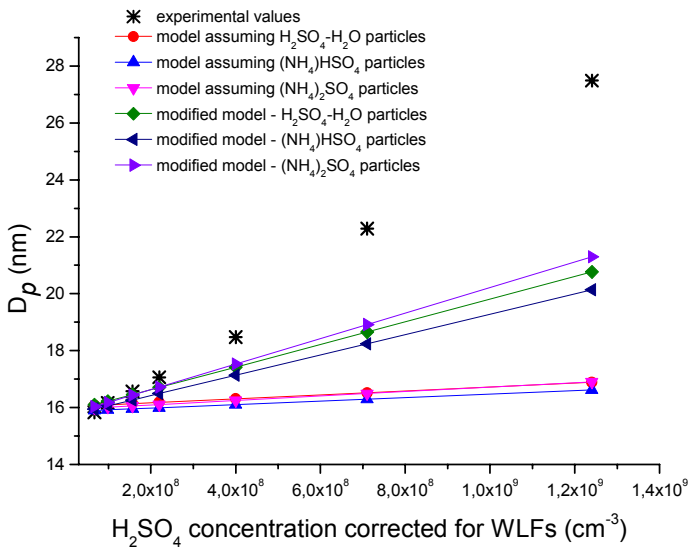

Fig. 29: The comparison of the experimental median particle diameters from a measurement conducted at T=283 K, with a RH of ~30% and a residence time of 60 s and values predicted theoretically from a model using the H_2SO_4 concentration corrected for wall losses, determined according to Hanson and Eisele (2000) and modified model, accounting for a diffusion coefficient of sulphuric acid in humidified air measured by Brus et al. (2011b).

As mentioned before, the carrier gas saturated with the nucleating vapours (H_2SO_4 and H_2O) was left flowing through the flow tube overnight between the experiments and the whole experimental setup was run for more than a month without an interruption. We therefore speculate, that the measurements were performed under close to wall-equilibrium conditions. The flow tube wall is therefore not an infinite sink for H_2SO_4 molecules as assumed by Hanson and Eisele (2000), but that there is also a flux of H_2SO_4 from the wall to the flow tube. Our results indicate that the wall losses of H_2SO_4 are not as great as is commonly presumed in case of long-lasting experiments. For this reason, the initial $[H_2SO_4]$ calculated from Eq. (5) corresponding to $[H_2SO_4]$ at the beginning of the flow tube was used as the input parameter for all the model calculations in the further analysis. As can be seen there, the calculations using initial $[H_2SO_4]$ agree with the experimental data much better (Fig. 30). The modelled growth rates, calculated from the model (section 3.1) with the initial $[H_2SO_4]_0$ using Eq. (11), range from 7 nm h^{-1} to 1100 nm h^{-1} under dry conditions and from 15 nm h^{-1} to 1300 nm h^{-1} under wet conditions. Growth rates over 1000 nm h^{-1} were reached only at very high H_2SO_4 concentrations of 8×10^9 molecule cm^{-3} and higher and at a residence time of 90 s. Most growth rates span the range from ~10 nm h^{-1} to ~500 nm h^{-1} under dry conditions and from ~15 nm h^{-1} to ~400 nm h^{-1} under wet conditions.

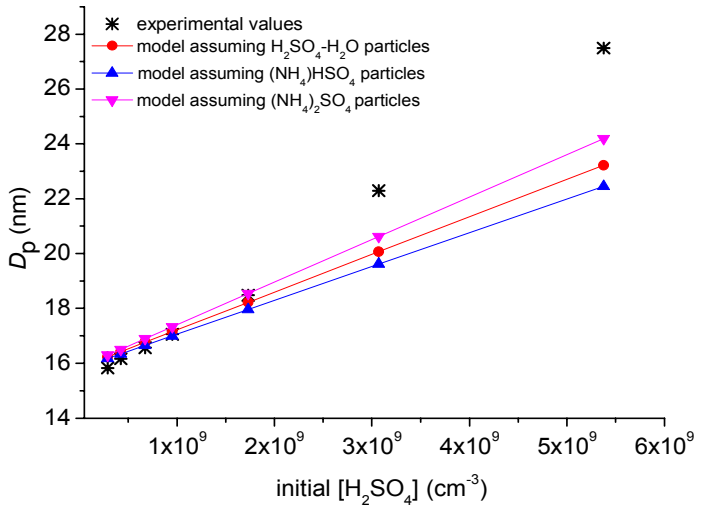

Fig. 30: The comparison of the experimental median particle diameters from a measurement conducted at T=283 K, with a RH of ~30% and a residence time of 60 s and the values predicted theoretically from a model using the initial H_2SO_4 concentration without a correction for wall losses.

Our model considered 3 different numbers of NH_3 molecules taken up by each molecule of H_2SO_4 during particle formation. All three tested degrees of neutralization provided results that are in good agreement with the experimental data and all of them capture the trends in the growth rate values in a similar manner (see Fig. 30). The highest growth rates were achieved for ammonium sulphate particles. The numerical results indicate that the presence of NH_3 enhances the growth of a freshly formed aerosol. Overall, the model predicts the growth rates of newly formed particles very well, despite the fact that the model slightly overestimates the growth rates at a residence time of 90 s (Fig. 31).

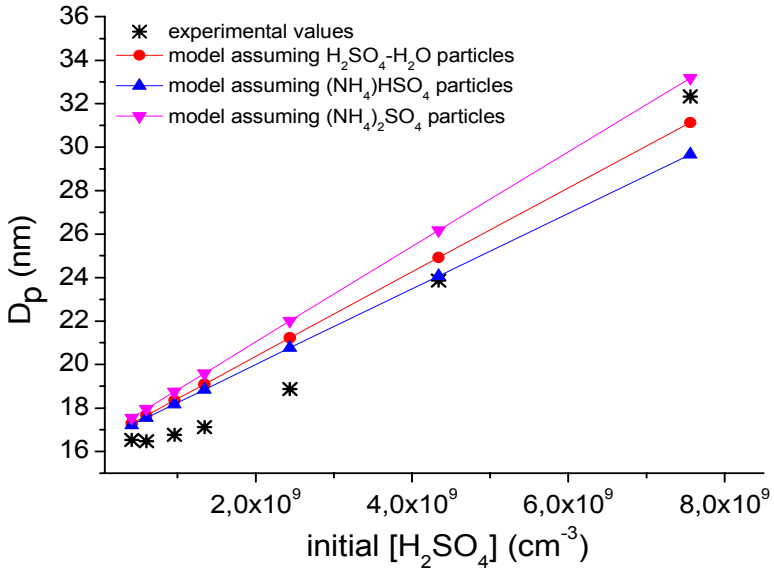

Fig 31: The comparison of the experimental median particle diameters determined from a measurement conducted at T=283 K, with a RH of ~30% and a residence time of 90 s and the values predicted theoretically from a model using the initial H_2SO_4 concentration without a correction for wall losses. As can be seen, the model overestimates the growth rates slightly in the case of experiments conducted at a residence time of 90 s.

An indirect way to determine the H_2SO_4 concentration in experimental devices is based on the measured growth rates of the freshly formed particles. The H_2SO_4 concentrations in our study derived solely from the growth rates determined experimentally and verified in our model indicate that the commonly assumed wall losses of H_2SO_4 on the inner surfaces calculated from Eq. (6) are not as significant as previously believed in case of long-lasting steady state experiments. Our observations suggest that the wall is not an infinite sink for H_2SO_4, but that there is also a flux of H_2SO_4 from the wall to

the flow tube. For example in the study by Hanson and Eisele (2000), the wall of a laminar flow tube was found to be a significant source of H_2SO_4 at a RH of <0.5% and the concentration of H_2SO_4 from the wall reached up to 3×10^8 molecule cm^{-3}. Another possible explanation for the discrepancy between the H_2SO_4 concentrations calculated from Eq. (6) and that leading to our experimental growth rates might be the limited adsorption capacity of the wall. The wall becomes saturated with H_2SO_4 during experiments and therefore further adsorption of H_2SO_4 molecules might be hindered after a certain time period. We estimated the "real" wall losses of H_2SO_4 in the flow tube by matching the predicted and observed growth rates through tuning the initial H_2SO_4 concentration in the model. Although the estimated wall losses were slightly scattered for different experimental conditions (RH, temperature and residence time), a reasonable agreement found for the experimental and modelled data yields an estimation of the wall losses to be ~10% for a residence time of 45 s, ~15% for a residence time of 60 s and ~25% for a residence time of 90 s, corresponding to WLFs of 1.11, 1.18 and 1.33, respectively.

3.3 Conclusions

In conclusion, we presented the results of an experimental study of sulphuric acid - water nucleation and nanoparticles growth. The main achievement of this experimental part is determination of the growth rates of newly formed particles and its dynamics under different conditions. The obtained growth rates were found to increase significantly with increasing H_2SO_4 concentration, which is in agreement with atmospheric observations. A slightly enhancing effect of increased temperature on growth rates was observed, whereas the effect of RH was not consistent - at lower H_2SO_4 concentrations the growth rates were higher under dry conditions and with increasing H_2SO_4 concentrations the growth rates were higher under wet conditions. The residence time was found to have a negligible effect on the growth rates. These experiments provide a dataset for comparison with the theoretical predictions of particle growth. Our experimental growth rates show a good agreement with a model, which accounts for the condensation of H_2SO_4, H_2O and NH_3 and investigates 3 different extents of neutralization of formed H_2SO_4 and H_2O particles by NH_3. Furthemore, the comparison of these experimental results with atmospheric observations is of special importance for identification of the compounds involved in the early growth of nucleated particles in different types of atmospheric environment. Our results show that H_2SO_4 is dominant condensating vapour involved in nanoparticles growth only in polluted and SO_2 rich environments. Presence of other condensating species is therefore assumed in order to fully explain field growth rates, which is an important atmospheric implication.

In addition to above described experiments dedicated to observation of growth dynamics of freshly nucleated particles, we also discussed the diffusional wall losses of H_2SO_4 in the flow tube. Due to long-lasting experiments (the experimental setup was run for more then a month without an interruption), the measurements are believed to be performed under close to wall-equilibrium conditions. We therefore speculate that the wall of the flow tube is not an infinite sink for H_2SO_4 molecules, but that there is also a flux of H_2SO_4 from the wall into the tube, which is more intense under dry conditions. The correct determination of the sulphuric acid concentration in nucleation measurements is a crucial factor for subsequent analysis and data interpretation. Our results show that neglecting the flux of H_2SO_4 from the wall may cause a significant underestimation of the residual H_2SO_4 concentration.

4 Atmospheric observation of new particle formation and particle shrinkage

We introduce atmospheric observations of new particle formation and growth of newly formed particles in this chapters. The measurements reported here were carried out at urban background station Prague - Suchdol. There are long-term observations of particle number size distributions from this station, starting in November 2007. Because the basic characteristics of observed new particle formation events, the measured growth rates and their variability have been reported from this site previously (Řimnáčová, 2011), we focused in our analysis on a recently reported phenomenon - a particle shrinkage following previous new particle formation event. More specifically, we will address the following issues: a) to study the seasonal variation of particle shrinkage events b) to investigate the connection of particle shrinkage to ambient conditions and to find the processes favouring this phenomenon.

4.1 Methodology

Measurement site

The measurements, reported here, were performed between May 2012 and April 2014 at the urban background station Prague - Suchdol (50.13°N, 14.38°E). The site is located in a northwest suburb approximately 5 km from the city centre (Fig. 32). The Prague region is densely populated (2357.6 inhabitants per km^2 (Czech Statistical Office, 2013)) and industrialized. The station is located on the edge of a plateau above Prague with an altitude of 277 m above sea level on the campus of the Institute of Chemical Process Fundamentals (ICPF). The site is exposed to emissions from local sources including residential houses (~30 m from the site), traffic from the nearest road – distance approximately 250 m (daily traffic ~15,000 cars) and the Václav Havel Airport Prague, located 9 km to the southwest. As mentioned above, long-term continuous sampling of aerosol particle size distributions using SMPS and Aerodynamic Particle Sizer (APS) spectrometers covering the range of diameters from 10 nm to 15 μm has been performed at this site. This campaign is focused on studying the particle number size distributions, its dynamics and dependence on ambient conditions. The results of a 2-year-long continuous measurement campaign (November 2007 to October 2009) are summarized in Řimnáčová et al. (2011). The observed particle number size distribution was often found to be bimodal with the peaks in the Aitken (25–

100 nm) and accumulation (> 100 nm) size range and the peaks were sometimes overlapping each other. When NPF events were observed, the peak in the nucleation size range (< 25 nm) was dominant in the whole size distribution. The average background particle number concentration was ~ 4×10^3 cm^{-3}, while the highest particle number concentrations were observed during NPF events reaching up to 2×10^5 cm^{-3}. When analysing the NPF events dynamics, the average values of J_{10} and GR_{10} were estimated to be 2.6 cm^{-3} s^{-1} and 5.4 nm h^{-1}, respectively. These values of nucleation and growth rates fall within the range of typical J and GR reported from field experiments (Kulmala et al., 2004). The NPF events were observed on 20.1% (136 days) of all measurement days and were much more frequent in the warmer periods of the year (spring and summer) than in the colder periods (autumn and winter). The observed frequency of NPF events is in line with values reported from other studies. For example, the Hyytiälä station, a regional background station in Finland with long-term time series of NPF events observations reports that the NPF event days account for 24.2% of all measurements days (Kulmala et al., 2004).

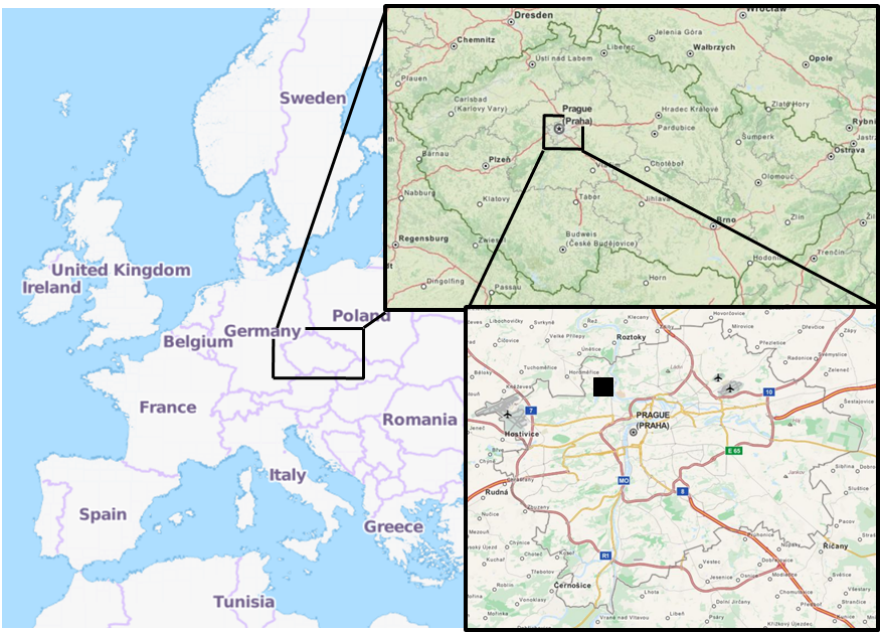

Fig. 32: The location of urban background station Prague – Suchdol. Figure taken from Skrabalova et al. (2015).

Sampling and instrumentation

The concentrations of atmospheric aerosol, used in this study, were measured using a Scanning Mobility Particle Sizer (SMPS), determining the particle number size distribution (PNSD) in the submicron size range, and providing information on the raw mobility size distributions and on the diagnostic parameters of the instrument as well. The diagnostic file consists of the values of temperature, relative humidity, absolute pressure, and flows of both aerosol and sheath air. The SMPS 3034 (TSI, USA) has been used in an upgraded version, so it meets the quality standards for ultrafine aerosol measurement networks described in Wiedensohler et al. (2012). The quality assurance is based on temperature and relative humidity in the SMPS system, and on the aerosol and sheath flow rates. The PNSD were computed using BY-HESS LabView shareware application software from the raw data and diagnostic files. The BY-HESS inversion routine is based on multiple charge inversion (Pfeifer et al., 2014) and contains also corrections on the Condensation Particle Counter (CPC) counting efficiencies (inbuilt CPC 3010, TSI, USA was used), particle losses in the connecting tubes and inside the SMPS, based on an equivalent pipe length (Wiedensohler et al., 2012), and Differential Mobility Analyser (DMA) transfer function (TSI 3034 DMA with 32.7 cm active length). At the given flows (1 l min^{-1} of aerosol flow and 4 l min^{-1} of sheath flow), the PNSD in the size range between 6.5 and 540 nm was measured every 5 minutes; due to the measurement uncertainties at both edges of the distribution, only PNSD between 10 and 500 nm were considered. In addition to the SMPS data, basic meteorological data (temperature, global radiation, relative humidity, wind speed and wind direction) from the meteorological station located in the same measurement container of automated immission monitoring (AIM) on the campus of ICPF were available. Also the concentrations of gaseous pollutants, namely sulphur dioxide (SO_2), nitric monoxide (NO), nitric dioxide (NO_2), ozone (O_3), carbon monoxide (CO), toluene, benzene, PM_{10} and $PM_{2.5}$ measured at AIM station by the Czech Hydrometeorological Institute (CHMI), were added to the analysis.

Data treatment

The whole measurement campaign was focused on studying of PNSD and processes influencing its dynamics, especially NPF events and the growth of the newly formed particles. The classification of NPF events was conducted according to the criteria proposed in Dal Maso et al. (2005). For this analysis, two years of data were taken (from May 2012 to April 2014). The daily contour plots of particle number size distributions, obtained by the inversion of raw SMPS data and the daily plots of the positions of the modes of the

multimodal distributions were considered. The method, used to determine the mode position using mathematical gnostics is described in Ždímal et al., (2008). Each measurement day was classified into one of the following categories: event day (a day when NPF event was observed), non-event day (no NPF event), undefined (nucleation was observed, but was not classified as NPF), or missing (when the SMPS scan was incomplete). NPF events are characterized by the appearance of freshly formed particles in the nucleation mode and the continuous growth of nucleated particles for at least several hours. Particle shrinkage presents the continuous decrease of the geometric mean diameter of the grown particles following a previous NPF event lasting for at least 2 hours. The identification of particle shrinkage was performed visually from the contour plots of the days with the NPF event. The identification was based on several distinct features of temporal changes of the particle size distributions and particle sizes. To illustrate the variability of PNSD and modes location, the plots of different classification categories are depicted in Figs. 33 and 34.

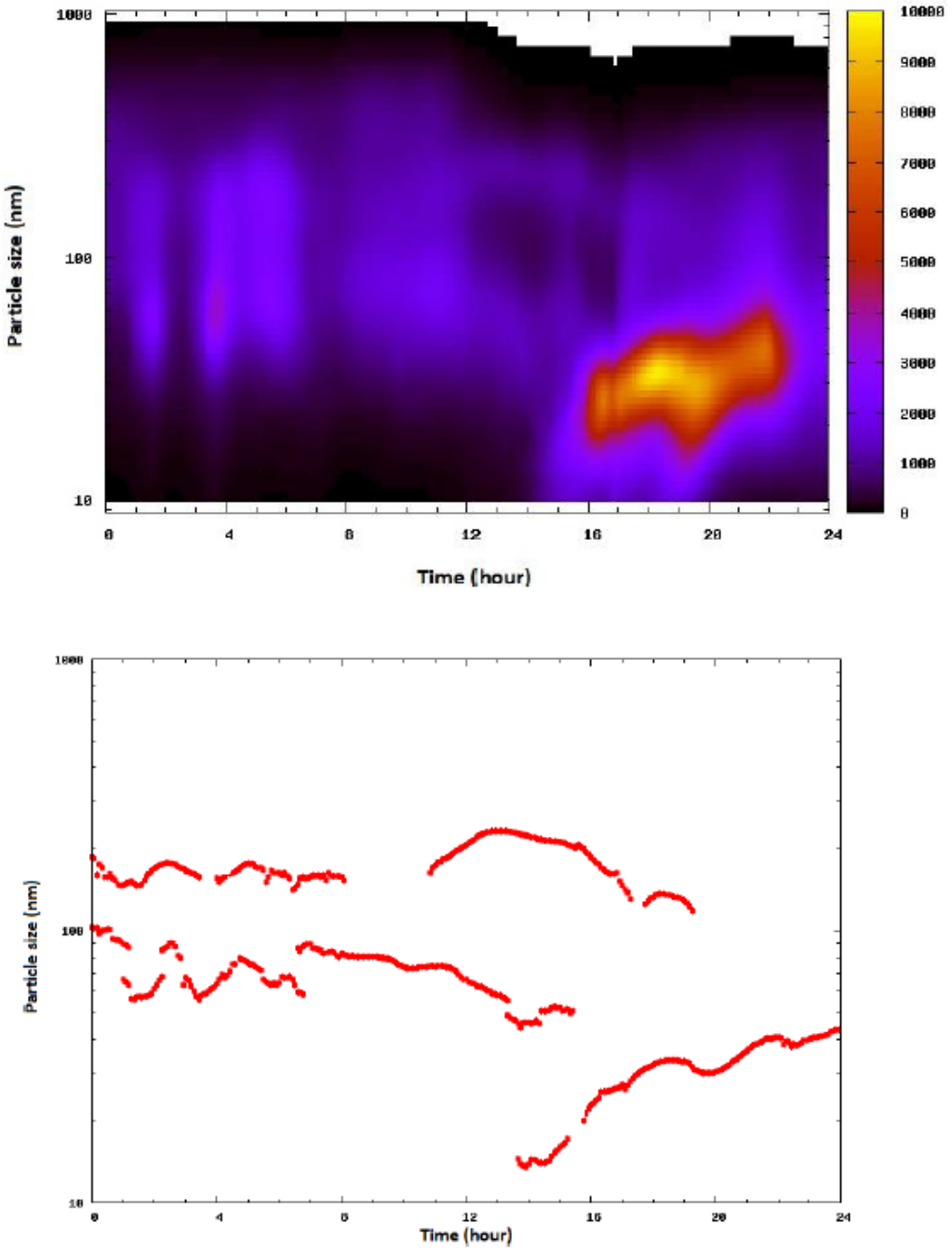

Fig. 33: An example of daily colour map of particle number size distribution and exhibition of modes positions on NPF event day.

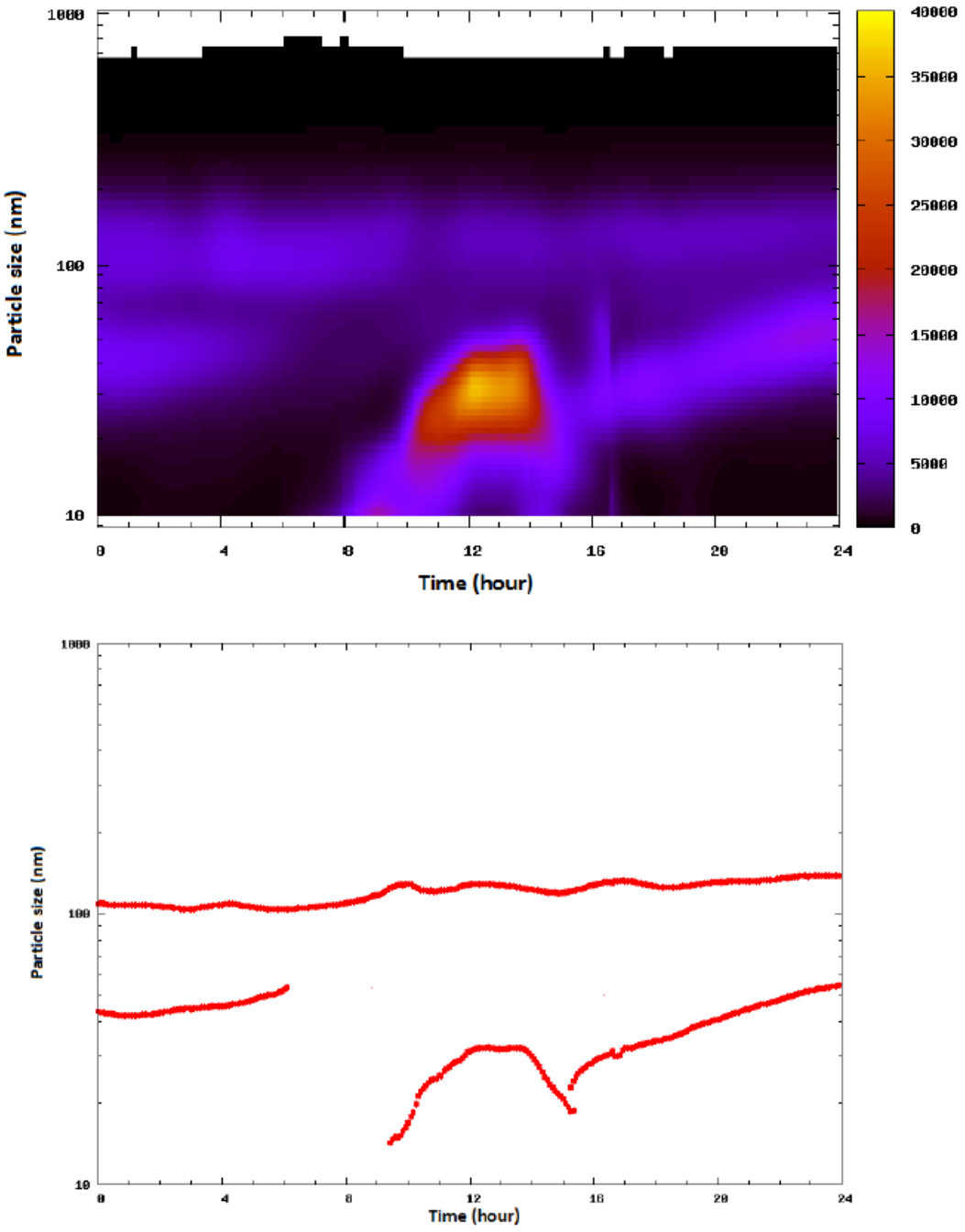

Fig. 34: An example of daily colour map of particle number size distribution and exhibition of modes positions on particle shrinkage event day.

Determination of particle shrinkage rate, condensational sink and H_2SO_4 proxy concentration

Concentrations of different precursors as well as the concentration of the pre-existing particles influence both NPF and subsequent growth of nucleated particles. In order to assess these interactions, some of the parameters characterizing these processes were determined. Condensational sink (CS) is a measure of the loss rate of condensable vapours onto the pre-existing aerosol. An elevated concentration of pre-existing aerosol particles can supress atmospheric nucleation due to the scavenging of freshly nucleated particles and condensable vapours. CS was calculated using size distributions measured with the SMPS as follows (Kulmala et al., 2001):

$$\mathrm{CS} = 2\pi D \sum \beta \mathrm{m}(D_{\mathrm{p,i}}) D_{\mathrm{p,i}} N_{\mathrm{i}}, \qquad (14)$$

where D is the diffusion coefficient of the vapour considered, $D_{\mathrm{p,i}}$ is the diameter of the particles in the size bin i and N_{i} is the number concentration of these particles. The term βm presents the transition regime correction factor for mass transfer and was calculated according to the equation given in Fuchs and Sutugin (1970) with a value of 1 for the mass accommodation coefficient. When calculating CS, the condensable species were assumed to have molecular properties of H_2SO_4 and thus negligible saturation vapour pressure corresponding to the assumption that H_2SO_4 behaves as a non-volatile vapour.

H_2SO_4 is the key component of atmospheric NPF (Sipilä et al., 2010; Brus et al., 2011). To investigate the connection of NPF events and growth dynamics to ambient sulphuric acid, the proxy of H_2SO_4 concentration presented in Petäjä et al. (2009) was determined:

$$[\mathrm{H_2SO_4}] = k.\ [\mathrm{SO_2}].\ \mathrm{GR/CS}, \qquad (15)$$

where $[SO_2]$ is the SO_2 concentration, GR is the intensity of solar radiation (both variables obtained from the measurements) and CS is the condensational sink of H_2SO_4 by pre-existing aerosols. Since this calculation of H_2SO_4 proxy concentration is based on measurements in a boreal forest in Finland (Petäjä et al., 2009), the absolute values of the proxy $[H_2SO_4]$ should be considered as indicatory $[H_2SO_4]$ only.

As mentioned above, the main focus of this study was to investigate the particle shrinkage. The shrinkage rate was determined using the mode fitting method presented in Dal Maso et al. (2005). The number size distributions obtained from the SMPS measurement were fitted with log-normal distribution and the geometric mean diameter (GMD) of the nucleation mode was

determined. The particle shrinkage rates were then obtained from the change of the modal GMD as a function of time:

$$\mathrm{SR} = \frac{\Delta(GMD)}{\Delta(t)}. \qquad (16)$$

4.2 Results

NPF and particle shrinkage events frequency and seasonal variability

The frequency of the NPF events during the measurement period was investigated. They occurred on 183 days, which represents 25% of all the considered days. Atmospheric nucleation is thus relatively often observed phenomenon at Prague - Suchdol site. The NPF frequency also exhibits significant seasonal variation. In spring (March – May) and summer (June - August) the frequencies were similar to each other with values of 38% and 32%. The occurrence of NPF events was considerably lower in Autumn (September - November) and Winter (December - February) accounting for 16% and 14%, respectively. The seasonal variability was similar in both campaign years. Řimnáčová et al. (2011), who analysed two-year PNSD dataset from Prague - Suchdol site reported NPF events to occur on 136 days, which represents 20% of all relevant days. Local features, i.e. meteorological or atmospheric conditions as well as pollution sources, are known to influence annual frequency and seasonal variability of NPF events reported from various sites. However, the NPF frequencies observed in our study are similar to those reported from other urban stations. Qian et al. (2007) analysed a two-year dataset of particle size distributions from urban station in St. Louis, USA and observed NPF events to occur on 24% of all days. Similar results are reported from Budapest (Salma et al., 2011), where NPF events were recorded on 27% of all days.

As mentioned above, since the observations of NPF events, particle growth rates and their variability have been reported from Prague – Suchdol site previously (Řimnáčová et al., 2011), we focused in our study on investigation of recently reported phenomenon - a particle shrinkage following previous NPF event. To clasify atmospheric nucleation as NPF event, a growth of nucleated particles must prevail at least for several hours. Recently, several studies have reported that under specific atmospheric conditions, which are unfavourable for the growth of freshly nucleated particles, a reversal process leading to particle shrinkage can occur. This phenomenon has been observed in Brazil (Backman et al., 2012), Taiwan (Young et al., 2013), Hong Kong (Yao et al., 2010) and Spain (Cusack et al., 2013). During the measurement period,

there were 22 particle shrinkage events following the NPF observed. The occurrence of particle shrinkage is strongly influenced by the seasonal variation of NPF events. The shrinkage events were most abundant during spring (50% of the total number of shrinkage event days) and summer (41%) and least in autumn (9%). No particle shrinkage was observed in the winter season. The particle shrinkage followed 12% of all observed NPF events. The study of Young et al. (2013) from Taiwan reports 14 NPF events and 5 shrinkage events following prior NPF during 137-day campaing. In their case the particle shrinkage followed 35% of observed NPF events, indicating that particle shrinkage might be an important process especially in warm climatic regions. Table 1 summarizes the frequencies of the NPF events and particle shrinkage events identified during the measurement period.

Table 1. Number of new particle formation and shrinkage events observed in different seasons (spring = March, April, May; summer = June, July, August; autumn = Sept., Oct., Nov., winter = Dec., Jan., Feb.)

season	NPF	% from all NPF event days	shrinkage event	% from all shrinkage events
spring	70	38%	11	50%
summer	58	32%	10	41%
autumn	29	16%	1	9%
winter	26	14%	0	0%

Observed particle shrinkage rates

The shrinkage rates were calculated using the Eq. (16). The determined shrinkage rates span the range from -2.5 to -12.5 nm h^{-1}. In the most intensive cases, the grown particles shrank back to the smallest measurable particle size of 10 nm. Both the minimum and the maximum shrinkage rates show slightly higher span of values from the ones reported in the earlier studies. The previously reported shrinkage rates were between -8.6 and -11 nm h^{-1} in Hong Kong (Yao et al., 2010), -5.1 and -7.6 nm h^{-1} in Taiwan (Young et al., 2013), -11 nm h^{-1} in Montseny, Spain (Cusack et al., 2013) and -5.2 nm h^{-1} in Sao Paulo, Brazil (Backman et al., 2012). Based on the analysis of 7 years of

particle size distribution measurements from Hyytiälä station in Finland, the growth rates of newly formed particles during NPF events were found to be dependent on particle size and have a clear seasonal pattern with the highest values during summer (Yli-Jutti et al., 2011). When analysing the seasonal variability of growth rates reported from Prague - Suchdol site (Řimnáčová, 2011), quite large spread of values was observed. Even though the growth rates tend to be somewhat higher during spring and summer time, no clear trend was observed and very high growth rates ≥ 10 nm h^{-1} were recorded in all seasons including winter. In this study, the seasonal variation of particle shrinkage was strongly influenced by the seasonal variation of NPF events. Although our results indicate that the shrinkage rates were highest during summer, it is not feasible to quantify this tendency owing to the limited number of observations (in particular for autumn and with no data available for the winter season).

Particle concentrations and size distributions evolution during particle shrinkage

The temporal change of the particle number size distribution of NPF directly followed by particle shrinkage has several characteristic features. At the beginning of NPF event, a distinctly new particle mode in the nucleation (≤ 25 nm) size range is observed, prevails for at least several hours and the newly formed particles grow to larger sizes by the condensation of various vapours. Under specific atmospheric conditions, which do not favour the further growth of the nucleated particles, a reversal process leading to particle shrinkage can occur. If so, the size of the grown particles starts to decrease when the geometric mean diameter of the nucleated particles reaches its maximum. In the most intensive cases, the particles shrank back to the smallest measurable sizes. These events, observed in Taiwan (Young et al., 2013) and Spain (Cusack et al., 2013), were characterized by an “arch-like” shape in the size distribution contour plots. An example of an intensive event, when the grown particles shrank back to the smallest detectable size of 10 nm is presented in Fig. 35 (a) - 35 (c).

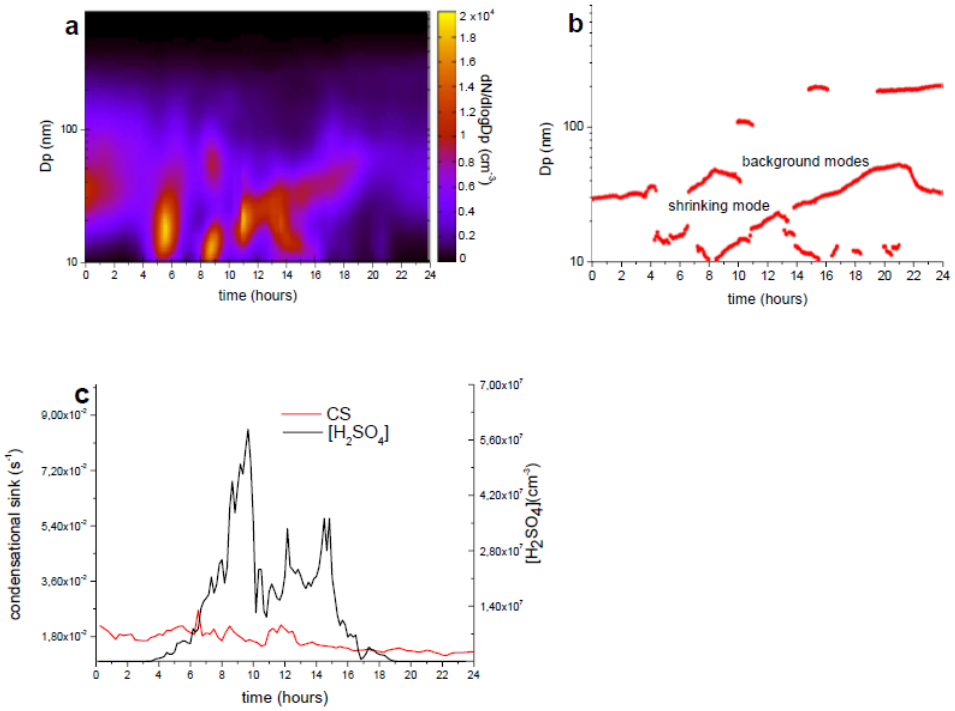

Fig. 35: The evolution of (a) particle size distribution, (b) modes location, (c) condensational sink and $[H_2SO_4]$ during the shrinkage event observed on 24 May 2013.

Intensive NPF events are characterised by a sharp increase of particle number concentration in the nucleation and Aitken modes. In our study, most of the particle shrinkage events following a previous NPF were found to exhibit a decrease of the particle number concentration in $N_{10\text{-}100}$ with a simultaneous decrease of particle size. However, in several cases an increase of the concentration of the particles with sizes < 30 nm with a decreasing geometric mean diameter was recorded during shrinkage. Yao et al. (2010) attributes this behaviour to a lower scavenging rate of the < 30 nm particles than the shrinkage rate of the particles with sizes > 30 nm. Young et al. (2013) who also recorded this phenomenon concluded that this behaviour was observed because of the arrival of new air masses (characterized by low condensational sink and SO_2-enrichment) due to atmospheric advection and mixing near the end of the particle shrinkage period, which might have initiated a new NPF event in new air mass. When comparing the particle number concentration at the end of the shrinkage period to the concentrations recorded at the onset of the NPF event, the vast majority of newly nucleated and grown particles was found to evaporate during intensive shrinkage events. In Fig. 36 (a) - 36 (c) the particle shrinkage recorded on 1 October 2013 is presented, where it is

evident that the particle number concentrations at the beginning of the NPF and at the end of particle shrinkage are almost identical.

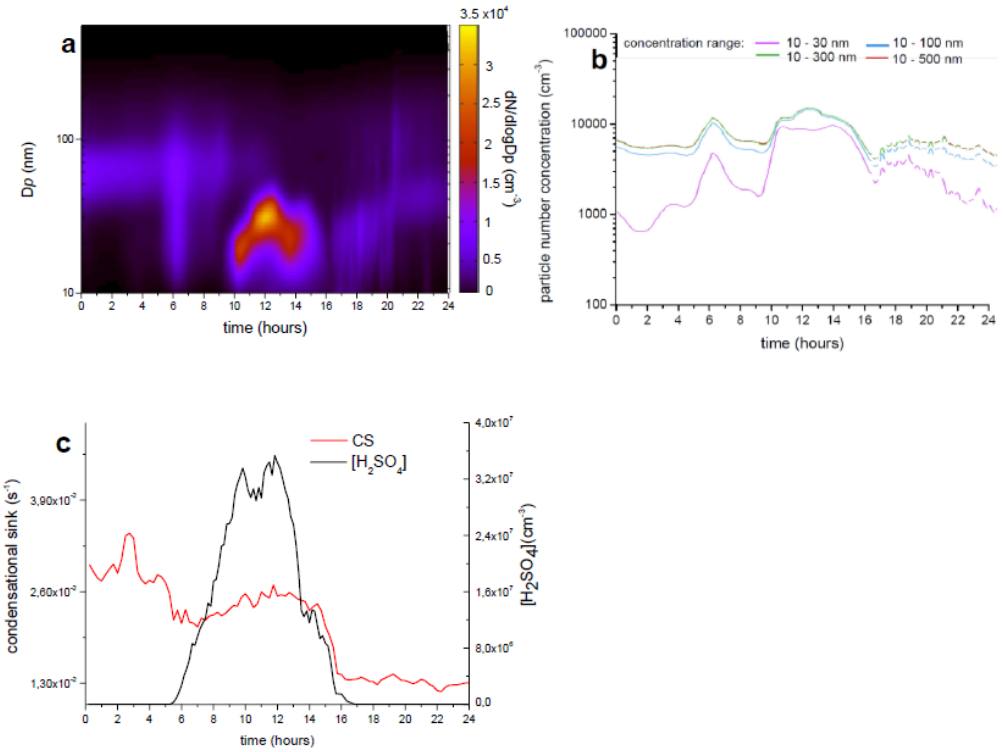

Fig. 36: The evolution of (a) particle size distribution, (b) total number concentrations, (c) condensational sink and [H_2SO_4] during the shrinkage event observed on 1 October 2013.

Particle shrinkage in relation to air pollutants concentration, H_2SO_4 proxy concentration and condensational sink

Atmospheric nucleation as well as particles growth are influenced by concentration of pre-existing aerosol and concentration of various gas phase species. The 10-minute averaged PM_{10}, $PM_{2.5}$, CO, NO_x, O_3, SO_2, benzene and toluene concentrations obtained from the automatic immission monitoring station (AIM) during particle shrinkage event days were therefore investigated. O_3 concentration had a distinct daily pattern with a rapid increase of [O_3] after sunrise followed by a decrease to a minimum concentration after sunset. In general, [O_3] was often found to decrease during particle shrinkage, with the lowest concentration at the end of the shrinkage event. This decrease of [O_3] was accompanied by lower global radiation causing decreased photochemical activity. No clear pattern in the PM_{10}, $PM_{2.5}$, NO_x, CO, benzene and toluene

concentrations variability during particle shrinkage was found – in some cases these concentrations were slightly increasing or decreasing, rapid hourly variations were observed several times and in few cases the concentrations were almost stagnant. The variation in concentrations can be attributed to the possible dilution of the air masses or arrival of polluted air during particle shrinkage; however, our observations indicate that the change in PM_{10}, $PM_{2.5}$, CO, NO_x, benzene and toluene concentrations does not affect particle shrinkage.

SO_2 is the precursor of gas phase H_2SO_4, which plays a key role in atmospheric nucleation and is also one of the major condensing vapours during early particle growth. Previous studies from Budapest (Salma et al., 2011) and Taiwan (Young et al., 2013) report that SO_2 concentration is not the limiting factor for NPF in urban environments, because SO_2 is always present in excess of the concentration needed for new particle formation. In this study, the SO_2 concentration was found to be rather stagnant during shrinkage events as compared to the observed concentration variability of other air pollutants (PM_{10}, $PM_{2.5}$, CO, NO_x, O_3, benzene and toluene) except for several events, which were accompanied by the arrival of polluted air masses with a subsequent distinct increase of $[SO_2]$. On the contrary, the proxy $[H_2SO_4]$ determined using Eq. (15) was found to have a distinct daily pattern since gas phase H_2SO_4 formation involves photochemical processes. The NPF burst was almost always preceded by an increase of the proxy $[H_2SO_4]$. On the other hand, $[H_2SO_4]$ was frequently observed to decrease during particle shrinkage, which is mainly due to lower global radiation, which was recorded during most of the particle shrinkage events. This trend is similar to the observed $[O_3]$ variation during shrinkage.

Condensational sink (CS) describes the loss of condensable vapours from gas phase onto the pre-existing particles and is proportional to the surface area of the aerosol particles. High CS might inhibit new particle formation and the growth of newly nucleated particles because a large fraction of the vapour could condense on larger particles. In our study, the beginning of NPF was often observed to coincide with the decrease of the condensational sink. CS then gradually increased over the course of the NPF and subsequent growth of the newly formed particles. On the contrary, particle shrinkage was often found to commence with decreasing CS, which could indicate air mixing leading to a lower concentration of volatile and semi-volatile vapours. A decrease of the concentration of these species might promote a subsequent evaporation of the volatile and semi-volatile vapours from the grown particles. This behaviour was

also observed in previous studies of particle shrinkage (Young et al., 2013; Cusack et al., 2013).

Meteorological conditions favouring particle shrinkage

Particle shrinkage following a previous NPF occurs under specific atmospheric conditions, which do not favour further particle growth. This phenomenon has been observed in both urban (Yao et al*.,* 2010; Backman et al., 2012; Young et al*.,* 2013) and regional background (Cusack et al*.,* 2013) stations. All particle shrinkage observations have so far been made in subtropical (Yao et al., 2010; Backman et al*.,* 2012; Young et al*.,* 2013) or a hot Mediterranean region (Cusack et al*.,* 2013) and the measurements in a mild climatic region have been reported for the first time in Skrabalova et al. (2015).

Particle shrinkage reported from studies, which provide precise meteorological information during shrinkage events (Backman et al., 2012; Young et al., 2013, Cusack et al*.,* 2013), have several common features. In general, particle shrinkage events appeared to start under intensive solar radiation, high ambient temperature and atmospheric dilution. A consistent feature of our observations is the global radiance (GR) dynamics. The vast majority of particle shrinkage events observed in our study started either at peak global radiation intensity, decreasing gradually over the course of shrinkage or at peak GR followed by a sharp drop in intensity. Similar variability has been reported from Brazil (Backman et al*.,* 2012) and Spain (Cusack et al*.,* 2013). Lowering global radiance intensity is also the reason for the decreasing concentrations of [O_3] and the proxy [H_2SO_4] recorded during most of the shrinkage events. Intensive solar radiance may initiate particle shrinkage due to the evaporation of condensed species from particles (Cusack et al., 2013), whereas a significant drop of GR intensity may interrupt a previously initiated growth process due to lower photochemical activity. The observed values of wind speed were quite variable - some shrinkage events occurred under almost stagnant air with wind speeds as low as 0.5 m s^{-1} while in other cases the wind speed reached up to 4 m s^{-1}. Previous observations have reported particle shrinkage taking place under relatively high ambient temperatures of ~18°C and above. In our study, the temperatures during shrinkage events ranged from 12°C to 27°C, however most events occurred at temperatures from 20 to 24°C. This temperature dependency also explains the observed seasonal variability - only 1 event was observed in autumn and none in winter. Evaporation of both organics (Denjean et al., 2015) and NH_4NO_3 (Dassios and Pandis, 1999) was observed to increase with increasing temperature. Our observations suggest that the evaporation of organics and NH_4NO_3 might be significantly hindered under ~12°C and temperature is very

likely one of the limiting factors for shrinkage events seasonal variability. Relative humidity was measured in a relatively wide range from 30 to 77% and was found to both increase and decrease during particle reverse growth.

When analysing the data set, we attempted to find some patterns in the particle shrinkage observations and possible correlation with meteorological parameters. Atmospheric nucleation rate *J*, which presents the formation rate of newly nucleated particles, reported from various NPF field studies, was often observed to correlate with ambient [H_2SO_4] and the dependence has been found to obey a power-law form with an exponent of 1 or 2 (Kulmala and Kerminen, 2008). The rate at which nucleated particles shrunk under certain size, for example < 30 nm, was therefore investigated. However, the number concentration of shrinking particles was observed to both increase and decrease along with decrease of geometric mean diameter of these particles. This process thus requires a complex model involving interactions with pre-existing aerosol and cannot be described by a simple correlation.

We also focused on the dependence of observed shrinkage rates on the meteorological variables. Investigating of 7-year long dataset of NPF and growth rates from Hyytiälä station in Finland revealed, that the growth rates of newly formed particles in range from 7 to 20 nm h^{-1} have a positive correlation with temperature (0.39) and UVB intensity (0.35), but did not have a notable correlation with any other variable (wind speed, RH, ambient pressure) (Yli-Juuti et al., 2011). In case of the shrinkage rates, the correlation factors were found to be negligible for relative humidity (R = -0.04) and wind velocity (R = -0.11), but showed the positive correlation with global radiation (R = 0.21) and temperature (R=0.24) (Fig. 37). However, since the shrinkage rate was calculated for the whole shrinkage period, the corresponding meteorological variables were averaged over the same period. T and RH were found to change only slightly during most of the shrinkage periods, but the opposite is truth for global radiation, which exhibited often sharp drops during particle shrinkage. Therefore the observed correlation between shrinkage rates and global radiation intensity may be spurious. Also the number of observations is low (a total of 22 shrinkage events) and a larger dataset would be therefore needed for deeper statistical analysis and verification of observed positive correlation of shrinkage rates with temperature and global radiation.

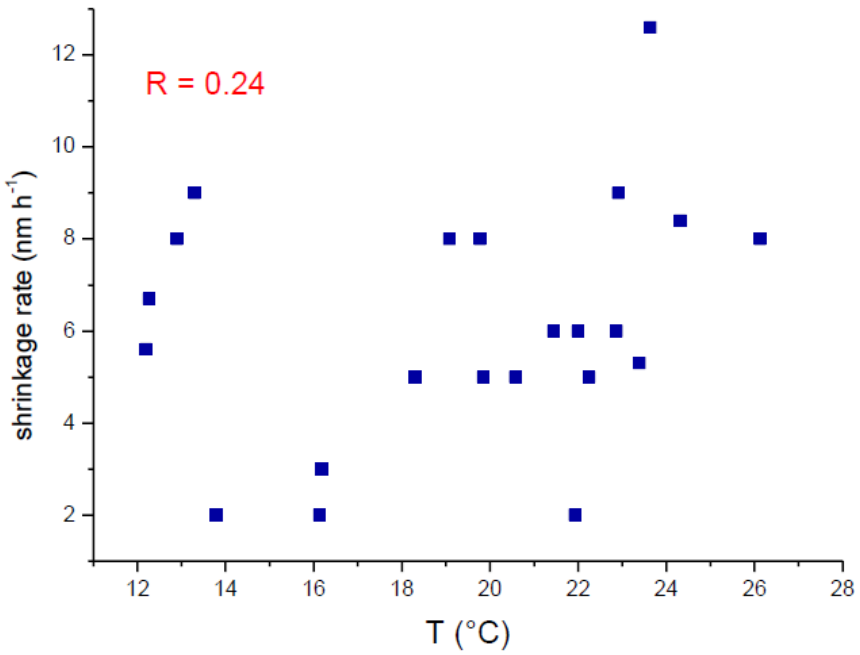

Fig. 37: A positive Spearman correlation coefficient R between shrinkage rates and temperature was observed, indicating that growing temperature is likely to enhance evaporation of previously condensed species from particles during shrinkage events.

Particle shrinkage mechanism

Several studies have recently focused on the chemical composition of particles grown after NPF. Bzdek et al. (2012) reports that NO_3^-, NH_4^+ and organics contribute to 54 - 59% of new particle growth, whereas sulphates are responsible for the remaining 41 - 46% of the observed growth. Smith et al. (2008) showed that the major compound of the newly formed particles are organics (~84%) and include organic acids (formate, acetate), hydroxyl organic acids and nitrogen-containing organic compounds. The vast majority of these organics are volatile or semi-volatile and can evaporate from the particles when the phase equilibrium favours the gas phase. Also the decrease of relative humidity can cause morphological changes resulting in particle size change. An example of such a reaction is the replacement of NH_3 with alkylamines in $(NH_4)_2SO_4$ resulting in formation of alkylaminium sulphates. This reaction causes the phase transition from the crystalline to the amorphous phase (Qui and Zhang, 2012), which enhances water uptake and consequently particle growth with increasing RH. This phase transition can be reversible with lowering relative humidity.

Yao et al. (2010), who report particle shrinkage in Hong Kong, attribute this behaviour to the evaporation of organics and NH_4NO_3 from the particles since these compounds can repartition between the gas and particulate phases. Backman et al. (2012) explained the observed particle shrinkage in Sao Paulo, Brazil by the evaporation of previously condensed species from particles when the precursor vapour concentration was decreased (likely due to dilution of air masses) and by the evaporation of NH_4NO_3. Although it was not possible to identify the chemical composition of the grown and shrinking particles from the available data, these processes are very likely the cause of the particle shrinkage observed in our study.

Organic species and NH_4NO_3 have different timescales of evaporation. The partitioning of atmospheric submicron NH_4NO_3 particles between the aerosol and gas phase was estimated to proceed in the time range from a few seconds to 15 minutes depending on the ambient temperature (Dassios and Pandis, 1999). The evaporation of organics was observed to proceed much slower. Grieshop et al. (2007) studied the dilution-induced evaporation of laboratory produced secondary organic aerosol (SOA) formed by α-pinene ozonolysis in a chamber study. The system was observed to reach evaporation equilibrium within two and half hour. The obtained relatively slow evaporation rate was attributed to the formation of low volatility oligomers. Another study (Vaden et al., 2011) studied evaporation kinetics of laboratory SOA produced by reaction of α-pinene with O_3 and atmospheric SOA. They concluded that the SOA evaporation has two separated regimes: a fast regime, which takes ~100 minutes and a second, very slow regime, which lasts more than a day. The SOA evaporation was also observed to be almost size independent and did not follow the evaporation of a liquid droplet indicating that the SOA particles were coated. However, the atmospheric particles contain wide range of organic and inorganic compounds and the chemical composition governs aerosol properties i.e. hygroscopicity or volatility. Several recent studies (Hakkinen et al., 2014; Yli-Jutti et al., 2013) report that the volatility of organic acids is influenced by the presence of inorganic salts in aerosol particles. Deeper investigation is therefore needed to gain a better insight into the particle phase chemistry and its influence on aerosol particles partitioning and aerosol mass loadings.

Case study of particle shrinkage events

Backman et al. (2012), who report particle shrinkage from Brazil, speculate that the decrease of vapour concentration due to changing atmospheric conditions is more rapid than the decrease of vapour concentration caused by lower photochemical activity. Intensive atmospheric mixing would thus

promote evaporation from particles more effectively when compared to lower global radiation and would also enhance shrinkage rates. In order to investigate this hypothesis, we present two particle shrinkage events, one which occurred under relatively stagnant atmospheric conditions and the other under atmospheric mixing.

On 13 July 2013, the start of morning NPF occurred at ~8:30 and the initial GMD of the particles was 11 nm (Fig. 38(a) - 38(f)). The NPF burst was followed by particle growth to 21 nm from 9:00 to 11:00 with a growth rate of 4.5 nm h^{-1}. The peak hourly concentration of particles in a size range of 10–30 nm reached 2.2×10^4 at 12:30. Between 11:00 and 15:00, the GMD decreased to 11 nm with a shrinkage rate of -2.5 nm h^{-1} and the $N_{10\text{-}30}$ decreased between 12:30 and 20:00 from 2.2×10^4 to 2.2×10^2. It is notable that the shrinkage of GMD occurred at ~11:00 when there was a sharp drop of global radiance intensity from 880 to 260 W m^{-2} likely due to a short period with cloud cover. This sharp decrease of GR intensity may have hindered the photochemical processes, thus lowering the condensable vapour concentrations and causing the reversal in the growth process and evaporation of particles. During the period of decreasing GMD between 11:00 and 15:00, there was a low wind speed of ~1.5 m s^{-1}, T increased from 20.6 to 22.7°C and RH decreased from 52 to 42%. These conditions further enhanced the particle evaporation. There were only slight changes in the air pollutants concentrations, implying no significant changes in air masses. The meteorological conditions were therefore very likely the driving force of the observed particle shrinkage event.

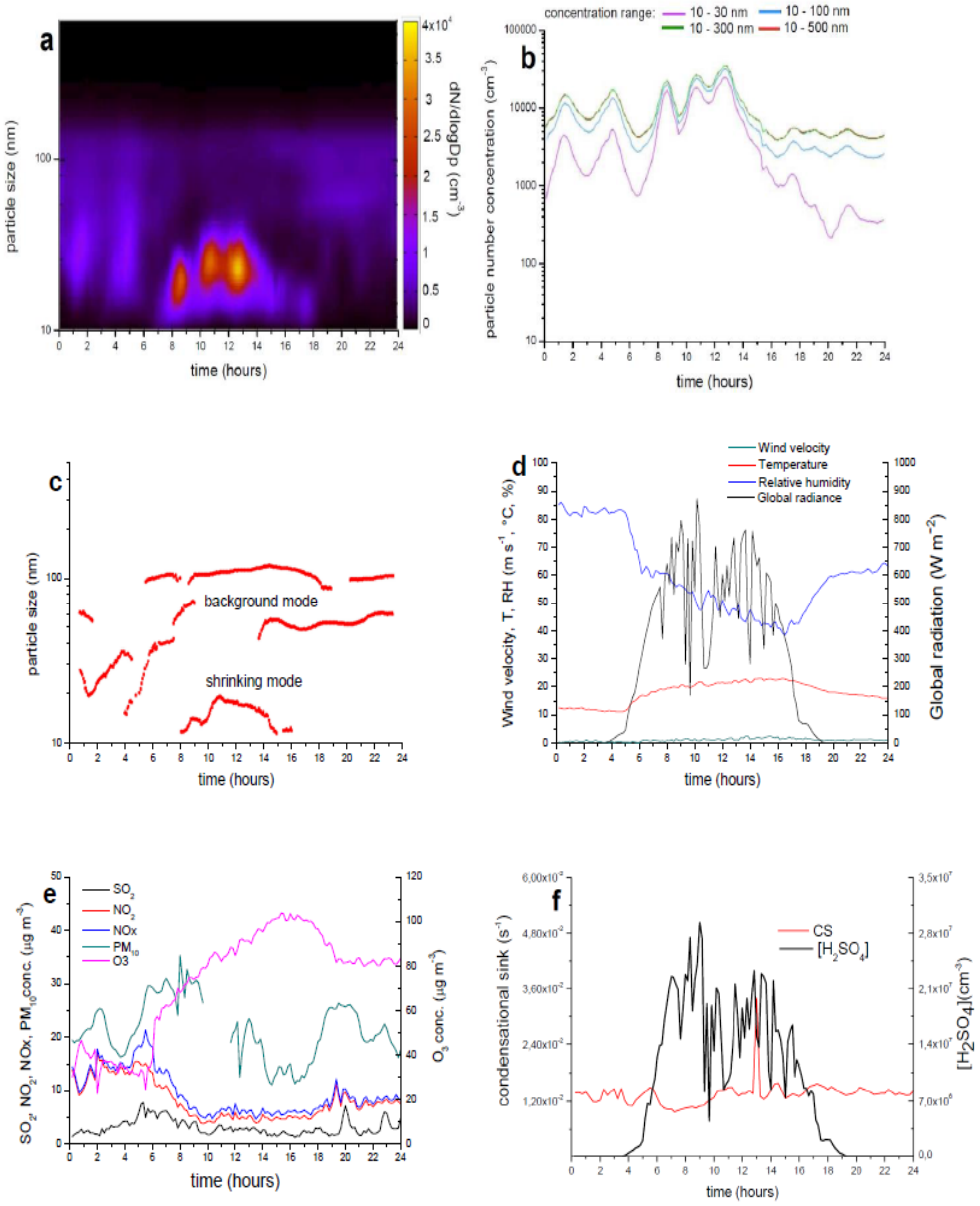

Fig. 38: The evolution of (a) particle size distribution, (b) total number concentrations, (c) modes location, (d) meteorological parameters (e) air pollutants concentrations, (f) condensational sink and $[H_2SO_4]$ during the shrinkage event observed on 13 July 2013, where meteorological conditions are assumed to be the driving force of particle shrinkage.

On 7 July 2013 the nucleation particle burst started at 9:00 and was followed by intensive particle shrinkage (Fig. 39 (a) - 39 (f)). After the start of NPF, the GMD grew rapidly from 13 nm to 50 nm with a growth rate of 12 nm h^{-1}. The $N_{10\text{-}30}$ decreased sharply at the beginning of NPF as the particles were

growing to sizes over 30 nm and increased again significantly when the particles started to evaporate and lower in size. The GMD decreased during particle shrinkage from 50 nm to 25 nm between 12:00 and 14:00 with a shrinkage rate of -12.5 nm h^{-1} and $N_{10\text{-}30}$ reached its minimum value of 2.7×10^3 at 18:00. Similarly to the previously described event, the particle shrinkage occurred during a substantial drop of GR intensity from 844 to 287 W m^{-2} suggesting a period of a cloudy sky between 12:00 and 13:20, which might have interrupted the growth process. The dynamics of T and RH was similar to the previously described event - T increased from 23 to 24.9°C, RH decreased from 46 to 39% and the wind speed varied between 0.7 and 2 m s^{-1}. There were reductions in the air pollutants concentrations during the shrinkage period, which indicate atmospheric mixing leading to a decrease of the condensable vapour concentrations, which would further enhance particle evaporation.

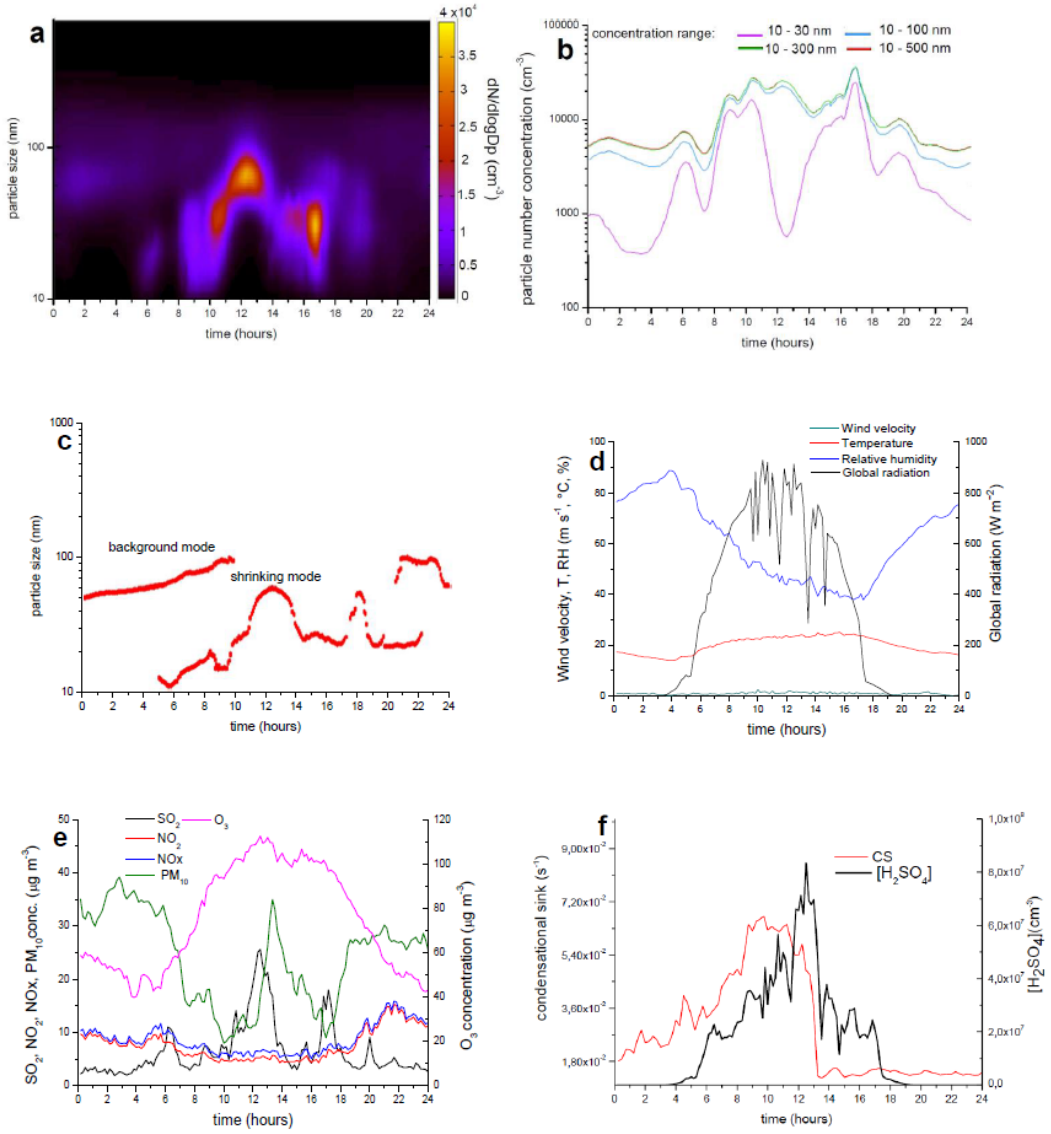

Fig. 39: The evolution of (a) particle size distribution, (b) total number concentrations, (c) modes location, (d) meteorological parameters and (e) air pollutants concentrations, (f) condensational sink and [H_2SO_4] during the shrinkage event observed on 7 July 2013, where particle shrinkage is assumed to be initiated by a meteorological condition change and further promoted by atmospheric mixing.

In general, particle shrinkage seems to appear when a significant shift in meteorological conditions interrupts the process of particle growth and in addition the reversal process leading to particle shrinkage is favoured by the ambient conditions. Furthermore, our results indicate that particle evaporation is very effectively enhanced under the conditions of atmospheric mixing. When comparing the 2 previously described shrinkage events, which occurred under similar meteorological conditions, we calculated the dew point temperature, which is a good indicator of the air mass origin (Kleinman et al., 2012). In both cases the dew point changed only slightly during particle shrinkage indicating no significant air mass changes. When comparing the concentrations of air pollutants, there were more significant changes in concentrations during particle shrinkage in the second case study. We conclude that in the second case study the particle shrinkage occurred under vertical mixing which very effectively enhanced particle evaporation and caused significantly higher shrinkage rates as compared to first case study. This observation is in agreement with the previously mentioned idea outlined in Backman et al. (2012) that the decrease of vapour concentration due to changing atmospheric conditions is more rapid than the decrease of vapour concentration caused by lower photochemical activity.

4.3 Conclusions

In conclusion, we observed the atmospheric nucleation and growth dynamics of newly formed particles at an urban background station Prague Suchdol. A special attention was given to a recently observed phenomenon - a particle shrinkage following previous new particle formation events. The particle shrinkage was attributed to specific atmospheric conditions unfavourable for the growth of nucleated particles. The lowered intensity of global radiance was identified as the most effective meteorological parameter contributing to particle shrikage. Also the occurrence of vertical atmospheric mixing was found to promote particle shrinkage very effectively. A large fraction of the originally condensed volatile and semi-volatile species is assumed to evaporate from the particulate phase during the shrinkage events. The particle shrinkage events thus not only directly influence the particle number concentrations, but also significantly affect the probability of nucleated particles to growth to cloud condensation nuclei sizes and subsequently participating in cloud formation processes.

5 Summary

In the last decades, the interest of scientists was attracted towards basic research of various physical phenomena, including phase transitions. The goal of this doctoral thesis was to explore the atmospheric particle formation via nucleation of sulphuric acid and water with emphasis on the growth dymanics of the formed particles including particle shrinkage. This work aims to unveil some of the mechanisms, which rule particle growth dynamics under various atmospheric conditions and to provide experimental growth rates dataset, which can be compared with atmopsheric observations and with models. The system of interest - sulphuric acid and water was chosen, because it is the key component of atmospheric new particle formation and has also wide applications in industry.

First, the nucleation of sulphuric acid and water and subsequent growth of formed particles was investigated in laboratory study. A thorough exploration of dependence of growth rates on various experimental conditions was made. We also proposed a model, which predicts the particle growth rates and very good agreement with experimental values was observed. A comparison of experimental growth rates with atmospheric ones shows that species other than H_2O or H_2SO_4 are important for particle growth, which is an important atmospheric implication. To our best knowledge, our measurements provide the first comprehensive experimental dataset of growth rates of particles formed via sulphuric acid and water nucleation. These data can serve as a basis for detailed investigation of ternary species enhancement of particle growth, which has not been performed in a laboratory study yet.

The second study was focused on the investigation of the atmospheric nucleation and growth dynamics of newly formed particles with a special interest in a particle shrinkage following previous new particle formation events. Our results are indicative that the growth and shrinkage of newly formed particles are very sensitive to changing atmospheric and meteorological conditions and both the concentration and geometrical mean diameter of these particles may evolve significantly in a short time period. The particle shrinkage seems to be quite often observed phenomenon especially in warm climatic regions (tropic and subtropic) and can thus very significantly influence the total particle number concentration of atmospheric aerosol particles. Further investigation is therefore needed to gain an insight into processes governing new particle growth and shrinkage and overall magnitude of this process in the atmosphere.

Bibliography

Andreae, M. O. and Rosenfeld, D.: Aerosol-cloud-precipitation interactions. Part 1: The nature and sources of cloud-active aerosols. *Earth Sciences Reviews*. 2008, 89, p. 13-41.

Ayers, G. P., Gillett, R. W. and Gras, J. L.: On the vapor pressure of sulfuric acid. *Geophysical Research Letters.* 1980, 7, 6, p. 433-436.

Backman, J., Rizzo, L.V., Hakala, J., Nieminen, T., Manninen, H.E., Morais, F., Aalto, P.P., Siivola, E., Carbone, S., Hillamo, R., Artaxo, P., Virkkula, A., Petäjä, T. and Kulmala, M.: On the Diurnal Cycle of Urban Aerosols, Black Carbon and the Occurrence of New Particle Formation Events in Springtime Sao Paulo, Brazil. *Atmos. Chem. Phys*. 2012, 12: 11733–11751, doi: 10.5194/acp-12-11733-2012.

Ball, S. M., Hanson, D. R. and Eisele, F. L.: Laboratory studies of particle nucleation: Initial results for H_2SO_4, H_2O, and NH_3 vapors. *Journal of Geophysical Research*. 1999, 104, D19, p. 23709-23718, doi:10.1029/1999JD900411.

Becker R. and Döring. W.: Kinetische Behandlung der Keimbildung in Übersättigten. *Dämpfen. Ann. Physics*. 1935, 24: p. 719–752.

Benson, D. R., Young, L.H., Kameel, F. R. and Lee, S. H.: Laboratory-measured nucleation rates of sulfuric acid and water binary homogenous nucleation from SO_2 + OH reaction. *Geophysical Research Letters*. 2008, 35, L11801.

Benson, D. R., Erupe, M. E. and Lee, S.-H.: Laboratory-measured H_2SO_4-H_2O-NH_3 ternary homogeneous nucleation rates: Initial observations. *Geophysical Research Letters*. 2009, 36, L15818, doi:10.1029/2009GL038728.

Benson, D. R., Yu, J. H., Markovich, A. and Lee, S.-H.: Ternary homogeneous

nucleation of H_2SO_4, NH_3, and H_2O under conditions relevant to the lower troposphere. *Atmospheric Chemistry and Physics.* 2011, 11, p. 4755–4766, doi: 10.5194/acp-11-4755-2011.

Berndt, T., Böge, O., Stratmann, F., Heintzenberg, J. and Kulmala, M.: Rapid formation of sulfuric acid particles at near-atmospheric conditions. *Science,* 2005, 307 (5710): 698 – 700.

Berndt, T., Stratmann, F., Sipilä, M., Vanhanen, J., Petäjä, T., Mikkilä, J., Grüner, A., Spindler, G., Lee Mauldin III, R., Curtius, J., Kulmala, M. and Heintzenberg, J.: Laboratory study on new particle formation from the reaction OH + SO_2: influence of experimental conditions, H_2O vapour, NH_3 and the amine tert-butylamine on the overall process. *Atmospheric Chemistry and Physics.* 2010, 10, p. 7101–7116, doi:10.5194/acp-10-7101-2010.

Berndt, T., Sipilä, M., Stratmann, F., Petäjä, T., Vanhanen, J., Mikkilä, J., Patokoski, J., Taipale, R., Mauldin R. L. III and Kulmala, M.: Enhancement of atmospheric H_2SO_4 / H_2O nucleation: organic oxidation products versus amines. *Atmospheric Chemistry and Physics.* 2014, 14, p. 751-764.

Biskos, G., Buseck, P. R. and Martin, S. T.: Hygroscopic growth of nucleation-mode acidic sulfate particles. *Aerosol Science*. 2009, 40, p. 338-347.

Brus D., Hyvärinen A.-P., Ždímal V., Lihavainen H.: Homogeneous Nucleation Rate Measurements of 1-Butanol in Helium: A Comparative Study of a Thermal Diffusion Cloud Chamber and a Laminar Flow Diffusion Chamber. *Journal of Chemical Physics.* 2005, 122, p. 214506.

Brus D., Ždímal V., and Smolík J.: Homogeneous nucleation rate measurements in supersaturated water vapour. *Journal of Chemical Physics. 2008,* 129, p. 174501.

Brus, D., Hyvärinen, A.-P., Viisanen, Y., Kulmala, M., and Lihavainen, H.: Homogeneous nucleation of sulfuric acid and water mixture: experimental setup and first results. *Atmospheric Chemistry and Physics*. 2010, 10, p. 2631-2641, doi:10.5194/acp-10-2631-2010.

Brus, D., K. Neitola, T. Petäjä, J. Vanhanen, A.-P. Hyvärinen, M. Sipilä, P. Paasonen, H. Lihavainen and M. Kulmala: Homogenous nucleation of sulfuric acid and water at atmospherically relevant conditions. *Atmospheric Chemistry and Physics*. 2011a, 11, p. 5277–5287, doi:10.5194/acp-11-5277-2011.

Brus, D., Neitola, K., Petäjä, T., and Lihavainen, H.: Diffusion coefficient measurements of sulphuric acid in air. *Abstract 456, European Aerosol Conference, Manchester, UK*. 4.-9.9 2011b.

Bzdek, B.R., Zordan, C.A., Pennington, M.R., Luther III, G.W., and Johnston, M.V.: Quantitative Assessment of the Sulfuric Acid Contribution to New Particle *Growth. Environ. Sci*. 2012, Technol. 46: 4365–4373.

Charlson, R. J., Schwartz, S. E., Hales, J. M., Cess, R. D., Coakley, J. A., Hansen, J. E. and Hofmann, D. J.: Climate forcing by anthropogenic aerosols. *Science*. 1992, 255, p. 423-430.

Cusack, M., Alastuey, A. and Querol, X.: Case Studies of New Particle Formation and Evaporation Processes in the Western Mediterranean Regional Background. *Atmos. Environ.* 2013, 81: 651–659.

Dal Maso, M., Kulmala, M., Riipinen, I., Wagner, R., Hussein, T., Aalto, P. P. and Lehtinen, K. E. J.: Formation and growth of fresh atmospheric aerosol: eight years of aerosol size distribution data from SMEAR II, Hyytiälä, Finland. *Boreal Environment Research*. 2005, 10, p. 323-336.

Dassios K.G. and Pandis S.N.: The Mass Accommodation Coeffcient of Ammonium Nitrate. *Aerosol. Atmos. Environ*. 1999, 33: 2993–3003.

Denjean, C., Formenti, P., Picquet-Varrault, B., Camredon, M., Pangui, E., Zapf, P., Katrib, Y., Giorio, C., Tapparo, A., Temime-Roussel, B., Monod, A., Aumont, B. and Doussin J.F.: Aging of Secondary Organic Aerosol Generated from the Ozonolysis of α-pinene: Effects of Ozone, Light and Temperature. *Atmos. Chem. Phys*. 2015, 15: 883–897.

Dusek, U., Frank, G. P., Hildebrandt, L., Curtius, J., Schneider, J., Walter, S., Chand, D., Drewnick, F., Hings, S., Jung, D., Borrmann, S. and Andreae, M.O.: Size matters more than chemistry for cloud-nucleating ability of aerosol particles. *Science*. 2006, 312, p. 1375-1378.

Ehn, M., Thornton, J. A., Kleist, E., Sipilä, M., Junninen, H. , Pullinen, I., Springer, M., Rubach, F., Tillmann, R., Lee, B., Lopez-Hilfiker, F., Andres, S., Acir, I. H., Rissanen, M., Jokinen, T., Schobesberger, S., Kangasluoma, J., Kontkanen, J., Nieminen, T., Kurtén, T., Nielsen, L. B., Jørgensen, S., Kjaergaard, H. G., Canagaratna, M., Dal Maso, M., Berndt, T., Petäjä, T., Wahner, A., Kerminen, V.-M., Kulmala, M., Worsnop, D. R., Wildt J. and Mentel, T. F.: A large source of low-volatility secondary organic aerosol. *Nature*. 2014, 506, p. 476–479, doi:10.1038/nature13032.

Erupe, M. E., Benson, D. R., Jingmin, L., Young, L. H., Verheggen, B., Al-Refai, M., Tahboub, O., Cunningham, V., Frimpong, F., Viggiano, A. A. and Lee, S. H.: Correlation of aerosol nucleation rate with sulfuric acid and ammonia in Kent, Ohio: An atmospheric observation. *Journal of Geophysical Research*. 2010, 115, D23216.

Fiedler, V., Dal Maso, M., Boy, M., Aufmhoff, H., Hoffmann, J., Schuch, T., Birmili, W., Hanke, M., Uecker, J., Arnold, F., and Kulmala, M.: The contribution of sulphuric acid to atmospheric particle formation and growth: a comparison between boundary layers in Northern and Central Europe, *Atmos. Chem. Phys.*, 2005, 5, 1773–1785.

Frenkel, D. and Smith, B.: Understanding molecular simulation: from algorithms to applications. 2nd edition. *Academic*: San Diego, CA, London, 2002.

Fuchs, N. A. and Sutugin, A. G.: Highly Dispersed Aerosols. Butteworth-Heinemann, Newton Mass., 1970.

Grieshop, A.P., Donahue, N.M. and Robinson, A.L.: Is the Gas-particle Partitioning in Alpha-pinene Secondary Organic Aerosol Reversible? *Geophys. Res. Lett.* 2007, 34: L14810.

Hakkinen, S.A.K., Faye McNeill, V. and Riipinen, I.: Effect of Inorganic Salts on the Volatility of Organic Acids. *Environ. Sci. Technol.* 2014, 48: 13718–13726.

Hanson, D.R. and F. Eisele: Diffusion of H_2SO_4 in Humidified Nitrogen: Hydrated H_2SO_4. *Journal of Physical Chemistry A*. 2000, 104, p. 1715-1719.

Hanson, D.R.: Mass Accommodation of H_2SO_4 and CH_3SO_3H on Water-Sulfuric Acid Solutions from 6% to 97% RH. *Journal of Physical Chemistry A*. 2005, 109, p. 6919-6927.

Heist, R. H. and He, H. H. *Journal of Physical and Chemical Reference Data*. 1994, 23, p. 781.

Herrmann, E., Brus, D., Hyvärinen, A.-P., Stratmann, F., Wilck, M., Lihavainen, H., and Kulmala, M.: A computational fluid dynamics approach to nucleation in the water-sulfuric acid–system. *Journal of Physical Chemistry A*. 2010, 114, p. 8033–8042.

Hinds W. C.: Aerosol Technology: Properties, Behavior and Measurement of Airborne Particles. John Wiley and Sons, Inc., 1999.

Hirsikko, A., Nieminen, T., Gagné, S., Lehtipalo, K., Manninen, H. E., Ehn, M., Hõrrak, U., Kerminen, V.-M., Laakso, L., McMurry, P. H., Mirme, A., Mirme, S., Petäjä, T., Tammet, H., Vakkari, V., Vana, M. and Kulmala, M.:

Atmospheric ions and nucleation: a review of observations. *Atmospheric Chemistry and Physics*. 2011, 11, p. 767–798, doi: 10.5194/acp-11-767-2011.

Hyvärinen, A.-P., T. Raatikainen, A. Laaksonen, Y. Viisanen, and H. Lihavainen, Surface tensions and densities of H_2SO_4 + NH_3 + water solutions. *Geophysical Research Letters*. 2005, 32, 16, L16806.

Kashchiev, D.: On the relation between nucleation work, nucleus size, and nucleation rate. Journal of Chemical Physics. 1982, 76, p. 5098–5102, doi:10.1063/1.

Kathman, S. M.: Understanding the chemical physics of nucleation. *Theoretical Chemistry Accounts*. 2006, 116, p. 169–182 DOI 10.1007/s00214-005-0018-8.

Kathmann, S. M., Schenter G. K., Garrett B. C., Chen B. and Siepmann J. I.: Thermodynamics and Kinetics of Nanoclusters Controlling Gas-to-Particle Nucleation. *Journal of Physical Chemistry C*. 2009, 113 (24), p. 10354–10370 DOI: 10.1021/jp8092226.

Katz, J. L. and Ostermier B. J.: Diffusion Cloud-Chamber Investigation of Homogeneous Nucleation. *The Journal of Chemical Physics*. 1967, 47 (2), 478-487.

Kerminen, V. M. and Kulmala, M.: Analytical fromulae connecting the real and apparent nucleation rate and the nuclei number concentration for atmospheric nucelation events. *Journal of Aerosol Science*. 2002, 33, p. 609 – 622.

Kerminen, V. - M. Petäjä, T., Manninen, H. E., Paasonen, P., Nieminen, T., Sipilä, M., Junninen, H., Ehn, M., Gagné, S., Laakso, L., Riipinen, I., Vehkamäki, H., Kurten, T., Ortega, I. K., Dal Maso, M., Brus, D., Hyvärinen, A.-P., Lihavainen, H., Leppä, J., Lehtinen, K. E. J., Mirme, A., Mirme, S., Horrãk, U., Berndt, T., Stratmann, F., Birmili, W., Wiedensohler, A., Metzger, A., Dommen, J., Baltensperger, U., Kiendler-

Scharr, A., Mentel, T. F., Wildt, J., Winkler, P. M., Wagner, P. E., Petzold, A., Minikin, A., Plass-Dülmer, C., Pöschl, U., Laaksonen, A. and M. Kulmala, M.: Atmospheric nucleation: highlights of the EUCAARI project and future directions. *Atmospheric Chemistry and Physics*. 2010, 10, 10829–10848, doi:10.5194/acp-10-10829-2010.

Kirkby, J., Curtius, J., Almeida, J., Dunne, E., Duplissy, J., Ehrhart, S., Franchin, A., Gagné, S., Ickes, L., Kürten, A., Kupc, A., Metzger, A., Riccobono, F., Rondo, L., Schobesberger, S., Tsagkogeorgas, G., Wimmer, D., Amorim, A., Bianchi, F., Breitenlechner, M., David, A., Dommen, J., Downard, A., Ehn, M., Flagan, R., Haider, S., Hansel, A., Hauser, D., Jud, W., Junninen, H., Kreissl, F., Kvashin, A., Laaksonen, A., Lehtipalo, K., Lima, J., Lovejoy, E., Makhmutov, V., Mathot, S., Mikkilä, J., Minginette, P., Mogo, S., Nieminen, T., Onnela, A., Pereira, P., Petäjä, T., Schnitzhofer, R., Seinfeld, J., Sipilä, M., Stozhkov, Y., Stratmann, F., Tomé, A., Vanhanen, J., Viisanen, Y., Aron Vrtala, A., Wagner, P., Walther, H., Weingartner, E., Wex, H., Winkler, P., Carslaw, K., Worsnop, D.,Baltensperger, U. & Kulmala, M.: Role of sulphuric acid, ammonia and galactic cosmic rays in atmospheric aerosol nucleation. *Nature*. 2011, 476, p. 429–433, doi:10.1038/nature10343.

Kleinman, L.I., Daum, P.H., Lee, Y.N., Lewis, E.R., Sedlacek A.J., Senum, G.I. Springston, S.R., Wang, J., Hubbe, J., Jayne, J., Min, Q., Yum, S.S. and Allen, G.: Aerosol Concentration and Size Distribution Measured Below, in, and Above Cloud from the DOE G-1 during VOCALS-Rex. *Atmos. Chem. Phys*. 2012, 12: 207–223, doi: 10.5194/acp-12-207-2012.

Korhonen, P., Kulmala, M., Laaksonen, A., Viisanen, Y., McGraw, R., and Seinfeld, J. H.: Ternary nucleation of H_2SO_4, NH_3 and H_2O in the atmosphere. *Journal of Geophysical Research.* 1999, 104, p. 26349–26353,

doi: 10.1029/1999JD900784.

Krejčí, P: Experimental Study of Homogeneous Nucleation in the Mixture of Water and Sulphuric Acid Vapours. Dizertační práce, České vysoké učení technické, 2010.

Kulmala M. and Laaksonen, A.: Binary nucleation of water-sulfuric acid system: Comparison of classical theories with different H_2S0_4 saturation vapor pressures. *Journal of Chemical Physics*. 1990, 93 (1), 11.

Kulmala, M, Toivonen, A., Mäkela, M and Laarsonen, A.: Analysis of the growth of nucleation mode particles observed in Boreal forest. *Tellus B: Chemical and Physical Meteorology.* 1998, 50, p. 449.

Kulmala, M., Pirjola, L. and Mäkelä, J. M.: Stable sulphate clusters as a source of new atmospheric particles. *Nature*. 2000, 404, p. 66–69.

Kulmala, M., Dal Maso, M., Mäkelä, J., Pirjola, L., Väkevä, M., Aalto, P., Miikkulainen, P., Hameri, K., and O'Dowd, C. D.: On the formation, growth and composition of nucleation mode particles. *Tellus B*, 2001, 53: 479–490.

Kulmala, M.: How particles nucleate and grow. *Science*. 2003, 302, p. 1000-1001.

Kulmala, M., Vehkamäki, H., Petäjä, T., Dal Maso, M., Lauri, A., Kerminen, V.-M., Birmili, W. And McMurry, P. H.: Formation and growth rates of ultrafine atmospheric particles: a review of observations. *Journal of Aerosol Science*. 2004, 35, p. 143-176.

Kulmala, M., Lehtinen, K. E. J., and Laaksonen, A.: Cluster activation theory as an explanation of the linear dependence between formation rate of 3 nm particles and sulphuric acid concentration. Atmospheric Chemistry and Physics. 2006, 6, p. 787–793.

Kulmala, M., Riipinen, I., Sipilä, M., Manninen, H. E., Petäjä, T., Junninen, H., Dal Maso, M., Mordas, G., Mirme, A., Vana, M., Hirsikko, A., Laakso,

L., Harrison, R. M., Hanson, I., Leung, C., Lehtinen, K. E. J., and Kerminen, V.-M.: Toward direct measurement of atmospheric nucleation. *Science.* 2007, 318, p. 89–92, doi:10.1126/science.1144124.

Kulmala, M. and and Kerminen, V. M.: On the formation and growth of atmospheric nanoparticles. *Atmospheric Research*. 2008, 90, p. 132-150.

Kulmala, M., Petäjä, T., Nieminen, T., Sipilä, M., Manninen, H. E., Lehtipalo, K., Dal Maso, M., Aalto, P. P., Junninen, H., Paasonen, P., Riipinen, I., Lehtinen K. E. J., Laaksonen A. and Kerminen, V-M.: Measurement of the nucleation of atmospheric aerosol particles. *Nature protocols.* 2012, 7, doi:10.1038/nprot.2012.091.

Kulmala, M., Kontkanen, J., Junninen, H., Lehtipalo, K., Manninen, H. E., Nieminen, T., Petäjä, T., Sipilä, M., Schobesberg, S., Rantala, P., Franchin, A., Jokinen, T., Järvinen, E., Äijälä, M., Kangasluoma, J., Hakala, J., Aaltp, P. P., Paasonen, P., Mikkilä, J., Vanhanen, J., Aalto, J., Hakola, H., Makkonen, U., Ruuskanen, T., Mauldin III, R. L., Duplissy, J., Vehkamäki, H., Bäck, J., Kortelainen, A., Riipinen, I., Kurtén, T., Johnson, M. V., Smith, J. N., Ehn, M., Mentel, T. F., Lehtinen, K. E. J., Laaksonen, A., Kerminen, V.-M. And Wornsop, D. R.: Direct observations of atmospheric aerosol nucleation. *Science*. 2013, 339, p. 943-946.

Kurten, K., Loukonen, V., Vehkamäki, H. and Kulmala, M.: Amines are likely to enhance neutral and ion-induced sulfuric acid-water nucleation in the atmosphere more effectively than ammonia. *Atmospheric Chemistry and Physics*. 2008, 8, p. 4095–4103.

Lee, S.-H., Reeves, J. M., Wilson, J. C., Hunton, D. E., Viggiano, A. A.,Miller, T. M., Ballenthin, J. O., Lait, L. R.: Particle Formation by Ion Nucleation in the Upper Troposphere and Lower Stratosphere. *Science*. 2003, 301, p. 1886-1889.

Lehtinen, K. E. J. and Kulmala, K.: A model for particle formation and growth in the atmosphere with molecular resolution in size. *Atmospheric Chemistry and Physics*. 2002, 3, p. 251 – 257.

Leppä, J., Antilla, T., Kerminen, V.-M., Kulmala, M. and Lehtinen, K. E. J.: Atmospheric new particle formation: real and apparent growth of neutral and charged particles. Atmospheric Chemistry and Physics. 2011, 11, p. 4939–4955.

Lovejoy, E. R., Curtius, J., and Froyd, K. D.: Atmospheric ion-induced nucleation of sulphuric acid and water. *Journal of Geophysical Research*. 2004, 109, D08204, doi: 10.1029/2003JD004460.

Luijten, C. C. M., Bosschaart, K. J. and van Dongen, M. E. H.: High pressure nucleation in water/nitrogen systems. *Chemical Physics.* 1997, .106, (19), p. 4152.

Mäkela, J. M., Yli-Koivisto, S., Hiltunen, V., Seidl, W., Swietlicki, E., Teinilä, K., Sillanpää, M., Koponen, I. K., Paatero, J., Rosman, K. and Hämeri, K.: Chemical composition of aerosol during particle formation events in boreal forest. *Tellus B*. 2001, 53, p. 380-393.

McMurry, P. H.; Fink, M.; Sakurai, H.; Stolzenburg, M. R.; Mauldin, R. L.; Smith, J.; Eisele, F.; Moore, K.; Sjostedt, S.; Tanner, D.; Huey, L. G.; Nowak, J. B.; Edgerton, E.; Voisin, D. J.: A criterion for new particle formation in the sulfur-rich Atlanta atmosphere. *Geophysical Research.* 2005, 110, D22S02, doi:10.1029/2005JD005901.

Merikanto, J., Napari, I., Vehkamäki, H., Anttila, T. and Kulmala, M.: New parameterization of sulfuric acid-ammonia-water ternary nucleation rates at tropospheric conditions. *Journal of Geophysical Research*. 2007, 112, D15207, doi:10.1029/2006JD007977.

Merikanto, J., Spracklen, D. V., Mann, G. W., Pickering, S. J. and Carslaw K.

S.: Impact of nucleation on global CCN. Atmospheric Chemistry and Physics. 2009, 9, p. 8601-8616.

Mirabel P. and Clavelin J. L.: Experimental study of nucleation in binary mixtures: The nitric acid-water and sulfuric acid-water systems. *Journal of Chemical Physics*. 1978, 68, p. 5020–5027.

Neitola, K., Brus, D., Makkonen, U., Sipilä, M., Mauldin III, R. L., Kyllönen, K., Lihavainen, H., and Kulmala, M.: Total sulphate vs. sulphuric acid monomer in nucleation studies: which represents the "true" concentration? *Atmospheric Chemistry and Physics Discussion.* 2013, 13, p. 2313-2350, doi:10.5194/acpd-13-2313-2013.

Nieminen, T., Lehtinen, K. E. J. And Kulmala, M.: Sub-10 nm particle growth by vapor condensation – effects of vapor molecule size and particle thermal speed. *Atmospheric Chemistry and Physics*. 2010, 10, p. 9773-9779.

Nowakowski B. and Ruckenstein, E.: A kinetic approach to the theory of nucleation in gases. *Journal of Chemical Physics*. 1991a, 94, p. 1397.

Nowakowski B. and Ruckenstein, E.: Homogeneous nucleation in gases: A threedimensional Fokker–Planck equation for evaporation from clusters. *Journal of Chemical Physics*. 1991b, 94, p. 8487; doi: 10.1063/1.460719.

O'Dowd, C.D. Colin D. O'Dowd, Hämeri, K. at al.: Dedicated study of New Particle Formation and Fate in the Coastal Environment (PARFORCE): Overview of objectives and achievements. *Journal of Geophysical Research*. 2002, 107, D19, p. 8108, doi: 10.1029/2001JD000555.

Petäjä, T., Mauldin III, R.L., Kosciuch, E., McGrath, J., Nieminen, T., Paasonen, P., Boy, M., Adamov, A. and Kulmala, M. (2009). Sulfuric Acid and OH Concentrations in a Boreal Forest Site. Atmos. Chem. Phys. 9: 7435–7448.

Peters F.: Homogeneous nucleation of ethanol and n-propanol in a shock tube.

Journal of Chemical Physics. 1982, 77, p. 4788.

Peters F.: A new method to measure homogeneous nucleation rates in shock tubes. *Experiments in fluids*. 1983, 1, p. 143 – 148.

Pfeifer, S., Birmili, W., Schladitz, A., Müller, T., Nowak, A. and Wiedensohler, A. (2014). A Fast and Easy-to-Implement Inversion Algorithm for Mobility Particle Size Spectrometers Considering Particle Number Size Distribution Information outside of the Detection Range. Atmos. Meas. Tech. 7: 95–105, doi: 10.5194/amt-7-95-2014.

Qian, S., Sakurai, H., and McMurry, P. H.: Characteristics of regional nucleation events in urban East St. Louis. *Atmospheric Environment*. 2007, 41, p. 4119–4127.

Qiu, Ch. and Zhang, R.: Physiochemical Properties of Alkylaminium Sulfates: Hygroscopicity, Thermostability, and Density. *Environmental Science and Technology*. 2012, 46, p. 4474–4480.

Reiss, R., D. I. Margolese, and F. J. Schelling: Experimental study of nucleation in vapor mixtures of sulfuric acid and water. *Journal of Colloid and Interface Science*. 1976, 56, p. 511–526.

Riipinen I., Sihto S. L., Kulmala M., Arnold F., Dal Maso M., Birmili W., Saarnio K., Teinila, K. Kerminen, V. M., Laaksonen A., and Lehtinen, K. E. J.: Connections between atmospheric sulphuric acid and new particle formation during QUEST III–IV campaigns in Heidelberg and Hyytiälä. *Atmospheric Chemistry and Physics*. 2007, 7, p. 1899–1914.

Řimnáčová, D.: Studium atmosférické nukleace a jejích mechanismů. Dizertační práce, Vysoká škola chemicko – technologická, 2011.

Řimnáčová, D., Ždímal, V., Schwarz, J., Smolík J. and Řimnáč, M.: Atmospheric aerosols in suburb of Prague: The dynamics of particle size distributions. Atmospheric Research, 2011; 101(3):539-552.

DOI: 10.1016/j.atmosres.2010.10.024

Salma, I., Borsós, T., Weidinger, T., Aalto, P., Hussein, T., Dal Maso, M. Kulmala, M. (2011). Production, growth and properties of ultrafine atmospheric aerosol particles in an urban environment. Atmos. Chem. Phys. 11: 1339-1353.

Seinfeld, J. H. and Pandis, S. N.: Atmospheric Chemistry and Physics: From Air Pollution to Climate Change, John Wiley, New York, 1998

Sihto, S.-L., Kulmala, M., Kerminen, V.-M., Dal Maso, M., Petäjä, T., Riipinen, I., Korhonen, H., Arnold, F., Janson, R., Boy, M., Laaksonen, A. And Lehtinen, K. E. J.: Atmospheric sulfuric acid and aerosol formation: implications from atmospheric measurements for nucleation and early growth mechanisms. *Atmospheric Chemistry and Physisc*. 2006, 6, p. 4079-4091.

Sipilä, M., Berndt, T., Petäjä, T., Brus, D., Vanhanen, J., Stratmann, F., Patokoski, J., Mauldin III., R. L., Hyvärinen, A.-P., Lihavainen, H. And Kulmala, M.: The role of sulfuric acid in atmospheric nucleation. *Science*. 2010, 327, p. 1243-1246.

Skrabalova, L., Brus, D., Antilla, T., Zdimal, V. and Lihavainen, H.: Growth of sulphuric acid nanoparticles under wet and dry conditions, Atmos. Chem. Phys., 14, 1-15, 2014.

Skrabalova, L., Zikova N. and Zdimal, V.: Shrinkage of Newly Formed Particles in an Urban Environment. Aerosol and Air Quality Research, 2015, 15: 1313 – 1324.

Smith, J. N., Dunn, M. J., VanReken, T. M., Iida, K., Stolzenburg, M. R., McMurry, P. H., and Huey, P. H.: Chemical composition of atmospheric nanoparticles formed from nucleation in Tecamac, Mexico: evidence for an important role for organic species in nanoparticle growth. *Geophysical Research Letters*. 2008, 35, L04808.

Spracklen, D.V., Carslaw, K.S., Kulmala, M., Kerminen, V-M., Mann, G.W., Sihto, S. - L.: The contribution of boundary layer nucleation events to total particle concentrations on regional and global scales. *Atmospheric Chemistry and Physics*. 2006, 6, p. 5631-5648.

Spracklen, D. V., Carslaw, K. S., Kulmala, M., Kerminen, V. M., Sihto, S.-L., Riipinen, I., Merikanto, J., Mann, G. W., Chipperfield, M. P., Wiedensohler, A., Birmili, W. and Lihavainen, H.: Contribution of particle formation to global cloud condensation nuclei concentrations. *Geophysical Research Letters*. 2008, 35, L06808.

Staples, B. R.: Activity and Osmotic Coefficients of Aqueous Sulfuric Acid at 298.15 K. *Journal of Physical and Chemical Reference Data.* 1981, 10 (3), p. 779-798.

Stolzenburg, M. R., P. H. McMurry, H. Sakurai, J. N. Smith, R. L. Mauldin III, F. L. Eisele, and C. F. Clement: Growth rates of freshly nucleated atmospheric particles in Atlanta. *J. Geophys. Res.* 110, 2005, D22S05, doi:10.1029/2005JD005935.

Strey, R., P.E. Wagner, and T. Schmeling: Homogenous nucleation rates for n-alcohol vapors measured in a two-piston expansion chamber. *Journal of Chemical Physics*. 1986, 84 (4), p. 2325-2335.

Tang, I. N., & Munkelwitz, H. R.: Water activities, densities, and refractive indices of aqueous sulfates and sodium nitrate droplets of atmospheric importance. *Journal of Geophysical Research.* 1994, 99, p. 18 801–18 808.

ten Brink, H., Otjes, R., Jongejan, P. and Slanina S.: An instrument for semi-continuous monitoring of the size-distribution of nitrate, ammonium, sulphate and chloride in aerosol. *Atmospheric Environment*. 2007, 41, 13, p. 2768-2779.

ten Wolde, P. R., Oxtoby D. W. and Frenkel, D.: Chain formation in

homogeneous gas-liquid nucleation of polar fluids. *Chemical Physics*. 1999, 111: p. 4762 – 4773.

Vaden, T.D., Imre, D., Beránek, J., Shrivastava, M and Zelenyuk A. (2011). Evaporation Kinetics and Phase of Laboratory and Ambient Secondary Organic Aerosol. Science 108: 2190–9195.

Vanhanen, J., Mikkilä, J., Lehtipalo, K., Sipilä, M. , Manninen, H. E. , Siivola, E. , Petäjä, T. and Kulmala, M.: Particle Size Magnifier for Nano-CN Detection*, Aerosol Sci. Technol.*, 2011, 45: 4, 533-542.

Viisanen Y. and Strey, R.: Homogeneous nucleation rates for n-butanol. *Journal of Chemical Physics*. 1994, 101 (9), p. 7835-7843.

Viisanen, Y., Kulmala M. and Laaksonen, A.: Experiments on gas-liquid nucleation of sulfuric acid and water. *Journal of Chemical Physics*. 1997, 107, p. 920-926.

Volmer M. and Weber A.: Nucleus formation in supersaturated systems. *Zeitschrift für Physikalische Chemie*. 1926, p. 119–277.

Vehkamäki, H., Kulmala, M., Napari, I., Lehtinen, K. E. J., Timmreck, C., Noppel, M. and Laaksonen A.: An improved parameterization for sulfuric acid–water nucleation rates for tropospheric and stratospheric conditions. *Journal of Geophysical Research.* 2002, 107(D22), p. 4622, doi:10.1029/2002JD002184.

Wagner P. E. and Strey, R.: Homogeneous nucleation rates of water vapor measured in a two-piston expansion chamber. *Journal of Chemical Physics*. 1981, 85 (18), p. 2694-2698.

Wiedensohler, A. and Fissan, H. J.: Bipolar Charge Distributions of Aerosol Particles in High-Purity Argon and Nitrogen. *Aerosol Science & Technology*. 1991, 14, 358-364, doi: 10.1080/02786829108959498.

Wiedensohler, A., Birmili, W., Nowak, A., Sonntag, A., Weinhold, K., Merkel,

M. and Wehner, B.: Mobility Particle Size Spectrometers: Harmonization of Technical Standards and Data Structure to Facilitate High Quality Long-Term Observations of Atmospheric Particle Number Size Distributions. *Atmos. Meas. Tech*. 2012, 5: 657–685.

Wilemski, G.: Composition of the critical nucleus in multicomponent vapor nucleation. *Journal of Chemical Physics*. 1984, 80, p. 1370-1372.

Wu, Z., Birmili, W., Poulain, L., Wang, Z., Merkel, M., Fahlbusch, B., van Pinxteren, D. Herrmann, H. and Wiedensohler, A. Particle hygroscopicity during atmospheric new particle formation events: implications for the chemical species contribution to particle growth. *Atmospheric Chemistry and Physisc*. 2013, 13, p. 6637-6646.

Wyslouzil, B. E., Seinfeld, J. H., Flagan, R. C. and Okuyama, K.: Binary nucleation in acid-water systems II: Sulfuric acid-water and a comparison with methanesulfonic acid-water, *Journal of Chemical Physics*. 1991, 94, p. 6842-6850.

Yao, X., Choi, M.Y., Lau, N.T., Lau, A.P.S., Chan, C.K., and Fang, M.: Growth and Shrinkage of New Particles in the Atmosphere in Hong Kong. *Aerosol Sci. Technol*. 2010, 44: 639–650.

Yli-Juuti, T., Nieminen, T., Hirsikko, A., Aalto, P., Asmi, E., Hõrrak, U., Manninen, H. E., Patokoski, J., Dal Maso, M., Petäjä, T., Rinne, J., Kulmala, M. and Riipinen, I.: Growth rates of nucleation mode particles in Hyytiälä during 2003−2009: variation with particle size, season, data analysis method and ambient conditions. *Atmos. Chem. Phys.* 2011, 11: 12865-12886.

Yli-Jutti, T., Zardini, A.A., Eriksonn, A.C., Hansen, A.M. K., Pagels, J.H., Swietlicki, E., Svenningsson, B., Glasius, M., Wornsop, D.R., Riipinen, I. and Bilde, M.: Volatility of Organic Aerosol: Evaporation of Ammonium

Sulfate//Succinic Acid Aqueous Solution Droplets. Environ. *Sci. Technol*. 2013, 47: 12123–12130.

Young, L. H., Benson, D. R., Kameel, F. R., Pierce, J. R., Junninen, H., Kulmala, M., Lee, S.-H.: Laboratory studies of H_2SO_4/H_2O binary homogenous nucleation from the SO_2+OH reaction: evaluation of the experimental setup and preliminary results. *Atmospheric Chemistry and Physisc*. 2008, 8, p. 4997-5016.

Young, L.H., Lee, S.H., Kanawade, V.P., Hsiao, T.C., Lee, Y.L., Hwang, B.F., Liou, Y.J., Hsu, H.T. and Tsai, P.J.: New Particle Growth and Shrinkage Observed in Subtropical Environments. *Atmos. Chem. Phys*. 2013, 13: 547–564.

Yu, F.: Updated H_2SO_4-H_2O binary homogeneous nucleation look-up tables. *Journal of Geophysical Research. 2008,* 113, D24201, doi:10.1029/2008JD010527.

Yu, F.: Ion-mediated nucleation in the atmosphere: Key controlling parameters, implications, and look-up table. *Journal of Geophysical Research*. 2010, 115, D03206, doi:10.1029/2009JD012630.

Yue, D. L., Hu, M., Zhang, R. Y., Wang, Z. B., Zheng, J., Wu, Z. J., Wiedensohler, A., He, L. Y., Huang, X. F. and Zhu, T.: The role of sulfuric acid in new particle formation and growth in the mega-city of Beijing, *Atmos. Chem. Phys.,* 2010, 10, 4953-4960.

Zhang, R., Suh, I., Zhao, J., Zhang, D., Fortner, E. C., Tie, X., Molina, L. T. and Molina M. J.: Atmospheric new particle formation enhanced by organic acids. *Science. 2004,* 304, p. 1487-1490.

Zhang, R. Getting to the Critical nukleus of aerosol formation. *Science*. 2010, 328, p. 1366, DOI: 10.1126/science.1189732.

Zhang, R., A.F. Khalizov, L. Wang, M. Hu, X. Wen: Nucleation and growth of

nanoparticles in the atmosphere. *Chem. Rev.* 2012, 112, 1957-2011, DOI: 10.1021/cr2001756.

Ždímal. V.: Experimentalní studium homogenní nukleace v plynných směsích. Dizertační práce, Vysoká škola chemicko-technologická, 1998.

Ždímal, V.; Brabec, M.; Wagner, Z. Comparison of Two Approaches to Modeling Atmospheric Aerosol Particle Size Distributions. *Aerosol and Air Quality Research*. 2008, 8, 4, p. 392.